

THE IMPACT OF LIPID NANOPARTICLE CHEMISTRY ON RNA DELIVERY AND
THERAPEUTIC OUTCOMES

APPROVED BY SUPERVISORY COMMITTEE

Daniel Siegwart, Ph.D.

Hao Zhu, M.D.

Yujin Hoshida, M.D., Ph.D.

Caroline de Gracia Lux, Ph.D.

Amit Singal, M.D.

DEDICATION

To everyone who showed support and encouragement throughout my Ph.D. journey.

ACKNOWLEDGEMENT

There are many people that I would like to thank for their contributions to my development both professionally and personally during my Ph.D. studies at UT Southwestern.

First and foremost, I would like to express my sincere gratitude to my Ph.D. supervisor and mentor, Dr. Daniel Siegwart for his invaluable advice, patience, positive attitude, and continuous support throughout the duration of my Ph.D. studies. Dr. Siegwart's passion towards advancing science and developing transformative therapies is truly inspiring and I will always admire him as I continue in my scientific career endeavors. It has been an honor to be a member of the Siegwart laboratory team and I am grateful for the opportunity to train and grow as a scientist here during my time at UT Southwestern.

I would also like to express my deepest appreciation to my dissertation committee members, Dr. Hao Zhu, Dr. Yujin Hoshida, Dr. Caroline de Gracia Lux, and Dr. Amit Singal. I could not have undertaken this journey without my dissertation committee, who generously provided their knowledge and expertise throughout my Ph.D. research. Additionally, I am grateful for the generous support from the PhRMA Foundation.

I also want to express my appreciation to all involved in the Mechanisms of Disease and Translational Sciences Program at UT Southwestern; this program helped shape my research and scientific training throughout my Ph.D. Additionally, many thanks are extended to the faculty of the Biomedical Engineering program at UT Southwestern.

Words truly cannot express my gratitude to my mentor and previous coworker, Dr. Kejin Zhou. Kejin, thank you for your insightful advice, invaluable constructive feedback, and

your continuous encouragement during these last five years. I am grateful for everything that I have learned from you.

I would like to extend a special thank you to Dr. Di Zhang for her helpful suggestions, assistance, and constant support during my training. I am very grateful for her mentorship during the last several years of my Ph.D.

I would like to express my sincere appreciation to all of the members within the Siegwart laboratory, including past and present members, for their experimental troubleshooting assistance, presentation feedback sessions, and moral support. It is the kind help and encouragement of the entire Siegwart laboratory family that has made my Ph.D. studies a time that I will always cherish.

My gratitude is extended to both past and present members of the Moody Foundation Flow Cytometry Core at UT Southwestern, for sharing their knowledge of flow cytometry with me during my Ph.D. studies.

I would like to acknowledge and thank my friends at UT Southwestern that helped me throughout my Ph.D. studies. I would also like to extend a special thank you to my Dallas running buddies, the Black Swan Yoga family, and close friends for truly keeping me grounded during the challenges of pursuing a Ph.D.

Lastly, I would like to extend a thank you to my parents for their unwavering support, encouragement, and belief in me. Finally, a very special thank you to my best friend and fiancé, thank you for your continuous patience, support and encouragement during these many years of my scientific endeavors. I am so excited to embark on our next journey and begin our lives together, finally in the same state and city.

THE IMPACT OF LIPID NANOPARTICLE CHEMISTRY ON RNA DELIVERY AND
THERAPEUTIC OUTCOMES

by

LINDSAY TAYLOR JOHNSON

DISSERTATION / THESIS

Presented to the Faculty of the Graduate School of Biomedical Sciences

The University of Texas Southwestern Medical Center at Dallas

In Partial Fulfillment of the Requirements

For the Degree of

DOCTOR OF PHILOSOPHY

The University of Texas Southwestern Medical Center at Dallas

Dallas, Texas

December, 2022

Copyright

by

Lindsay Taylor Johnson, 2022

All Rights Reserved

AN INVESTIGATION OF THE IMPACT OF LIPID NANOPARTICLE CHEMISTRY ON
RNA DELIVERY AND THERAPEUTIC OUTCOMES

Publication No. _____

Lindsay Taylor Johnson

The University of Texas Southwestern Medical Center at Dallas, 2022

Supervising Professor: Daniel Siegwart, Ph.D.

Abstract: This dissertation aims to understand how two individual components of the traditional four-component lipid nanoparticle system, the PEG lipid component and the ionizable cationic lipid component, impact RNA delivery. To systematically investigate how PEG lipid chemistry impacted LNP formulation and RNA delivery, a series of linear-dendritic poly(ethylene glycol) (PEG) lipids were synthesized with modulated hydrophobic domains. The chemical structure of the hydrophobic domain did not impact the formulation of 5A2-SC8 LNPs, including nanoparticle size, RNA encapsulation, and stability. However, the chemical structure did affect RNA delivery efficacy both *in vitro* and *in vivo*. The chemical structure of

the hydrophobic domain of the PEG lipids impacted the escape of 5A2-SC8 LNPs from endosomes at early cell incubation time points. Overall, the results indicated that PEG lipid anchoring and chemical structure modulated RNA delivery.

Although most LNPs accumulate in the liver after intravenous administration (suggesting that liver delivery is straightforward), it was observed that two similar LNP formulations (5A2-SC8 and 3A5-SC14 LNPs) resulted in distinct RNA delivery within the liver organ. Despite both LNPs possessing similar physical properties, the ability to silence RNA *in vitro*, strong accumulation within the liver, and sharing a pKa of 6.5, only 5A2-SC8 LNPs were able to functionally deliver RNA to hepatocytes. Protein corona analysis indicated that 5A2-SC8 LNPs bind Apolipoprotein E (ApoE), which can drive LDL-R receptor mediated endocytosis in hepatocytes. In contrast, the surface of 3A5-SC14 LNPs was enriched in Albumin but depleted in ApoE, which likely led to Kupffer cell delivery and detargeting of hepatocytes. In an aggressive MYC-driven liver cancer model, 5A2-SC8 LNPs carrying let-7g miRNA were able to significantly extend survival compared the non-treatment group. Since disease targets exist in an organ- and cell-type specific manner, the clinical development of RNA LNP therapeutics will require an improved understanding of LNP cellular tropism within organs. Overall, the results from this work illustrates the importance of understanding the cellular localization of RNA delivery and incorporating further checkpoints when choosing nanoparticles beyond biochemical and physical characterization, as small changes in the chemical composition of LNPs can have an impact on both the biofate of LNPs and therapeutic outcomes.

TABLE OF CONTENTS

ABSTRACT	VII
TABLE OF CONTENTS	IX
PRIOR PUBLICATIONS	XV
LIST OF DEFINITIONS.....	XXII
CHAPTER ONE.....	1
INTRODUCTION: REVIEW OF THE LITERATURE.....	1
1.1 A GENE THERAPY OVERVIEW	1
1.2 THE THERAPEUTIC POTENTIAL OF NUCLEIC ACIDS.....	3
1.2.1 NUCLEIC ACIDS FOR GENE MEDIATED SILENCING	4
1.2.2 NUCLEIC ACIDS FOR PROTEIN REPLACEMENT: MRNA	8
1.2.3 GENE EDITING PLATFORMS.....	9
1.3 EFFICIENT TARGETED DELIVERY IS A SIGNIFICANT BARRIER FOR EFFECTIVE GENE THERAPY	10
1.4 NUCLEIC ACIDS REQUIRE A DELIVERY VEHICLE	10
1.4.1 VIRAL CARRIERS FOR NUCLEIC ACIDS	13
1.4.1A ADENO-ASSOCIATED VIRUS (AAV) DELIVERY	14
1.4.1B LENTIVIRAL (LV) DELIVERY	15
1.4.1C ADENOVIRAL DELIVERY	15
1.4.2 NON-VIRAL NUCLEIC ACID CARRIERS	15
1.4.2A THE EARLY GENERATION OF LIPID NANOPARTICLES (LNPS)	16
1.4.2B POLYMERIC NANOCARRIERS	18

1.4.2C PEPTIDE BASED CARRIERS	18
1.4.2D INORGANIC BASED CARRIERS	18
1.5 LIPID NANOPARTICLES AS DELIVERY VEHICLES FOR NUCLEIC ACIDS	19
1.5.1 LNPS ARE TRADITIONALLY COMPRISED OF FOUR COMPONENTS	20
1.5.2 IONIZABLE CATIONIC LIPIDS	21
1.5.3 PEG LIPID	24
1.5.4 HELPER LIPIDS (CHOLESTEROL AND PHOSPHOLIPIDS)	25
1.6 ROUTES OF ADMINISTRATION FOR LNPS	26
1.6.1 THE FATE OF SYSTEMICALLY ADMINSTERED LNPS	27
1.7 LIVER NANOPARTICLE CLEARANCE	27
1.7.1 PROTEIN CORONA AND LIVER DELIVERY	28
1.8 PRECISE RNA DELIVERY FOR HCC AND LIVER DISEASE THERAPY	29
1.9 OUTLOOK	32
CHAPTER TWO: THE HYDROPHOBIC DOMAIN STRUCTURE OF LINEAR-	
DENDRITIC POLY(ETHYLENE GLYCOL) LIPIDS AFFECTS RNA DELIVERY OF	
LIPID NANOPARTICLES	
2.1 INTRODUCTION	33
2.2 RESULTS AND DISCUSSION.....	37
2.2.1 SYNTHESIS AND CHARACTERIZATION OF LINEAR DENDRITIC	
POLY(ETHYLENE GLYCOL) (PEG) LIPIDS PEG-GNCM	37
2.2.2 FORMULATION AND CHARACTERIZATION OF DENDRIMER-BASED	
LIPID NANOPARTICLES (DLNPS) WITH PEG LIPIDS PEG-GN-CM	39

2.2.3 IN VITRO AND IN VIVO SMALL DELIVERY OF DLNPS	41
2.2.4 EXAMINATION OF ENDOSOMAL ESCAPE FOR DLNPS CONTAINING DIFFERENT PEGGNCM	45
2.2.5 IN VIVO SMALL RNA DELIVERY OF DLNPS IN TUMORS	51
2.3 MATERIALS AND METHODS	53
2.3.1 MATERIALS	53
2.3.2 CHARACTERIZATION.....	54
2.3.3 EXPERIMENTAL METHODS	54
2.3.3.1 SYNTHESIS OF FIRST, SECOND, AND THIRD GENERATION DENDRIMERS TB-GNDB	54
2.3.3.2 SYNTHESIS OF LINEAR DENDRITIC PEG LIPIDS PEG-GNCM	55
2.3.3.3 FORMULATION OF DLNPS	56
2.3.3.4 EVALUATION OF IN VITRO RNA DELIVERY OF 5A2-SC8 DLNPS .	57
2.3.3.5 EVALUATION OF CELLULAR UPTAKE, STABILITY AND HEMOLYSIS OF 5A2-SC8 DLNPS	57
2.3.3.6 EVALUATION OF IN VIVO DELIVERY OF 5A2-SC8 DLNPS.....	58
CHAPTER THREE: LIPID NANOPARTICLE (LNP) CHEMISTRY CAN ENDOW UNIQUE IN VIVO RNA DELIVERY FATES WITHIN THE LIVER THAT ALTER THERAPEUTIC OUTCOMES IN A CANCER MODEL	60
3.1 INTRODUCTION.....	60
3.2 RESULTS AND DISCUSSION.....	65

3.2.1 5A2-SC8 AND 3A5-SC14 LNPS POSSESS SIMILAR PHYSICAL PROPERTIES	65
3.2.2 5A2-SC8 AND 3A5-SC14 LNPS EXHIBIT DIFFERENTIAL SIRNA DELIVERY CAPABILITIES TO HEPATOCYTES	69
3.2.3 KUPFFER CELLS IMPACT 3A5-SC14 LNPS RNA DELIVERY OF HEPATOCYTES AND DO NOT AFFECT 5A2-SC8 LNPS	72
3.2.4 THE PROTEIN CORONA FORMED ON 5A2-SC8 AND 3A5-SC14 LNPS AIDS OR RESTRICTS DELIVERY TO HEPATOCYTES	76
3.2.5 CELLULAR TROPISM WITHIN THE LIVER AFFECTS THERAPEUTIC OUTCOMES IN AN AGGRESSIVE LIVER CANCER MOUSE MODEL	84
3.3 MATERIALS AND METHODS	89
3.3.1 MATERIALS AND REAGENTS.....	89
3.3.2 NUCLEIC ACIDS USED	90
3.3.3 REAGENTS USED FOR BIOLOGICAL ASSAYS	91
3.3.4 ANTIBODIES USED.....	91
3.3.5 INSTRUMENTATION.....	92
3.3.6 CELL CULTURE MATERIALS.....	92
3.3.7 EXPERIMENTAL PROCEDURES	93
3.3.7.1 FORMULATION AND CHARACTERIZATION OF 5A2-SC8 AND 3A5- SC14 LNPS	93
3.3.7.2 NANOPARTICLE SIZE AND SURFACE CHARGE MEASUREMENT	94
3.3.7.3 RNA BINDING RIBOGREEN ASSAY	95

3.3.7.4 EVALUATION OF IN VITRO LUCIFERASE DELIVERY OF 5A2-SC8 AND 3A5-SC14 LNPS.....	95
3.3.7.5 LUCIFERASE MRNA DELIVERY ASSAY WITH AND WITHOUT PROTEIN INCUBATION TO PRIMARY KUPFFER CELLS AND HEPATOCYTES...	96
3.3.7.6 EVALUATION OF IN VIVO TOXICITY OF SIFVII 5A2-SC8 AND 3A5-SC14 LNPS AT VARYING DOSES	96
3.3.7.7 EVALUATION OF LUCIFERASE MRNA DELIVERY IN VIVO.....	97
3.3.7.8 EVALUATION OF IN VITRO SIRNA DELIVERY OF 5A2-SC8 AND 3A5-SC14 LNPS	97
3.3.7.9 ANIMAL RELATED STUDIES	98
3.3.7.10 EVALUATION OF IN VIVO RNA DELIVERY OF 5A2-SC8 AND 3A5-SC14 LNPS TO HEPATOCYTES.....	98
3.3.7.11 ANALYSIS OF SIFVII-CY5.5 BIODISTRIBUTION OF 5A2-SC8 AND 3A5-SC14 LNPS	99
3.3.7.12 KUPFFER CELL DEPLETION AND IN VIVO RNA DELIVERY OF 5A2-SC8 AND 3A5-SC14 LNPS TO HEPATOCYTES.....	99
3.3.7.13 ISOLATION OF PLASMA PROTEINS ABSORBED TO 5A2-SC8 AND 3A5-SC14 LNPS	100
3.3.7.14 SODIUM DODECYL SULFATE-POLYACRYLAMIDE GEL ELECTROPHORESIS (SDS-PAGE) CHARACTERIZATION OF PLASMA PROTEINS ADSORBED ONTO 5A2-SC8 AND 3A5-SC14 LNPS.....	101

3.3.7.15 VALIDATION OF APOE AND ALBUMIN ADSORPTION OF LNPS USING WESTERN BLOT.....	101
3.3.7.16 PREPARATION OF PLASMA PROTEIN SAMPLES FOR MASS SPECTROMETRY PROTEOMICS	102
3.3.7.17 LUCIFERASE MRNA DELIVERY ASSAY WITH AND WITHOUT PROTEIN INCUBATION OF CELL LINES.....	102
3.3.7.18 LUCIFERASE MRNA DELIVERY ASSAY WITH AND WITHOUT PROTEIN INCUBATION TO PRIMARY CELLS.....	103
3.3.7.19 GENERATION OF MYC-DRIVEN AGGRESSIVE CANCER MOUSE MODEL	103
3.3.7.20 IN VIVO LET-7G MIRNA THERAPEUTIC STUDY IN AGGRESSIVE CANCER MOUSE MODEL USING 5A2-SC8 AND 3A5-SC14 LNPS.....	104
3.3.7.21 IMMUNOHISTOCHEMISTRY AND HISTOLOGICAL TISSUE ANALYSIS	104
CHAPTER FOUR: CONCLUSIONS AND FUTURE DIRECTIONS	106

PRIOR PUBLICATIONS

1. Zhou, K., **Johnson, L.T.**, Xiong, H., Minning, J., Yan, Y., Barrios, S., Abram, B., Yu, X., Siegwart, D.J., Linear-dendritic poly (ethylene glycol) lipid tail chemical structure switch RNA delivery of lipid nanoparticles. *Molecular Pharmaceutics* **2020**, 17 (5), 1575-1585.
2. Cheng, Q., Wei, T., Farbiak, L., **Johnson, L.T.**, Dilliard, S.A., Siegwart, D.J., Selective ORgan Targeting (SORT) nanoparticles for tissue specific mRNA delivery and CRISPR/Cas gene editing. *Nature Nanotechnology* **2020**, 15, 313-320.
3. Liu, S., Cheng, Q., Wei, T., Yu, X., **Johnson, L.T.**, Farbiak, L., D.J. Siegwart. Membrane destabilizing ionizable phospholipids for organ selective mRNA delivery and CRISPR/Cas gene editing. *Nature Materials* **2021**, 20, 701-710.
4. Lee, S.M., Q. Cheng, X. Yu, S. Liu, **Johnson, L.T.**, and Siegwart, D.J. A systematic study of unsaturation in lipid nanoparticles leads to improved mRNA transfection in vivo. *Angewandte Chemie International Edition* **2020**, 60, 5848-5853.
5. Farbiak, L., Cheng, Q., Wei, T., Benedicto, E.A., **Johnson, L.T.**, Lee, S.M., Siegwart, D.J. All-In-One Dendrimer-Based Lipid Nanoparticles enable Precise HDR-Mediated Gene Editing In vivo. *Advanced Materials* **2021**, 33, 200619

6. Yu, X., Liu, S., Cheng, Q., Lee, S.M., Wei, T., Zhang, D., Farbiak, L., **Johnson, L.T.**, Wang, X., Siegwart, D.J. Hydrophobic Optimization of Functional poly(TPAE-co-suberoyl chloride) for Extrahepatic mRNA Delivery Following Intravenous Administration. *Pharmaceutics* **2021**, 13 (11), 1914.
7. Liu, S., Wang, X., Yu, X., Cheng, Q., **Johnson, L.T.**, Chatterjee, S., Zhang, D., Lee, S.M., Sun, Y., Ting-Chih, T., Liu, J., Siegwart, D.J. Zwitterionic phospholipidation of cationic polymers facilitates systemic mRNA delivery to spleen and lymph nodes. *Journal of the American Chemical Society* **2021**, 143 (50), 21321-21330.
8. Alvarez-Benedicto, E., Farbiak, L., Ramirez, M., Wang, X., **Johnson, L.T.**, Mian, O., Guerrero, E.D., Siegwart, D.J. Optimization of phospholipid chemistry for improved lipid nanoparticle (LNP) delivery of messenger RNA (mRNA). *Biomaterials Science* **2022**, 10 (2) 549-229.
9. Zhang, D., Wang, G., Yu, X., Wei, T., Farbiak, L., **Johnson, L.T.**, Taylor, A., Hong, Y., Zhu, H., Siegwart, D.J. Enhancing CRISPR/Cas gene editing through modulating cellular mechanical properties for cancer therapy. *Nature Nanotechnology* **2022**.
10. **Johnson, L.T.**, Zhou, K., Lee, S.M., Liu, S., Dilliard, S., Farbiak, L., Chatterjee, S., Lin, Y., Siegwart, D.J. Lipid nanoparticle (LNP) chemistry can endow unique In Vivo

RNA delivery fates within the liver that alter therapeutic outcomes in a cancer model.

Molecular Pharmaceutics **2022** (Accepted).

LIST OF FIGURES

FIGURE 1.1 A SIMPLE ILLUSTRATION FO RNAI FOR SIRNAS	5
FIGURE 1.2 A SIMPLE ILLUSTRATION OF THE EXTRACELLULAR AND INTRACELLULAR BARRIERS FOR NON-VIRAL DRUG DELIVERY CARRIERS ..	12
FIGURE 1.3 VIRAL DELIVERY SYSTEMS FOR NUCLEIC ACIDS	14
FIGURE 1.4 NON-VIRAL DELIVERY SYSTEMS FOR NUCLEIC ACIDS	16
FIGURE 1.5 MODERNA AND PFIZER FDA APPROVED COVID 19	19
FIGURE 1.6 AN EXAMPLE OF A FOUR COMPONENT LNP FORMULATION	21
FIGURE 1.7 IONIZABLE CATIONIC LIPIDS UTILIZED IN LNPS	23
FIGURE 1.8 ROUTES OF ADMINISTRATION FOR DRUG DELIVERY AND LNPS	26
FIGURE 2.1.1 A SCHEMATIC STUDY ON THE IMPACT OF LINEAR DENDRITIC PEG LIPIDS AND RNA DELIVERY	36
FIGURE 2.2.1 CHEMICAL ROUTE FOR THE SYNTHESIS OF LINEAR DENDRITIC PEG LIPIDS	37
FIGURE 2.2.2 CHARACTERIZATION OF NINE LINEAR DENDRITIC PEG LIPIDS AND THEIR SYNTHETIC PRECURSOS T3-G1DB, T3-G2DB, T3-G3DB	39
FIGURE 2.2.3 THE PEG LIPID STRUCTURE DOES NOT IMPACT LNP FORMULATION	41
FIGURE 2.2.4 THE DENDRTICI STRUCTURE OF PEG-GNCM HAS AN IMPACT ON SIRNA DELIVERY EFFICACY IN VITRO	43
FIGURE 2.2.5 THE DENDRITIC STRUCTURE OF PEG-GNCM HAS AN IMPACT ON SIRNA DELIVERY EFFICACY IN VIVO.....	44

FIGURE 2.2.6 5A2-SC8 DLNPS FORMULATED WITH VARYING PEG LIPID STRUCTURES EFFECTIVELY INTERNALIZE INTO HELA CELLS	46
FIGURE 2.2.7 PEG-G1C16, PEG-G2-C12 5A2-SC8 DLNPS REMAIN STABLE UNDER ENDOSOME MIMICKING CONDITIONS	48
FIGURE 2.2.8 THE HYDROPHOBIC DOMAIN OF THE PEG LIPID IMPACTS ENDOSOMAL ESCAPE AT EARLY TIME POINTS.....	50
FIGURE 2.2.9 THE SIRNA DELIVERY CAPABILITY OF PEG-G1C12 AND PEG-G2C12 5A2-SC8 DLNPS EVALUATED IN A CANCER MODEL.....	52
FIGURE 3.1 SMALL CHANGES IN LNP CHEMISTRY CAN HAVE AN IMPACT ON CELLULAR TROPISM WITHIN THE LIVER AND CANCER THERAPEUTIC EFFICACY.....	64
FIGURE 3.2.1 5A2-SC8 AND 3A5-SC14 LNPS CONTAINING SIRNA FORM LNPS WITH SIMILAR PHYSICAL PROPERTIES	67
FIGURE 3.2.2 SIFVII 5A2-SC8 AND 3A5-SC14 LNPS WERE WELL TOLERATED IN VIVO AT VARYING DOSES (0.25, 0.5, 1, AND 1.5 MG/KG.	68
FIGURE 3.2.3 5A2-SC8 AND 3A5-SC14 LNPS CONTAINING SIRNA HAVE DISTICNT IN VIVO ACTIVITY IN REGARDS TO HEPATOCYTE DELIVERY.....	71
FIGURE 3.2.4 DEPLETION OF KUPFFER CELLS ENABLES RNA DELIVERY OF 3A5- SC14 LNPS TO HEPATOCYTES BUT DOES NOT IMPACT THE RNA DELIVERY OF 5A2-SC8 LNPS	75
FIGURE 3.2.5 3A5-SC14 AND 5A2-SC8 LNPS HAVE UNIQUE PROTEIN CORONAS	78

FIGURE 3.2.6 A COMPARSION OF THE FUNCTIONAL DELIVERY OF PROTEIN COATED OR UNCOATED 5A2-SC8 AND 3A5-SC14 LNPS IN VITRO WITH AND WITHOUT SERUM CONTAINING MEDIA	81
FIGURE 3.2.7. FUNCTIONAL LUCIFERASE MRNA DELIVERY OF UNCOATED OR PROTEIN COATED 5A2-SC8 AND 3A5-SC14 LNPS TO HUH-7 CELL LINE AND PRIMARY HEPATOCYTES	83
FIGURE 3.2.8 THERAPEUTIC EFFICACY OF 5A2-SC8 AND 3A5-SC14 LET-7G MIRNA LNPS AND 3A5-SC14 LET-7G MIRNA LNPS WERE EVALUATED IN MYC- DRIVEN LIVER CANCER MODEL.....	88

LIST OF APPENDICES

APPENDIX A SUPPLEMENTARY FIGURES..... 108

LIST OF DEFINITIONS

DNA – Deoxyribonucleic acid

NIH – National Institute of Health

RNA – Ribonucleic acid

RNAi – RNA interference

siRNA – Small interfering RNA

miRNA – Micro ribonucleic acid

mRNA – Messenger ribonucleic acid

shRNA – Short hairpin RNA

ASO – Antisense oligonucleotide

dsDNA – Double-stranded deoxyribonucleic acid

RISC – RNA-induced silencing complex

LNP – Lipid nanoparticle

pDNA – Plasmid DNA

FDA – Food and Drug Administration

TALEN – Transcription activator-like effector nucleases

CRISPR – Clustered Regularly Interspaced Short Palindromic Repeats

ZFN – Zinc finger nucleases

Cas9 – CRISPR associated protein 9

AGO2 – Argonaute RISC Catalytic Component 2

RNAses – Ribonucleases

IVT – In-vitro translation

Bp- Base pair

gRNA – Guide RNA

NHEJ – Non-homologous end joining

HDR – Homology directed repair

TTR – Transthyretin

AAV – Adeno-associated virus

LV –Lentivirus

hATTR – Hereditary transthyretin amyloidosis

HCC – Hepatocellular carcinoma

RSV – Rous sarcoma virus

PEG – Poly(ethylene glycol)

PLL – Poly-l-lysine

CPP – Cell penetrating peptide

PEI – Polyethyleneimine

PAMAM – Poly(amidoamine)

PLGA – poly(lactide-co-glycolic acid)

MC3 – DLin-MC3-DMA

I.V. – Intravenous injection

ApoE – Apolipoprotein E

DODAP – Dioleoyl-3-trimethylammonium propane

DOTAP –1,2- dioleoyl-3-trimethylammonium propane

DLin-KC2-DMA – 2,2-dilinoleyl-4-(2-dimethylaminoethyl)-[1,3]-dioxolane

DSPC – Distearoylphosphatidylcholine

DOPE – 1,2-dioleoyl-sn-glycero-3-phosphoethanolamine

SORT – Selective organ targeting

18PA – 1,2-dioleoyl-sn-glycero-3-phosphate

RES – Reticular endothelial system

MPS – Mononuclear phagocyte system

LDL – Low density lipoprotein

LDLR – Low density lipoprotein receptor

NASH – Non-Alcoholic fatty liver steatohepatitis

KC – Kupffer cells

DLNP – Dendrimer lipid nanoparticle

FAH – Fumarylacetoacetate hydrolase

FVII – Factor seven

AST – Aspartate transaminase

ALT – Alanine aminotransferase

CREA – Creatinine

BUN – Blood urea nitrogen

IHC – Immunohistochemistry

WB – Western blot

ASCVD – Atherosclerotic cardiovascular disease

CHAPTER ONE

Review of the Literature

1.1 A gene therapy overview

The field of gene therapy has evolved over the years with the ultimate goal of treating and curing genetic disease. In the past decade, over 20 gene therapies have been approved by the United States Food and Drug Administration (FDA) for clinical use.¹ There are many important milestones that have contributed to the exciting progression of gene therapy.^{2, 3} In the 1960s, scientists hypothesized that deoxyribonucleic acid (DNA) sequences could be introduced into the cells of patients to cure genetic disorders and in 1990, the National Institute of Health (NIH) approved the first-in-human gene therapy clinical trial.^{4, 5} With the completion of the Human Genome Project and the human DNA blueprint available, the door was opened for making gene therapy a reality for multiple diseases.⁶ Genetic information is expressed when genomic DNA is translated into a functional protein product by a messenger ribonucleic acid (mRNA) intermediate.² Ribonucleic acid (RNA) molecules are utilized to regulate the specific expression of the protein product through a process known as RNA interference (RNAi). Gene therapies provide the potential for treating most diseases by silencing disease causing genes or expressing genes for therapeutic proteins. These therapies use gene altering applications through the delivery of cargos like small interfering RNA (siRNA), messenger RNA (mRNA), plasmid DNA (pDNA), or clustered regularly interspaced palindromic repeats (CRISPR)/Cas9.⁷ Gene therapies offer advantages over conventional small molecule drugs

because they have a wide variety of targets that have otherwise been inaccessible, unlike small molecule drugs which are confined to active binding sites on proteins.⁸

More recently, the development of gene editing therapies utilizing CRISPR has enabled the editing of disease genes. Building off of the discoveries and knowledge from research on zinc finger nucleases, transcription activator-like effector nucleases (TALENs), and CRISPR-Cas9-based genome editing technologies, base and prime editing has emerged as an exciting gene editing technology for the treatment of disease. Base editing is a more fine-tuned approach to gene editing that can permanently change a single letter of a genetic code at a specific location.⁹ Base editors are one of the latest genomic editing technologies to enter the clinic. This year, the first patient was administered with the base editor VERVE-101, developed in a collaboration between Verve Therapeutics and Beam Therapeutics. The VERVE-101 base editor's goal is to turn off PCSK9 by the replacement of an Adenosine with a Guanine. This change in a single base has a great affect towards lowering low-density lipoprotein cholesterol (LDL-C) levels, which greatly reduces the risk for atherosclerotic cardiovascular disease (ASCVD).¹⁰ Furthermore, Beam therapeutics is preparing to begin a clinical trial for second base editor, BEAM-101, for the treatment of sickle cell disease.

Gene editing technology will continue to revolutionize medicine because it provides new opportunities to modulate specific genes for therapeutic intervention and the potential to provide patients with curative options. Millions of people worldwide suffer from genetic disorders or from diseases with little to no treatments. These diseases can in-theory be corrected with therapies utilizing DNA editing technology that can precisely manipulate

and edit sequences of DNA in human cells.¹¹ We have entered a new and exciting era of gene therapy where ongoing clinical trials utilize gene editing with the first FDA approved mRNA LNP vaccines on the market. However, the major challenge that prevents the widespread implementation of gene therapy is delivery. This challenge exists with most genetic cargos such as RNA, DNA, or CRISPR/Cas9. Gene delivery may appear as a straightforward problem, but large complexities exist, as delivery varies not only based on the cargo, but also the target tissue and/or cell type of interest. Naked DNA or RNA molecules rapidly degrade in the bloodstream and have trouble reaching the intended target tissues or cell types of interest. Further, the immune system can recognize and destroy genetic cargos. Over the years, significant progress has been made towards solving this challenge with the development of viral and non-viral delivery carriers. The remainder of chapter one will focus on laying out the foundation and the building blocks of gene therapy and explain how the field has begun to tackle the challenge of delivery by utilizing lipid nanoparticle (LNP) systems.

1.2 The therapeutic potential of nucleic acids

RNA interference (RNAi) is an evolutionary conserved mechanism where double stranded RNA (dsRNA) molecules silence the post-transcriptional expression of a target gene. The discovery of RNAi completely revolutionized the biomedical research field, as RNAi has the potential to develop new therapies that can treat human disease by interfering with disease associated genes. RNAi based therapies have opened the door to new treatment avenues for patients by addressing disease targets that are otherwise “undruggable” with conventional

therapeutics.¹² 20 years after the discovery of RNAi, the FDA approved ONPATRRO (Patisran), the first siRNA drug in August 2018.¹³ The second siRNA drug, GIVLAARI (Givosiran) was approved in 2019, and a third siRNA drug, OXLUMO (Lumaisran) was approved in November 2020.¹⁴ In addition to siRNAs, mRNAs have also been developed for therapeutic use.

With the approval of mRNA vaccines to treat COVID-19, we have seen first-hand that RNA therapeutics are now a reality for the prevention of viral disease and that other RNA based therapies have great potential to treat other diseases. According to the CDC, about 260 million people have received at least one dose of a COVID-19 vaccine, where 205 million doses of Moderna mRNA COVID-19 vaccine have been administered in the United States. Overall, RNAi therapeutics are a multipurpose platform that has unlimited capacity to treat unmet clinical needs.

1.2.1 *Nucleic acids for gene mediated silencing*

Multiple types of RNAi molecules are utilized for gene silencing, such small interfering RNA (siRNA), microRNA (miRNA), short hairpin RNA (shRNA) and antisense oligonucleotides (ASO). These RNAi molecules are delivered into cells and initiate the degradation or silencing of complementary messenger RNA (mRNA) molecules (Figure1.1).

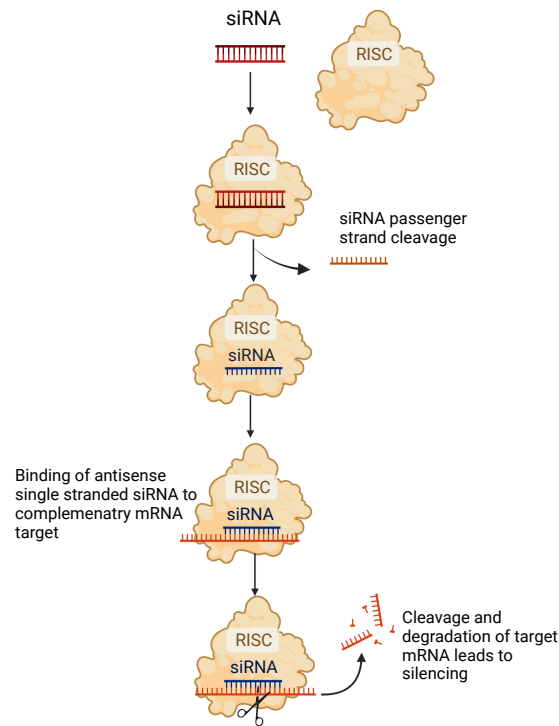


Figure 1.1. A simple illustration of the RNAi mechanism of siRNAs. Created with BioRender.com.

ASOs were one of the first molecules discovered that enabled gene mediated silencing. ASOs are short single stranded DNAs that are utilized to target a certain region of an RNA strand. In order to promote the RNAi mechanism, ASOs bind to a target RNA sequence through Watson-Crick base pairing.¹⁶ Differing from double stranded small RNAs, an ASO is delivered as a single strand and must find its target site on its own. ASOs will alter mRNA expression by a variety of mechanisms, such as cleavage of mRNAs by RNase H, direct steric blockage or modulating exons. In 1970, Zamecnick and Stephenson, pioneers of ASOs,

focused on utilizing ASOs to design a treatment strategy for Rous sarcoma virus (RSV).¹⁶ About twenty years later, the first ASO drug was approved by the FDA in 1998. The first ASO drug Fomivirsen (Vitavene) was a drug developed for treatment for human cytomegalovirus (CMV) retinitis.^{17, 18} Unfortunately, in 2006 Fomivirsen was withdrawn in the United States due to its high cost compared to similar drugs on the market. Despite the withdrawal of Fomivirsen, 10 ASO drugs have been FDA approved to date. Currently, hundreds of ASO drugs are in the clinical drug development or pre-clinical stage.¹⁷ Although ASO drugs are promising options for treatment compared to conventional small molecule drugs, concerns remain regarding adverse reactions. Mipomersen, approved in 2013, was taken off the market in 2019 due to hepatotoxicity risks. The removal of the FDA approved ASOs illustrates the importance of further understanding the molecular mechanisms underlying gene therapies.

Another class of RNA molecule that can mediate gene silencing is siRNA. siRNAs are naturally occurring noncoding RNAs. An siRNA is a chemically synthesized double stranded RNA that consists of around 21 to 23 base pairs (bp) in length and is designed to silence expression of a target gene. siRNAs can target individual genes for silencing *in vivo*. However, intravenous (I.V.) delivery of siRNA is a complex and multistep process. For example, in order for siRNAs to reach their target site, they must avoid degradation by ribonucleases (RNases) within the bloodstream or degradation by renal excretion. Once siRNAs reach their target site, the siRNA must then enter into the target cell by endocytosis. During this process, siRNA's cross the endosomal membrane and are released into the cytosol after escaping from the endosome. Once siRNAs are inside the cytosol, they will bind to and get loaded onto the RNA-induced silencing complex (RISC) for silencing of a target gene.¹⁹ The two strands of an siRNA

molecule serve as a “guide strand” and “passenger strand”. The mechanisms of siRNA gene mediated silencing is depicted in Figure 1.1. Briefly, siRNAs are incorporated into Argonaute 2 (AGO2) and the RISC. Next, the siRNA guide strand will guide RISC to the target mRNA site. Lastly, AGO2 cleaves the target mRNA leading to mRNA degradation, and silencing of the target gene.²⁰ SiRNAs offer a promising therapeutic approach to treat disease because they are highly specific and can induce silencing of target genes without disturbing endogenous mRNA pathways. However, during the delivery of siRNAs to their target sites they encounter both extracellular and intracellular barriers. A variety of chemical modifications to siRNAs may help overcome these barriers and are explained in the next section.

MiRNAs are small noncoding RNAs that function in RNA silencing by negatively regulating gene expression at the mRNA level.²¹ These endogenous small RNAs can regulate normal physiological processes and can play a role in disease.¹⁶ The first two miRNAs, *lin-3* and *let-7* were discovered in *C. elegans*.²² In 2000, the first human miRNA, *let-7* was discovered. Typically, miRNAs range from 20-25 nucleotides in length and regulate post transcriptional gene expression by targeting mRNA for cleavage or translational repression utilizing RNAi.^{16, 21} While miRNA and siRNA share similarities such as size and charge, there are distinct differences between the two. The major difference between these two types of RNA molecules is that siRNA has a specific target site for the degradation of mRNA and that miRNA molecules can have multiple target sites.²³ When the miRNA has a precise match to its target sequence mRNA degradation occurs; whereas an imperfect match leads to inhibition of mRNA expression.²⁴

Another type of RNAi molecule utilized for gene knockdown are short hairpin RNAs (shRNAs). Once inside the cell, Dicer will convert the hairpin structure of shRNA into siRNA, which then utilizes RISC to induce gene silencing. Utilizing an shRNA offers advantages over the alternatives such as fewer off target effects, ability to use viral vector carriers, and the possibility of controlling shRNA expression through an inducible or tissue specific promoters. Furthermore, if the therapeutic intention is to achieve long-term protein knockdown through the RNAi pathway, an shRNA molecule can be used.

1.2.2 *Nucleic acid therapies for protein replacement: mRNA*

Over two decades ago, the first mRNA therapeutic approach was reported by Wolff et al. when expression of an encoded protein was observed in the skeletal muscle of mice after a direct injection of in vitro transcribed (IVT) mRNA and plasmid (pDNA) into the skeletal muscle of mice.²⁵ Since mRNAs encode for a specific protein, mRNAs can be utilized therapeutically as they allow for selective introduction of a protein or up-regulation of a target protein. Clinically, mRNA has been utilized by companies such as Moderna and Pfizer-BioNTech in the development of vaccines during the SARS-Cov-2 pandemic. Both of these mRNA vaccines utilize a mRNA sequence that encodes for a portion of the SARS-Cov-2 spike protein in order to elicit production of viral neutralizing antibodies in over 92% of study participants.^{26, 27} With the approval of mRNA for use in vaccines and several ongoing clinical trials for protein replacement therapies, there is a bright future ahead in the development of mRNA-based therapeutics.

1.2.3 *Gene editing platforms*

One drawback to RNAi therapies is the need for repeated administrations, as gene silencing by siRNAs or protein replacement by mRNA is a transient process. Gene editing technologies offer advantages for therapeutics as they allow for the permanent modification of DNA at specific sites. The well-known gene editing systems are made up of CRISPR/Cas9, zinc-finger nucleases (ZFNs) and TALENs. More recently, base editors and prime editors have been added to the gene editing toolbox.

The CRISPR/Cas9 systems can either activate or repress gene expression by utilizing a guide RNA (gRNA) that guides and binds Cas9 and induces cleavage of the target DNA site. After the cleavage and DNA double stranded break, a donor repair template with homology identical to the area of double stranded cleaved DNA is introduced. DNA repair mechanisms are typically done through either a homology directed repair (HDR) or non-homologous end joining (NHEJ) repair process. NHEJ does not require a DNA template and repairs the DNA cut by joining the two ends of the double stranded break together. Through this repair pathway, there are often small insertions or deletions introduced into the break site. On the other hand, HDR is a repair mechanism that requires a template DNA and directs the accurate repair of a double stranded break. The HDR repair pathway is advantageous because it can introduce changes in a single nucleotide.

Research efforts in the gene editing field have made great process over the years and in November 2020 patients were enrolled in a clinical trial (NCT04601051) utilizing NTLA-2001, an LNP that delivers a modified sgRNA that targets the transthyretin (TTR) gene and Cas9 mRNA that encodes for Cas9 protein, which inactivates the target gene. Patients with

TTR amyloidosis, a rare and fatal disease, have a buildup of TTR protein in their livers. In the interim clinical trial results, a single dose of NTLA-2001 was able to reduce serum TTR in patients by up to 93%, compared to the 80% serum reduction with other drugs on the market that require continuous dosing. Further, serum TTR levels after NTLA-2001 were stable for up to 12 months with no reported safety concerns.²⁸ The two TTR targeting drugs currently used in the clinic are Anylam's siRNA LNP drug, ONPATPRO, and Ionis's ASO drug, Inotersen. Both current therapies reduce serum TTR around 80%, however, both siRNA and ASO are not permanent solutions and patients must receive multiple infusions of the therapy.²⁹

1.3 Efficient drug delivery is a significant barrier for effective gene therapy

Despite much research in the field, efficient targeted delivery remains a significant barrier for gene therapy. Effective gene delivery must overcome both extracellular and intracellular barriers as illustrated in Figure 1.2 and mentioned in Section 1.2.1. The extracellular barriers for delivery include reaching the target site and intracellular barriers include delivering RNA into the cytosol after escaping from the endosome. Further, efficacious carriers must enable cytoplasmic delivery of their cargos via endosomal escape before lysosomal degradation. To overcome these delivery barriers, delivery of nucleic acid cargos has relied on two main types of delivery carriers: viral and non-viral carriers.

1.4 Nucleic acids require a delivery vehicle

Despite the therapeutic potential of siRNA and mRNA, delivery remains a challenging barrier to overcome. In order to be effective, RNA must be delivered to the cytoplasm of

diseased cells *in vivo* and the field must overcome these barriers to access the full therapeutic potential of siRNA and mRNAs.

While RNAs can be delivered *in vivo* in their “naked” state, RNAs have a very short half-life *in vivo* due to rapid degradation by numerous circulating exonucleases and endonucleases in the bloodstream.¹⁴ In order to access the full potential of RNAi based machinery, nucleic acids must be able to reach the cytoplasm of their target site inside cells as shown in Figure 1.2. Due to nucleic acids’ inherent physical characteristics such as their negatively charged phosphate backbones and their high molecular weight (miRNA/siRNA ~13 kDa, mRNA >1000 kDa), nucleic acids cannot readily diffuse across negatively charged and hydrophobic cell membranes.³⁰ Due to these characteristics, nucleic acids benefit from special modifications and from the use of carriers for *in vivo* delivery applications. Other delivery challenges for RNA molecules include avoiding clearance by the kidneys, avoiding accumulation in the liver and avoiding activation of the immune system as RNAs may be recognized as foreign materials by the immune system when administered.

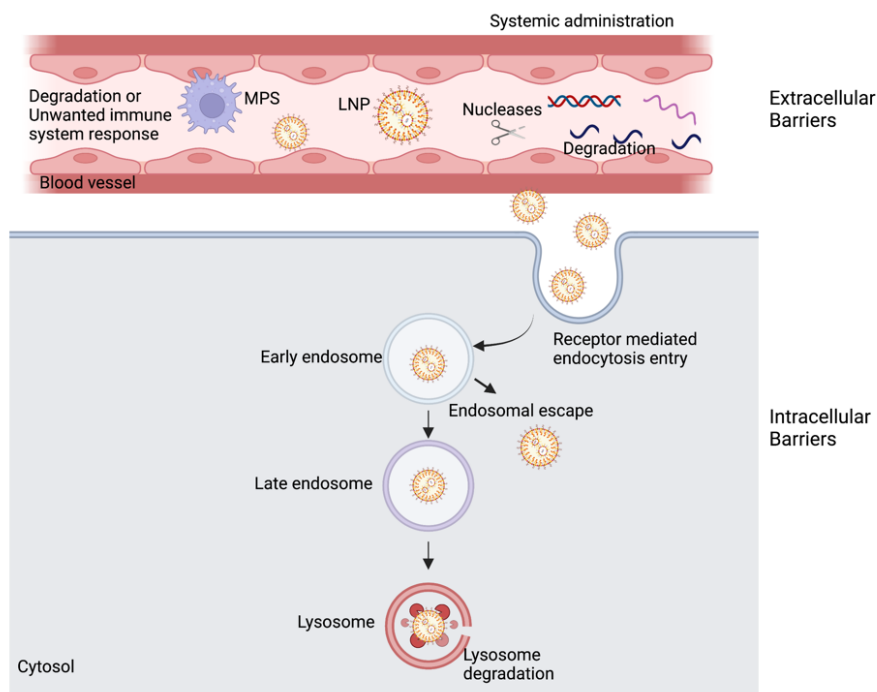


Figure 1.2. A simple illustration of the extracellular and intracellular barriers for non-viral drug delivery carriers adapted from Torres-Vanegas and created with BioRender.com.³¹

There are a wide range of chemical modifications that can be made to improve the stability, durability and potency of RNAs. Chemical modifications of nucleic acids can improve potency and selectively and are typically made to 3' or 5' ends of nucleic acids, the sugar, backbone, or nucleobase.³² To improve RNA stability, ribose modifications are typically made on the 2' OH site. Further, other common chemical modifications to RNA include a 2'-O-methyl (2'-O-Me), 2'-fluoro (2'F), and 2'-O-methoxyethyl (2'-MOE) modification.¹⁶ Once RNAs localize to their appropriate target, the next obstacle to delivery is cellular uptake. Both siRNA and mRNA are negatively charged molecules and cannot freely diffuse across the

hydrophobic cellular membrane. Cell uptake can occur through a variety of mechanisms such as receptor mediated endocytosis, caveolae mediated endocytosis, clathrin mediated endocytosis, and/or micropinocytosis.³³ For effective gene silencing or protein translation, an endocytosed RNA must escape from the endosome in order to enter the cytoplasm of the cell. Failure to escape the endosome will result in accumulation inside the lysosome, ultimately resulting in the degradation of RNA. The process of endosomal escape for siRNA and understanding how much siRNA is actually released into the cytosol of a cell is not well understood as it has been reported that only 1-2% of siRNA is released into the cytosol.³⁴

1.4.1. Viral carriers for nucleic acids

Viral vectors have been utilized for the delivery of nucleic acid cargos through the use of DNA and RNA viruses. Since viruses have a natural ability to deliver RNA into specific cells, the use of viral vectors became an exciting delivery tool for *in vivo* RNA delivery. Examples of viral carriers that deliver nucleic acids or genes into target cells through transduction include adenovirus, retrovirus, and lentivirus. Viral RNA carriers for treatments of disease such as HIV, cancer and muscular dystrophy have been researched for many years.¹ However, the use of viral delivery systems for therapeutic purposes gives rise to delivery challenges that reduce their clinical potential. For example, viral carriers demonstrate issues with immunogenicity, mutagenesis, limited loading of cargo and are costly to scale up.

Viral Delivery Systems

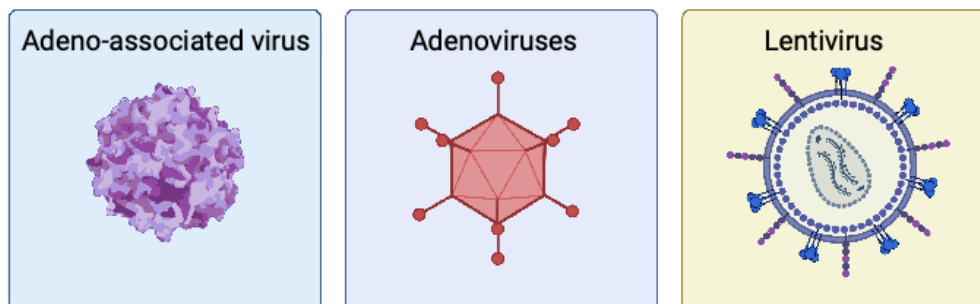


Figure 1.3. Viral delivery systems for nucleic acids created with BioRender.com.

1.4.1a Adeno-associated virus (AAV) delivery

Adeno-associated virus (AAV) are a popular viral vector as they have been used in a wide variety of clinical applications, from animal models of human disease, clinical trials and are even utilized in FDA-approved therapies.³⁵ AAVs are a type of virus that is composed of 60 copies of viral proteins VP1, VP2 and VP3 that are assembled into a capsid around the size of 25 nm. AAVs are a type of non-integrating vector that is relatively well understood and can carry cargo efficiently to a variety of relevant tissues. An important consideration when using an AAV as a carrier is to consider the size of the cargo as AAV's have a capacity of only ~5 kb.³⁶ Despite these size limitations, multiple research efforts have overcome the limitations by dividing gene editing agents into two parts. For example, each half of the gene editing material can be packaged into a separate AAV and administered simultaneously.³⁷

1.4.1b Lentiviral (LV) delivery

Lentiviruses (LVs) are single stranded RNA viruses that can accommodate up to 10 kb of a transgene, double to that of AAVs. One of the most well-known lentiviruses are from the virus HIV-1. Lentiviruses can be integrated into the host genome for the prolonged expression of a therapeutic gene.³⁸ A delivery system comprised of a recombinant lentivirus offers advantages because it can be used for either *ex vivo* or *in vivo* delivery applications.

1.4.1c Adenoviral delivery

Overall, viral vectors have been utilized for delivering gene editing agents *in vivo* across both pre-clinical and clinical studies. Adenovirus was one of the very first viral vendors used in the gene therapy field and is based on a virus that causes the common cold. Adenoviruses are non-enveloped double stranded DNA viruses that can package up to a 37 kb transgene.

1.4.2 Non-viral nucleic acid carriers

Over the last 40 years, a wide variety of non-viral carriers have been developed and tested.³² Non-viral carriers comprise a large class of materials such as lipid-based systems, polymer-based systems, peptide-based systems, and inorganic compounds. A major breakthrough in non-viral nucleic acid carriers was the approval of the first RNAi-based drug, ONPATRO, for the treatment of hereditary transthyretin-mediated amyloidosis (hATTR).³⁹ ONPATRO is a lipid nanoparticle-based formulation that encapsulates siRNA and efficiently targets the liver hepatocytes after I.V. administration to silence the transthyretin gene. The

approval of ONPATRO set the stage for other siRNA-based therapies, such as GIVLAARI (givosiran) and OXLUMO (lumaisran), as well as the COVID-19 mRNA vaccines, which utilizes similar four-component LNP system for carry the mRNA that encodes for a portion of the spike protein.¹⁴

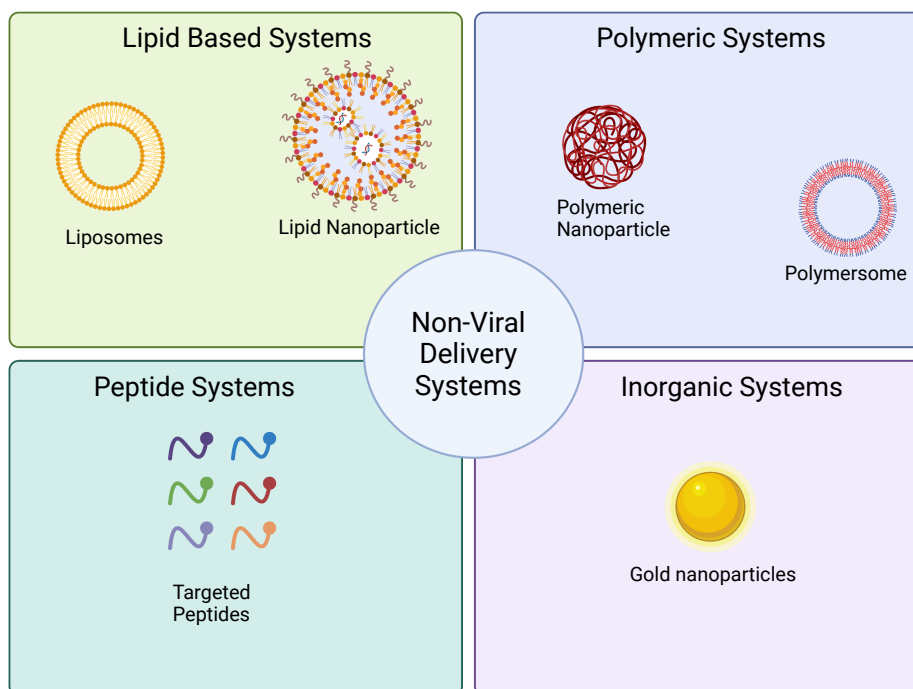


Figure 1.4 Non-Viral Delivery Systems for nucleic acids created with BioRender.com.

1.4.2a. The early generation of liposomes and lipid nanoparticles

The term “liposomes” was coined in the 1960s after researchers discovered that closed lipid bilayer vesicles form spontaneously in water.^{40, 41} Liposomes as drug carriers became quickly appreciated as a delivery carrier to combat delivery challenges present in the small molecule drug delivery field for cancer therapy. For example, a large number of the small

molecule drugs for cancer treatment exhibit low solubility in water and liposomes had the potential to improve delivery of these anticancer agents. Liposomes were one of the earliest nanomedicine delivery platforms to successfully proceed quickly from an idea into clinical application, with a large number of FDA approved therapeutics on the market today. For example, the first FDA approved liposomal drug known as Doxil was a liposome drug formulation of the anticancer drug doxorubicin, which is used to treat ovarian cancer.⁴² Since Doxil, many other liposomes continue to be used in the clinic or are at the clinical trial stage for the delivery of anticancer agents, anti-inflammatory therapies, antibiotic therapies, antifungal therapies, and other drugs as well as gene therapies.⁴³

In the 1990s, the term lipid nanoparticle was coined, and the first LNP patent filing took place a year later.⁴³ Some of the early generations of LNPs were cationic LNPs. Cationic LNPs can be divided further into two categories: liposomes prepared with cationic lipids such as DOTAP, or liposomes modified with cationic peptides.⁴⁴ Negatively charged nucleic acids are complexed by positively charged lipids or peptides to form the lipid nanocarrier with a final positive charge. However, while positively charged materials performed well *in vitro*, they had toxicity issues *in vivo*. Liposomes spontaneously self-assemble into vesicles and are made up of polar head group and non-polar tail containing phospholipids and cholesterol. Various cationic lipids such as DOTMA, DOTAP, DOPE have been utilized to form cationic liposomes by taking advantage of the electrostatic interactions between positively charged lipids and negatively charged nucleic acid cargo.^{1, 45}

1.4.2b Polymeric nanocarriers

Polymers such as dextran, chitosan, cyclodextrins or synthetic polymers such as poly-L-lysine (PLL), Polyethyleneimine (PEI), Poly(amidoamine) (PAMAM), or poly(lactide-co-glycolic acid) (PLGA) have been utilized in the formulation of polymeric nanoparticles.¹ Polymeric nanoparticles offer high advantages as a nucleic acid delivery system due to their simple method of synthesis, structural versatility, tunability scalability, high transfection efficiency, biocompatibility, and low immunogenicity.¹

1.4.2.c Peptide based carriers

Peptide based carriers are advantageous due to their sequence variety and functional diversity. In nature, there are various combinations of 20 amino acids that can result in peptides with different properties such as their 3-D conformations, polarity, hydrophobicity, electric charges, and hydrophilicity.⁴⁶ Unique peptide sequences serve as attractive siRNA delivery tools because peptide sequences can elicit various functions such as siRNA binding, membrane penetration, endosome disruption, and have targeting capabilities. In addition to natural peptide sequences, techniques such as phage and bacteria display can be utilized to create sequences that do not exist in nature. One class of peptides that have gained increasing popularity are cell-penetrating peptides (CPPs), which are able to penetrate the cell membrane and translocate into the cytoplasm.⁴⁶

1.4.2.d Inorganic based carriers

Commonly used inorganic based nanoparticles are nanocarriers such as gold nanoparticles, silica nanoparticles and iron oxide nanoparticles. Inorganic nanoparticles can be

utilized for nucleic acid delivery or utilized for imaging. Further, these types of carriers can be tuned for specific size or shapes.⁴⁷

1.5 Lipid nanoparticles (LNPs) as delivery vehicles for nucleic acids

Lipid nanoparticles are the most clinically advanced drug delivery system for RNA medicines.⁴⁸⁻⁵² In 2018, the first siRNA LNP drug, ONPATTRO, was approved by the United States Food and Drug Administration (FDA) for treating the hereditary amyloidogenic transthyretin amyloidosis following intravenous infusion. More recently, similar LNPs were used to deliver mRNA encoding for the spike protein of the SARS-Cov-2 virus to vaccinate billions of people against COVID-19 following intramuscular injection.^{26, 53} The three FDA approved LNPs share similar four-component LNP systems as shown in Figure 1.1.

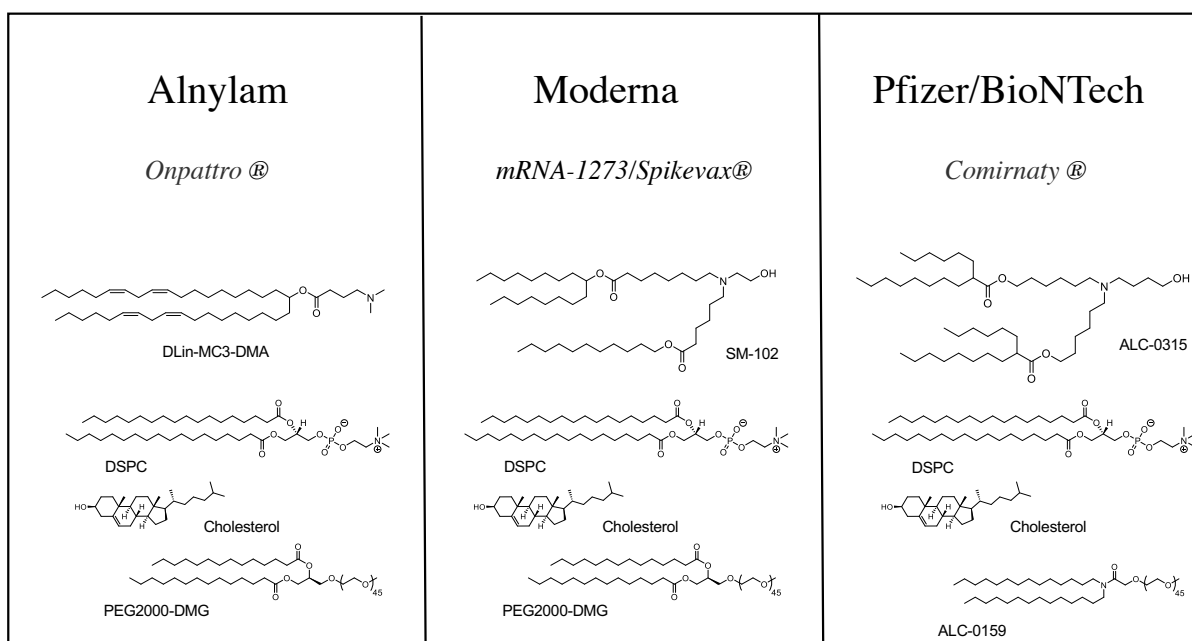


Figure 1.5. Moderna and Pfizer/BioNTech FDA approved COVID-19 vaccine utilizing LNPs share similar 4 components to ONPATTRO.

1.5.1 Lipid nanoparticles are traditionally comprised of four-components

Lipid nanoparticles have been utilized for the delivery of RNA and are traditionally composed of four components: an ionizable cationic lipid, a poly(ethylene glycol) (PEG)-lipid, cholesterol and a helper lipid as shown in Figure 1.2. LNPs are typically made using two methodologies known as lipid film rehydration and extrusion or ethanol dilution method.^{43, 54} Depending on the application, the ethanol dilution method can be done via hand-mixing, vortex-mixing or microfluidic mixing using a herringbone T junction chip. In the ethanol dilution formulation method, the RNA is dissolved in aqueous acidic buffer that is below the pKa of the cationic lipid and the lipid components are dissolved in ethanol. These two solutions are then rapidly mixed at a 3:1 ratio of acid buffer to ethanol. The rapid mixing of the two solutions allows for the initial complexation of the nucleic acids with cationic lipids via electronic interactions. During the preparation of LNP formulations, nucleic acids are first dissolved in an acidic aqueous buffer. The mixing of the acid aqueous buffer with the lipid components in ethanol promotes a charge interaction between both the ionizable cationic lipid and the negatively charged nucleic acid. Following a buffer exchange process into a pH neutral buffer, the final LNP suspension is generated with an almost neutral net charge. The uncharged state of LNPs is important in preventing recognition by the immune system as positively charged materials can contribute to toxicity. Each component within the LNP formulation serves a specific purpose and will be described in the sections below.

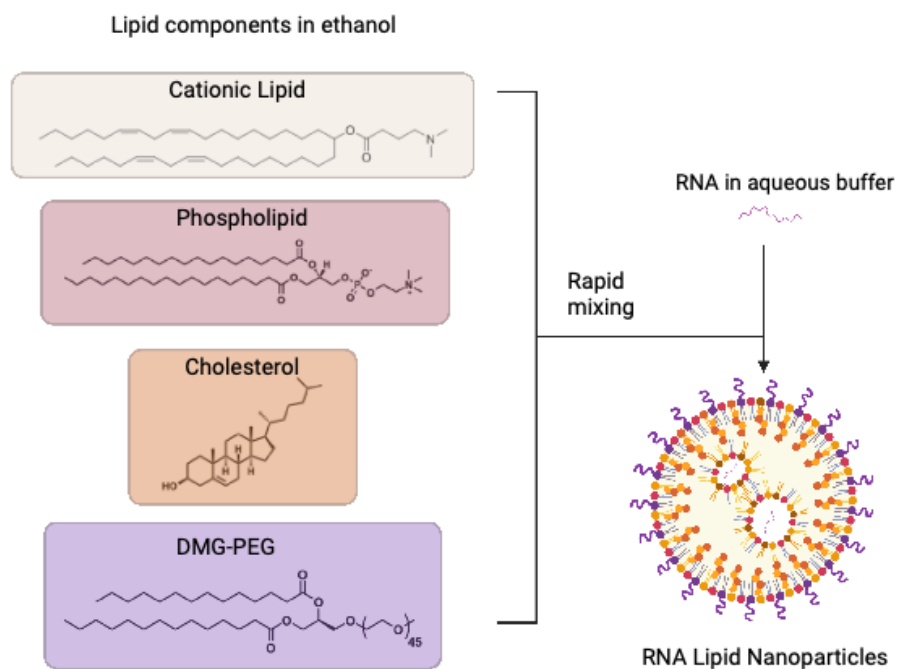


Figure 1.6. An example of a four-component LNP formation created with BioRender.com.

1.5.2 Ionizable cationic lipids

Ionizable cationic lipids were developed to overcome toxicity related issues that were occurring from the use of cationic lipids. The ionizable cationic lipid binds negatively charged nucleic acid via electrostatic interactions. While a variety of ionizable cationic lipids have been developed, the majority of ionizable cationic lipids utilized in LNPs share a few key features that are important for LNP formulation and delivery of RNAs.

All ionizable cationic lipids have a headgroup that typically contains a tertiary amine that can acquire charge and become protonated under acidic pH conditions and are typically

uncharged at physiological or neutral pH conditions. Further, ionizable cationic lipids also share lipid tail structures. Following internalization by a target cell, the protonated lipids help generate structures that assist in membrane fusion with acidified endosomes.⁵⁵ Another mechanism of endosomal escape is a process known as the “proton sponge” effect.^{56, 57} Cationic polyplexes have been suggested to undergo endosomal escape through this process by inducing osmotic swelling of the endosome by an influx of protons.⁵⁶ Another function of the ionizable cationic lipid of LNPs is to maintain positive charge in the acidified endosome and promote membrane fusion to allow for cytosolic delivery of nucleic acid cargos. Significant research efforts have been made in the LNP field in regards to the balance between these charged states for *in vivo* nucleic acid delivery.

The first FDA approved siRNA drug ONPATRO utilized an ionizable lipid known as DLin-MC3-DMA (MC3).⁵⁸ The ionizable cationic MC3 is a foundational lipid known as the gold standard and it has laid the groundwork for the development of other classes of ionizable cationic lipids and has been a key player in the future development of LNPs therapeutics.

Prior to the development of DLin-MC3-DMA (MC3), previous generations of ionizable lipids were utilized in LNPs as shown in Figure 1.6. The first generation ionizable lipid that lead to the development of MC3 was a lipid known as 2-dilinoleyloxy-*N,N*-dimethyl-3-aminopropane (DLin-DMA). DLin-DMA is an ether analog of 1,2-dioleoyl-3-(*N,N*-dimethylamino)propane (DODAP). The structure of DODAP includes oleic acid chains and is a pH-responsive ionizable lipid. After the development of DLin-DMA, subsequent studies revealed that ionizable lipids with linoleic acid chains are superior to oleic acid chains for the use of gene mediated silencing using siRNA LNPs. Through systematic research efforts

investigating the linker moiety and the head group of the ionizable lipid in DLin-DMA, a new ionizable lipid called 2,2-dilinoleyl-4-(2-dimethylaminoethyl)-[1,3]-dioxolane (DLin-KC2-DMA) was identified to have excellent *in vivo* delivery at a low dose of 0.1mg/kg siRNA when incorporated into LNPs.⁵⁸ In 2012, further optimization of the head group structure of DLin-KC2-DMA was performed, creating what is now known as MC3. LNPs containing MC3 as their ionizable cationic lipid had significantly improved gene mediated silencing in liver hepatocytes at a low dose of 0.005mg/kg of siRNA.

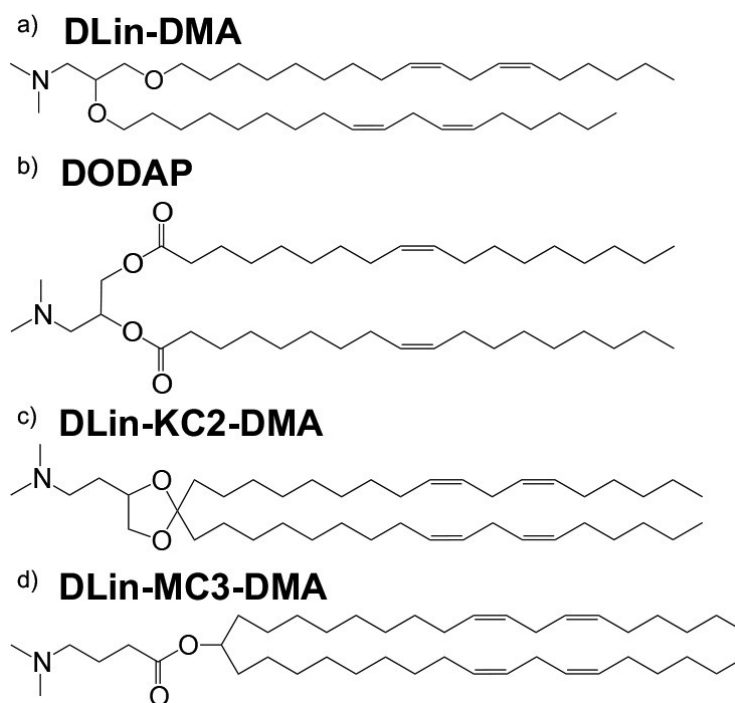


Figure 1.7 Examples of the previous generations of ionizable lipids leading to development of DLin-MC3-DMA utilized in LNPs. Figure adapted from Yonezawa et al.⁵⁹.

An important improvement of the ionizable cationic lipid formulation resulted from research on the incorporation of degradable ester linkages. In order to help introduce biodegradability, researchers incorporated degradable ester linkages into the ionizable cationic lipids where the ester linkage is stable at neutral pH but can become enzymatically hydrolyzed within tissues and cells that have a lower pH value. The incorporation of degradable ester linkages was an important consideration for *in vivo* therapy purposes.⁶⁰ Further, the pKa of the ionizable lipid has been reported to be an important parameter for the efficiency of RNA LNPs. For example, the optimal pKa range for gene silencing in hepatocytes falls within the range of 6.2-6.5.⁵⁹

Additionally, the ionizable cationic lipids utilized in the two LNP based mRNA vaccines (mRNA-1273 and BNT162b2) have structural similarities to that of the ionizable cationic lipid used in siRNA LNP ONPATRO. Both the ionizable cationic lipid SM-102 developed by Moderna and ionizable cationic lipid ALC-0315 developed by Biotech's Acuitas share a few distinct characteristics in their chemical structures. For example, both ionizable cationic lipids share a tertiary amine, ester linkages, and multibranch tail structures as shown in Figure 1.5.⁶⁰

1.5.3 PEG Lipids

The PEG-lipid component is another crucial component for the formulation of LNPs and serves a multitude of purposes. One of them is to promote stability by preventing particle aggregation, prolonging half-life in the bloodstream, and preventing immune system recognition.^{61, 62} The molecular weight of the PEG lipid as well as the molar percentage of the

PEG lipid incorporated in the LNP formulation can affect the characteristics of LNPs and its physiochemical properties. For example, work done in regards to the molar % of PEG lipid in the LNP has shown that when PEG lipid is increased from 0.25% to 5 molar %, a reduction in LNP size is observed and when this percentage increases beyond 5%, there is no longer a difference in the LNP size.^{63,64} In addition to molar percentage of PEG lipid, another important consideration when choosing an appropriate PEG lipid is the length of the acyl chain of the PEG lipid. The length of the acyl chain tail has been shown to correlate with dissociation of the PEG lipid from the LNP surface in circulation. For example, PEG lipids that are composed of 14-carbons in length dissociate rapidly from the LNP in circulation in comparison to PEG lipids with 18-carbon acyl chains which does not dissociate from the LNP in circulation.^{64, 65} PEG lipid dissociation is especially important in the context of delivery to target tissues or cells due to protein recognition that occurs when LNPs are in systemic circulation. It has been shown that PEG lipids with 14-carbon acyl chains can dissociate from the surface and aid in absorption of ApoE serum protein which plays a crucial role in recognition LDL-receptors present on the hepatocyte surface.⁵⁹ In chapter two, a systematic investigation of the chemistry of the PEG lipid and its impact on LNP formulation and RNA delivery efficacy will be discussed.

1.5.4 Helper lipids (Cholesterol and Phospholipids)

Helper lipids have been known to contribute towards the stabilization of LNPs during formulation.⁶⁶ Two examples of helper lipids utilized in four component LNPs are cholesterol and phospholipids. Cholesterol aids in membrane fusion and helps stabilize the hydrophobic

interactions within the nanoparticle. The helper lipid most commonly used for siRNA LNPs is 1,2-distearoyl-sn-glycero-3-phosphocholine (DSPC) and aids in stabilization and contributes to the nanoparticles structure.⁵⁹ The helper lipid has also been shown to be important in regards to the type of cargo for LNPs, for example, 1,2-dioleoyl-sn-glycero-3-phosphoethanolamine (DOPE) has been shown to aid in delivery of mRNA, whereas DSPC is commonly used for siRNA LNPs.⁶⁷

1.6 Routes of administration for LNPs

The fate of LNPs in the body varies depending on the design of the nanoparticle system and the route of administration. LNPs that are administered intravenously have been primarily limited to the liver organ. The unique physiochemical properties of LNPs such as particle size and surface charge are critical for RNA delivery through systemic administration.

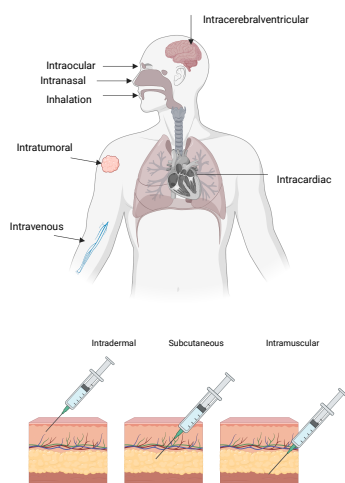


Figure 1.8. The various routes of administration for delivery adapted from Xou et al and created with BioRender.com.⁶⁸

1.6.1 The fate of systemically administered LNPs

Historically, it has been accepted that the majority of systemically administered LNPs will accumulate within the liver. LNPs have been widely restricted to liver hepatocyte delivery, however, significant progress has been made in extrahepatic delivery. Recently, work done by Cheng et al. provided explanation towards the rational design of LNPs that are capable of predictably targeting extrahepatic tissues such as the lung and spleen by an inclusion of a selective organ targeting (SORT) molecule.⁶⁹ The inclusion of a fifth component, SORT molecule, into the traditional 4-component LNP is able to achieve functional delivery to the lung and spleen. For example, inclusion of 50% DOTAP, a permanent cationic lipid, delivery is rerouted to the lung. Further, inclusion of 18PA as a sort molecule, an anionic charged lipid, delivery is shifted to the spleen.⁶⁹ Work done by Dilliard and Cheng et al. has showed that the chemical identity of the SORT molecular affects biodistribution, pKa and protein corona formation to alter the specific organ tropism for mRNA delivery.⁷⁰

While SORT and other methods of active and endogenous targeting are beginning to open the door to organ targeted delivery, the specific cellular fate of LNPs *within the organ* remains poorly defined (including in the liver).

1.7 Liver nanoparticle clearance

The liver is the largest organ in the body and has the essential role of filtering the blood. This organ has important metabolic functions as it converts nutrients from the diet to substances that cells can use. Additionally, the liver breaks down toxic substances so they can be cleared from the body. The anatomy of the liver is unique as it is divided into lobules that

are each connected and supplied by the branches of the portal vein, hepatic artery and the bile duct. It is widely accepted in the nanomedicine drug delivery field, that after administration into the body, the majority of nanoparticles do not reach their intended target and are eliminated through the kidney (if < 6 nm in size) or sequestered by the reticuloendothelial system (RES) that is also called mononuclear phagocytic system (MPS) (if > 6 nm).⁷¹⁻⁷⁴ The liver is a major clearance organ (the major part of MPS), as its role is to filter the blood, as such nanoparticles often end up within the liver as a result. However, nanoparticle delivery to liver cells, especially hepatocytes, is not as straightforward as commonly assumed.

When LNPs are administered by an intravenous injection and enter into the liver, Kupffer cells are one of the first cell types encountered.⁷⁵ The liver structure is comprised of multiple cell types, where 60-80% of parenchymal cells are hepatocytes.⁷⁵ Hepatocytes are involved in many functions such as protein synthesis, protein storage, detoxification and metabolism.⁷⁶ The remainder of the liver are the non-parenchymal cells which are comprised of Kupffer cells, sinusoidal endothelial cells, and hepatic stellate cells. Kupffer cells are an important first line of defense to foreign materials as these particular cells are tissue resident macrophages that will phagocytose and destroy pathogens and other foreign bodies and materials within the blood.⁷⁵ They are responsible for the majority of phagocytic activity within the liver tissue and make up of 80-90% of the total macrophage population within the body.^{75,}

77

1.7.1 Protein Corona and liver delivery

Once LNPs are administered into the bloodstream, the surface of lipid nanoparticles can become modified by a layer of proteins from the biological fluid, known as the protein

corona. The protein corona has been thought to define the biological identity of nanoparticles from the organ to cellular levels.⁷⁸⁻⁸⁵ Individual proteins associated with the surface of nanoparticles could serve as ligands guiding nanoparticles to specific cell surface receptors.⁸⁶ For example, it has previously been shown that Apolipoprotein E (ApoE) binds to DLin-MC3-DMA ONPATTRO LNPs and that efficacy is lost in ApoE knockout animals.⁸⁷ Thus, there is evidence that ApoE is required for receptor-mediated targeting and uptake in hepatocytes, likely by low-density lipoprotein (LDL) receptor (LDLR) that mediate cell uptake.^{78, 87} Additionally, it has been reported that ApoE plays a critical and determinate role for both uptake and clearance of nanoparticles by hepatocyte cells within the liver.⁸⁶⁻⁸⁸ One can utilize the intricacies of cell-level delivery for precise therapeutic intervention in the context of liver cancer.

1.8 Precise RNA delivery for HCC and liver disease therapy

Hepatocellular Carcinoma (HCC), the most common type of liver cancer, has poor prognosis due to diagnosis at the late stage.⁸⁹ If diagnosed early, HCC can be treated with surgery, radiation, transarterial chemoembolization, chemotherapy, and systemic therapies. However, the type of treatment a patient may receive is limited by their clinical condition and their liver function. Whenever feasible, a surgical resection of the liver tumor is the ideal method because it has the best prognosis. However, surgical resection is not always an option for patients. Conversely, the treatment of late-stage liver cancer is even more challenging because many of the current treatment options have intrinsic hepatotoxicity which can exacerbate underlying liver disease and drastically limit treatment options further. Over the

past two decades, the incidence rates of HCC in the United States have been on the rise due to an increasing number of patients with Hepatitis C virus and/or Non-Alcoholic steatohepatitis (NASH).^{90, 91} The liver can become inflamed due to a chronic liver injury as a result from various etiologies, such as Hepatitis B, NASH, or alcohol abuse. Chronic liver injury causes liver inflammation and can ultimately result in the development of cirrhosis.⁹¹ Devastatingly, the majority of HCC cases in the US occur in the presence of liver cirrhosis as patients with cirrhosis are at an even high risk for developing HCC.⁹² Overall, liver cancer is a challenging disease for therapeutic intervention because patients with liver cancer have poor liver function and drug-induced toxicity can exacerbate the compromised liver function even further.^{93, 94}

In 2007, Sorafenib was approved, thus increasing therapeutic options for patients with HCC. After the approval of Sorafenib, many other small molecule drugs for HCC failed in Phase III clinical trials and it took nearly 10 years for new systemic therapy options to come into the clinic for both first- and second-line HCC treatments.⁹³ Recently, Lenvatinib was approved as another first-line therapy while Regorafenib, Cabozantinib and Ramucirumab were approved as second-line therapies.⁹⁵⁻⁹⁷ However, Sorafenib and Lenvatinib only marginally extended patient survival by 1-2 years.^{98, 99} In addition, immunotherapies are also being investigated for the treatment of HCC.¹⁰⁰ Atezolizumab and bevacizumab are two immune checkpoint inhibitors that have been recently used as a therapy for advanced HCC in clinical studies.¹⁰¹ Atezolizumab is a checkpoint inhibitor that targets the PD-L1 pathway in order to prevent interaction with receptors PD-1 and B7-1 and bevacizumab is a monoclonal antibody that targets VEGF in order to inhibit tumor growth.¹⁰⁰⁻¹⁰²

In a recent phase Ib clinical trial, advanced HCC patients who received a combination therapy of atezolizumab plus bevacizumab had improved survival outcomes overall in comparison to patients who received sorafenib.¹⁰⁰

Nucleic acid therapies, including RNA interference, offer a promising alternative for treating liver cancer. Advantages include high efficacy, selectivity, and numerous target choices. However, delivery remains a major challenge for nucleic acid therapeutics.¹⁰³ In 2016, Mirna Therapeutics terminated its clinical trial of MRX34 (miR-34a liposome) for HCC due to adverse effects.¹⁰⁴ The failure was in part caused by nanoparticle targeting of the wrong cells, which induced an adverse immune response. MRX34 was assumed to target hepatocytes and cancer cells, but instead unexpectedly delivered to Kupffer cells. While it is important to understand organ level delivery, it is also necessary to understand delivery at the cellular level, a point underappreciated in the field. Failure of MRX34 has illustrated the importance of understanding cell level delivery of nucleic acid therapies.

Hepatocytes, which account for about 80% of liver mass, can become cancerous when mutated, and the oncogene *c-MYC* is a major driver for human HCC.¹⁰⁵ Another major cell type within the liver are the Kupffer cells (KCs) that make up approximately 80% of the total macrophage population in the entire body and around 20% of the liver nonparenchymal cells.^{106,107} KCs also have a critical role in liver damage. Once the liver is damaged, the state of the liver can quickly progress to HCC.¹⁰⁸

Currently, most of the HCC drugs on the market are based on targeting pathologic proteins through the use of recombinant proteins or antibodies. This approach is challenging because it is difficult for these methods to reach their target inside the specific cell. RNA therapy offers

great promise because RNAs can be designed to target a specific mRNA. Further, LNPs can be used to carry RNAs to specific locations inside the cell or tissue. While great progress has been made as a field in LNP delivery, there is still much to be learned on cell-specific delivery within the liver as well as other tissues. Currently, there is not a cure for HCC and it continues to be a devastating disease that affects about 1 million people worldwide every year.^{93, 95, 109.} The work described in chapter three identifies key biochemical and physical factors that impact the biofate of lipid nanoparticles and alter therapeutic outcomes in an aggressive liver cancer model.

1.9 Outlook

There is a need to understand how the chemistry of the components in lipid nanoparticle impact RNA delivery not only at the organ level but at the cellular level. The halt of Phase I clinical trial for miRNA-34a nanoparticle MRX34 illustrates that cellular tropism can have catastrophic consequences when there is delivery to unexpected cell types. This survey of the literature has provided an overall review of nucleic acid therapeutics for gene mediated silencing and other modalities that utilize RNAi. In addition, barriers for effective RNA delivery were reviewed, and the various delivery carriers for nucleic acids were discussed. Further, the need to target specific cell types was highlighted. Despite these advances, there is still a need to understand what aids in delivery to specific cells within a tissue and how this can be utilized for disease treatment.

CHAPTER TWO

THE HYDROPHOBIC DOMAN STRUCTURE OF LINEAR-DENDRITIC POLY(ETHYLENE GLYCOL) LIPIDS AFFECTS RNA DELIVERY OF LIPID NANOPARTICLES

This chapter consists of a research article written by the authors (Zhou, Johnson, et al., 2020)

2.1. INTRODUCTION

RNA therapeutics are emerging as a promising modality for the prevention and/or treatment of human diseases including cancer, genetic diseases, and infectious diseases.¹¹⁰⁻¹¹⁹ The approval of the first RNA interference drug, ONPATRO, by the FDA in August 2018 for the treatment of hereditary transthyretin-mediated amyloidosis was an important event for demonstrating the utility of RNA-based drugs.¹²⁰ There is high potential for future use of RNA-based drugs for treating a wide range of diseases.¹²¹ Various viral and non-viral delivery strategies have been developed to deliver RNA molecules ranging from small RNAs to long messenger RNAs (mRNAs).^{110, 118, 122-124} To discover suitable RNA carriers for the treatment of diseases with high liver dysfunction, we recently reported a library of >1,500 ester-based dendrimers containing ionizable amino groups that self-assemble with excipients into dendrimer-based lipid nanoparticles (DLNPs) to effectively deliver small RNAs to compromised livers.¹²⁵ The screen identified a dendrimer named 5A2-SC8, which was able to extend survival in an aggressive and challenging genetically engineered mouse model (GEMM) of *MYC*-driven liver cancer and toggle the polyploid state in the liver via delivery of

siRNAs and miRNAs.¹²⁵⁻¹²⁷ 5A2-SC8 DLNPs are multicomponent formulations that contain four-components consisting of an cationic ionizable dendritic lipid, phospholipid, cholesterol, and poly(ethylene glycol) (PEG) lipid with the optimized molar ratio of 50/10/38/2 (mol/mol).¹²⁵

The RNA delivery potency of LNPs is influenced not only by the chemical structure of each component but also the formulation composition and the cargo molecules themselves, such as short rigid small RNAs or long flexible mRNAs.¹²⁸⁻¹³⁵ For example, we determined that for long mRNA delivery, the formulation composition of 5A2-SC8 DLNPs should be optimized to a molar ratio of 5A2-SC8/DOPE/Chol/PEG lipid = 24/24/47/5 (mol/mol).⁶⁷ This formulation could deliver 1,300 nucleotide long fumarylacetoacetate hydrolase (FAH)-encoded mRNA effectively into hepatocytes of FAH knockout mice to completely normalize liver function and eliminate hepatorenal tyrosinemia type I symptoms.⁶⁷ In addition to the molar composition, the molecules themselves, such as the PEG lipid, modulate delivery efficacy.

The hydrophilic polymer, poly(ethylene glycol) (PEG), is a commonly used excipient in drug development to increase *in vivo* stability, evade recognition by the reticuloendothelial system (RES), pro-long circulation half-life, and reduce immunogenicity.^{62, 136} It has been found that the percentage of the PEG lipid has a huge impact on formulation, pharmacokinetics, pharmacodynamics, and *in vivo* delivery potency of siRNA-loaded LNPs.^{61, 65, 137-140} Without the PEG-lipid, the formulated siRNA LNPs dissociate immediately after being exposed in the blood stream and lose *in vivo* siRNA delivery potency.⁶¹ Interestingly, the high percentage of the PEG lipid substantially compromises hepatocyte gene knockdown

of siRNA lipid nanoparticles.⁶⁵ Although the chemistry of PEG lipids has been examined extensively as a critical component in the formulation of LNPs for RNA delivery, there has been little work studying the hydrophobic domains of PEG lipids beyond commercially available natural tails from natural lipids. We envisioned that the dendrimer growth chemistry previously used for the design and synthesis of ionizable dendrimers¹²⁵ could also be applied to investigation of branching within the hydrophobic domains to understand “anchoring” effects of PEG lipids.

The work included in chapter two, comprises efforts of a systematic investigation of the effect of lipid tail chemical structure on siRNA delivery of 5A2-SC8 DLNPs by synthesizing a series of linear-dendritic poly(ethylene glycol) (PEG) lipids (PEG-GnCm) with different lipid length (C8, C12, and C16) and different generations (first, second, and third) (**Figure 2.2.2**). Linear-dendritic block copolymers are exciting molecules whose unusual topology enables new chemical and biophysical properties of materials.^{141, 142} It was found that the PEG lipid tail chemical structure dramatically affects RNA delivery of 5A2-SC8 DLNPs (**Figures 2.2.4** and **2.2.5**). All PEG lipids formed nanoparticles with size from 50 to 100 nm and siRNA encapsulation up to 90%. The PEG lipid tail chemical structure did not affect nanoparticle stability, with some increase in size after 6 days. (**Figure 2.2.3**). First generation PEG lipids (PEG-G1C8, PEG-G1C12, and PEG-G1C16) and second-generation PEG lipid (PEG-G2C8) enabled 5A2-SC8 DLNPs to deliver siRNAs effectively *in vitro* and *in vivo*. 5A2-SC8 DLNPs formulated with second generation PEG lipids (PEG-G2C12 and PEG-G2C16) and all three third generation PEG lipids (PEG-G3C8, PEG-G3C12 and PEG-G3C16) lost the ability to deliver RNA *in vitro* and *in vivo*. Collectively, the data indicate that

PEG lipid tail chemical structure impacts the ability of 5A2-SC8 DLNPs to overcome the intracellular RNA delivery barriers.

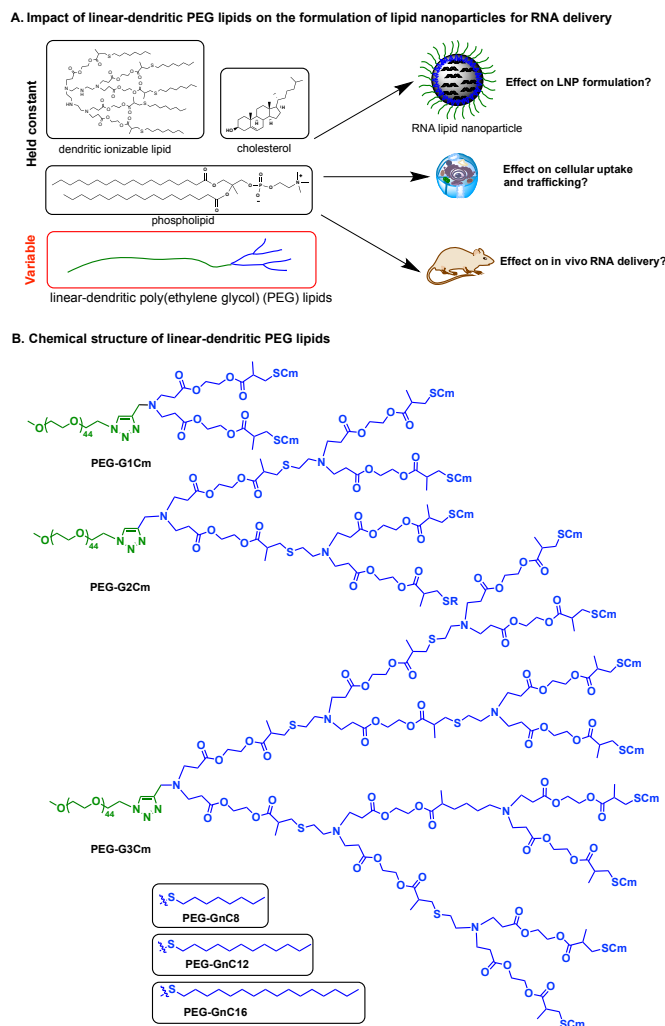


Figure 2.1.1 A systematic study on the impact of linear dendritic polyethylene glycol (PEG) lipids and RNA delivery. (A) Schematic illustration of the impact of linear dendritic polyethylene glycol (PEG) lipids on the formulation of established dendrimer-base lipid nanoparticles for small RNA delivery. (B) The chemical structure of the nine linear dendritic PEG lipids.

2.2 RESULTS AND DISCUSSION

2.2.1 Synthesis and characterization of linear-dendritic poly(ethylene glycol) (PEG) lipids

PEG-GnCm.

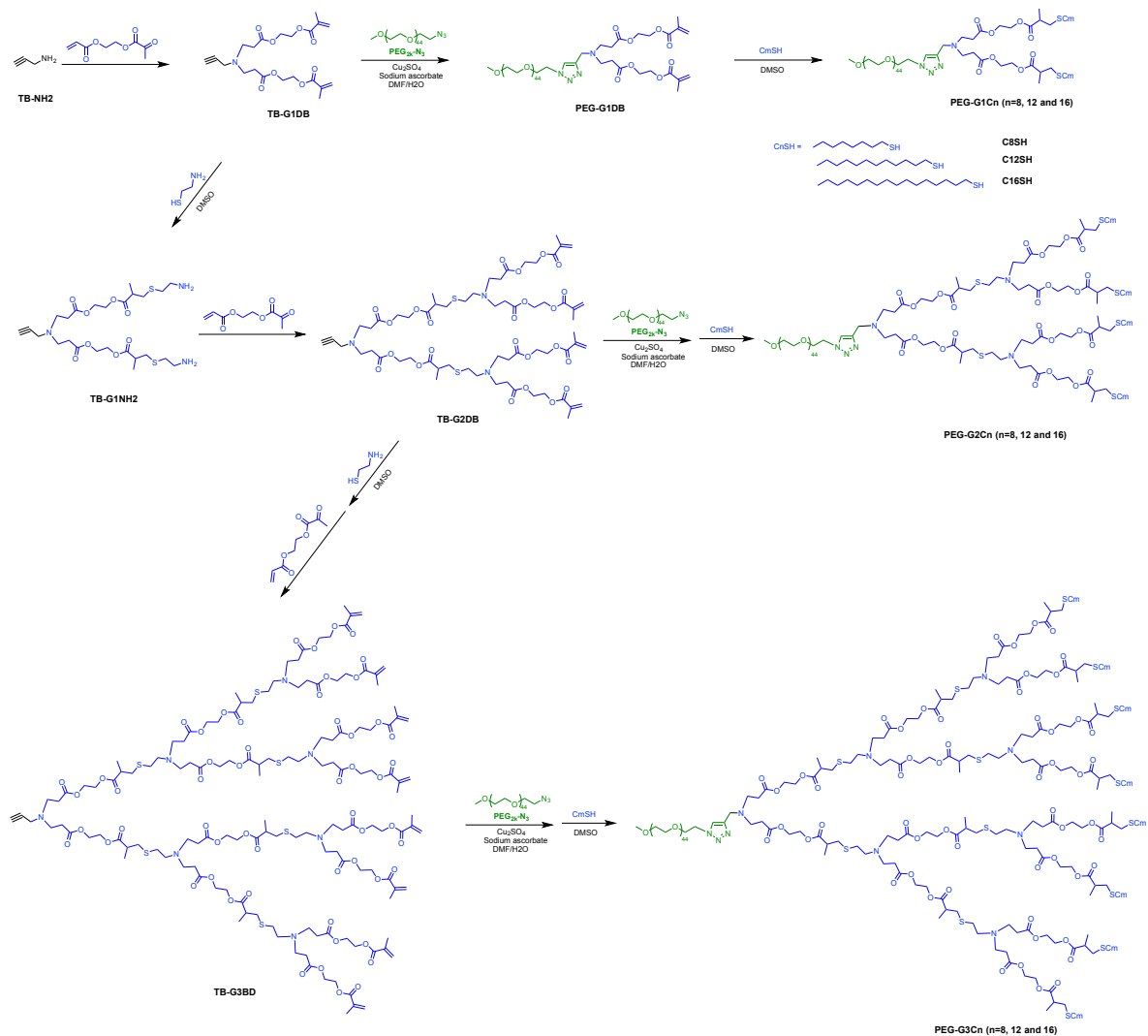


Figure 2.2.1 Chemical route for the synthesis of linear dendritic PEG lipids.

As shown in **Figure 2.2.1**, linear-dendritic poly(ethylene glycol) (PEG) lipids PEG-GnCm were prepared through three steps. First, the dendritic motifs TB-GnDB (n=1, 2, 3)

were synthesized through a strategy of using sequential aza- and sulfa-Michael additions that was used to construct a library of more than 1,500 degradable dendrimers in our previous studies.¹²⁵ Second, the above dendritic motifs TB-GnDB were conjugated with poly(ethylene glycol) azide (PEG-N₃) through copper(I)-catalyzed azide-alkyne cycloaddition to give the linear-dendritic PEG intermediates (PEG-GnDB) that contains double bonds (DB). Finally, PEG-GnDB were reacted with different alkyl thiols: 1-octanethiol (C8-SH), 1-decanethiol (C12-SH), and 1-hexadecanethiol (C16-SH), to give PEG-GnCm with different lipid length (C8, C12, and C16). The dendritic motifs TB-GnDB (n=1, 2, 3) were constructed through alternatively using two sequential orthogonal reactions: aza-Michael addition and sulfa-Michael addition. Propargylamine TB-N3 reacted quantitatively with the less sterically hindered double bond of 2-(acryloyloxy)ethyl methacrylate (AEMA) to give first generation dendrimer TB-G1DB with the more sterically hindered double bond untouched. The double bonds of TB-G1DB reacted with cysteamine via sulfa-Michael addition to give TB-G1NH₂. Then TB-G1NH₂ reacted with AEMA to give second generation dendrimer TB-G2DB. TB-G2DB led to third generation dendrimer TB-G3DB, as indicated by mass spectrometry (**Figure 2.2.2A**). TB-GnDB reacted with poly(ethylene glycol) azide (PEG-N₃) through copper(I)-catalyzed azide-alkyne cycloaddition to give PEGylated dendrimers PEG-GnDB, as indicated by the increase of molecular weight in the GPC curves. PEG-GnDB reacted with 1-octanethiol (C8-SH), 1-decanethiol (C12-SH), and 1-hexadecanethiol (C16-SH) to give PEG lipids, PEG-GnCm. After normalization to the retention time of the peaks in the GPC curves, the curves of PEG-GnCm nearly superimposed on those of PEG-GnDB and that of PEG-N₃, indicating that PEG-GnCm were uniformly synthesized (**Figure 2.2.2B-C**).

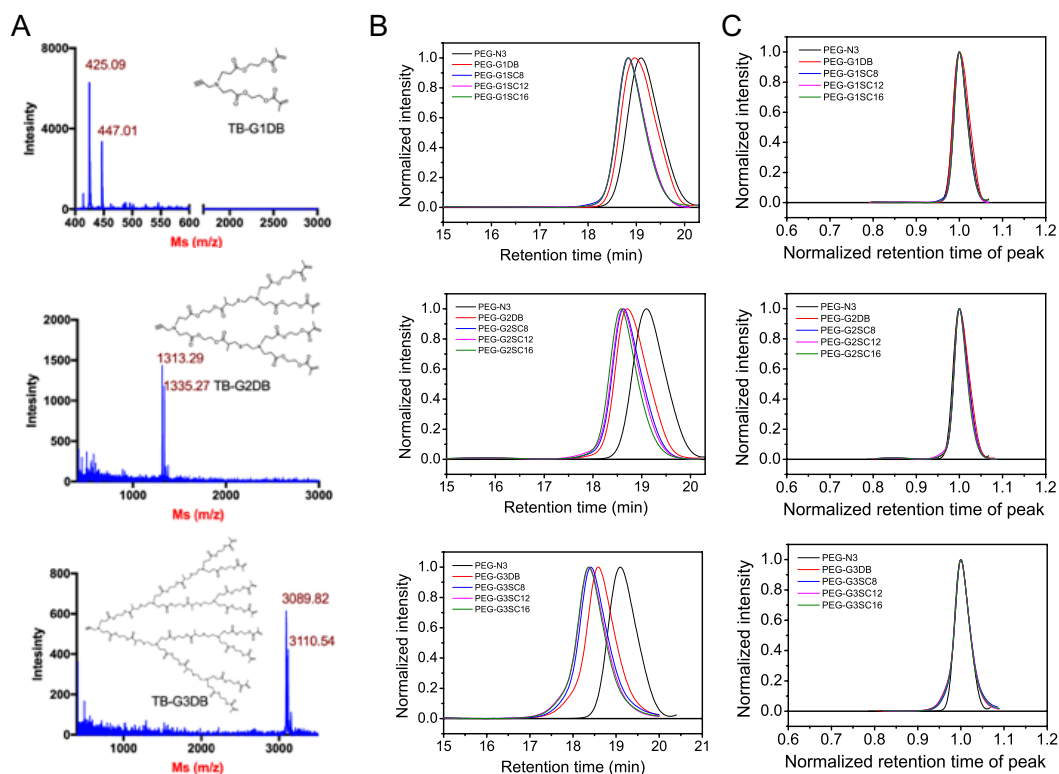


Figure 2.2.2 Characterization of nine linear dendritic PEG lipids and their synthetic precursors T3-G1DB, T3-G2DB, and T3-G3DB. (A) T3-G1DB, T3-G2DB, and T3-G3DB structures were confirmed by mass spectrometry. (B) Nine linear dendritic PEG lipids were characterized with Gel Permeation Chromatography (GPC). (C) Narrow polydispersity of nine linear dendritic PEG lipids was confirmed through normalization of their maximum retention time of the GPC curves.

2.2.2 Formulation and characterization of dendrimer-based lipid nanoparticles (DLNPs) with PEG lipids PEG-GnCm.

The ionizable and degradable amino dendrimer, 5A2-SC8, that emerged from our previous screen as being non-toxic and potent for siRNA delivery, was used to formulate

siRNA-loaded multicomponent dendrimer lipid nanoparticles (DLNPs) with the molar ratio of 50/10/38/2 (ionizable dendrimer/ phospholipid DSPC/cholesterol/PEG-GnCm). Despite having different chemical structures and molecular weight, all synthesized PEG-GnCm were able to formulate into stable 5A2-SC8 DLNPs. As shown in **Figure 2.2.3A**, 5A2-SC8 can form well-defined RNA nanoparticles across different PEG-GnCm with the size ranging from 50 to 100 nm. The formulated 5A2-SC8 DLNPs were stable for at least 11 days without visible aggregation (**Figure 2.2.3A**). Interestingly, the size of PEG-G1C8 and PEG-G2C8 5A2-SC8 DLNPs increased after eight days while the size of PEG-G3C12 and PEG-G3C16 5A2-SC8 DLNPs increased after 6 days. All the 5A2-SC8 DLNPs encapsulated siRNA molecules up to 90% across the nine different PEG-GnCm. The siRNA molecules stayed encapsulated for up to 8 days, with a slight release from PEG-G1C8 and PEG-G1C12 5A2-SC8 DLNPs after that time point (**Figure 2.2.3B**).

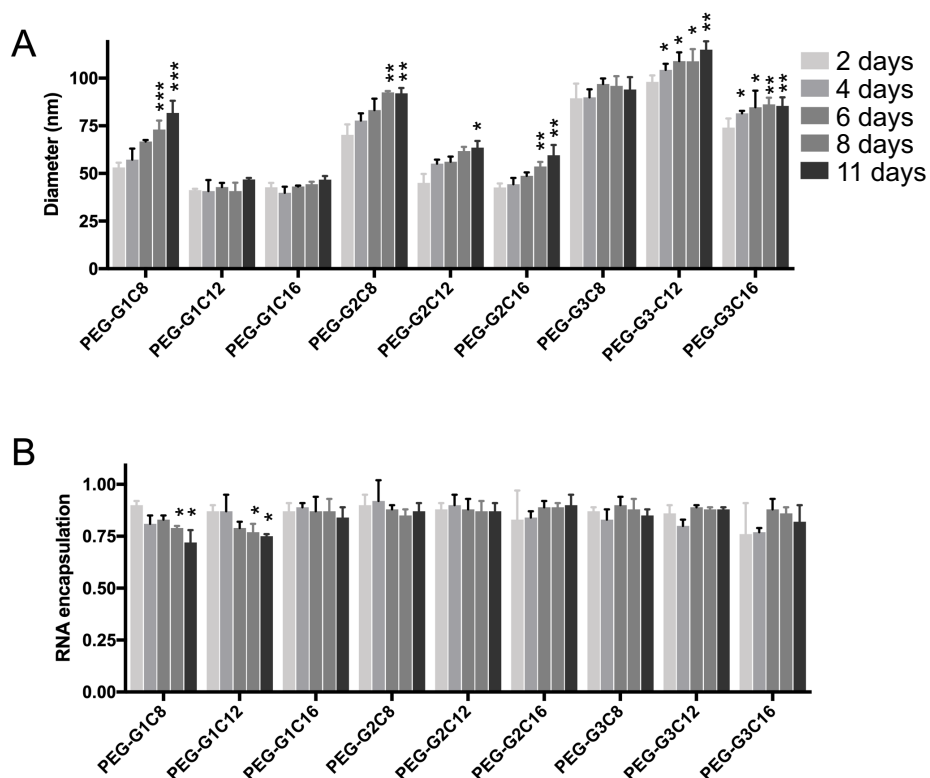


Figure 2.2.3. The PEG lipid structure does not impact LNP formulation. Time-dependent (A) size and (B) RNA encapsulation of 5A2-SC8 DLNPs formulated with nine linear dendritic PEG lipids. Stars indicate significant difference based on a comparison of the size and RNA encapsulation between the different days and second day within each of the PEG lipid 5A2-SC8 DLNPs. * $p < 0.05$, ** $p < 0.01$, and *** $p < 0.001$ (Student's two-tailed t-test).

2.2.3 *In vitro* and *in vivo* small RNA delivery of dendrimer-based lipid nanoparticles (DLNPs).

5A2-SC8 DLNPs were loaded with siLuc to enable silencing of reporter Luciferase protein. Then the nanoparticles were incubated with Luciferase-expressed HeLa cells at a

series of concentrations of siLuc from 0.7 to 66.9 nM. The PEG lipids, PEG-GnCm, dramatically affected the activity of 5A2-SC8 DLNPs for silencing Luciferase in HeLa cells (**Figure 2.2.4A**). First generation PEG lipids (PEG-G1C8, PEG-G1C12, and PEG-G1C16) enabled 5A2-SC8 DLNPs to deliver siLuc efficaciously into the Luciferase-expressed HeLa cells. The IC₅₀s were as low as 10 nM. Second generation PEG lipid (PEG-G2C8) had comparable silencing activity as PEG-G1C8 in HeLa cells. Surprisingly, the IC₅₀ values of other second generation and third generation PEG lipids increased to 66.9 nM. This indicates that the dendritic structure of PEG-GnCm had a major impact on the siRNA delivery. 5A2-SC8 DLNPs were well tolerated in HeLa cells across all different PEG lipids and broad incubation concentrations (**Figure 2.2.4B**).

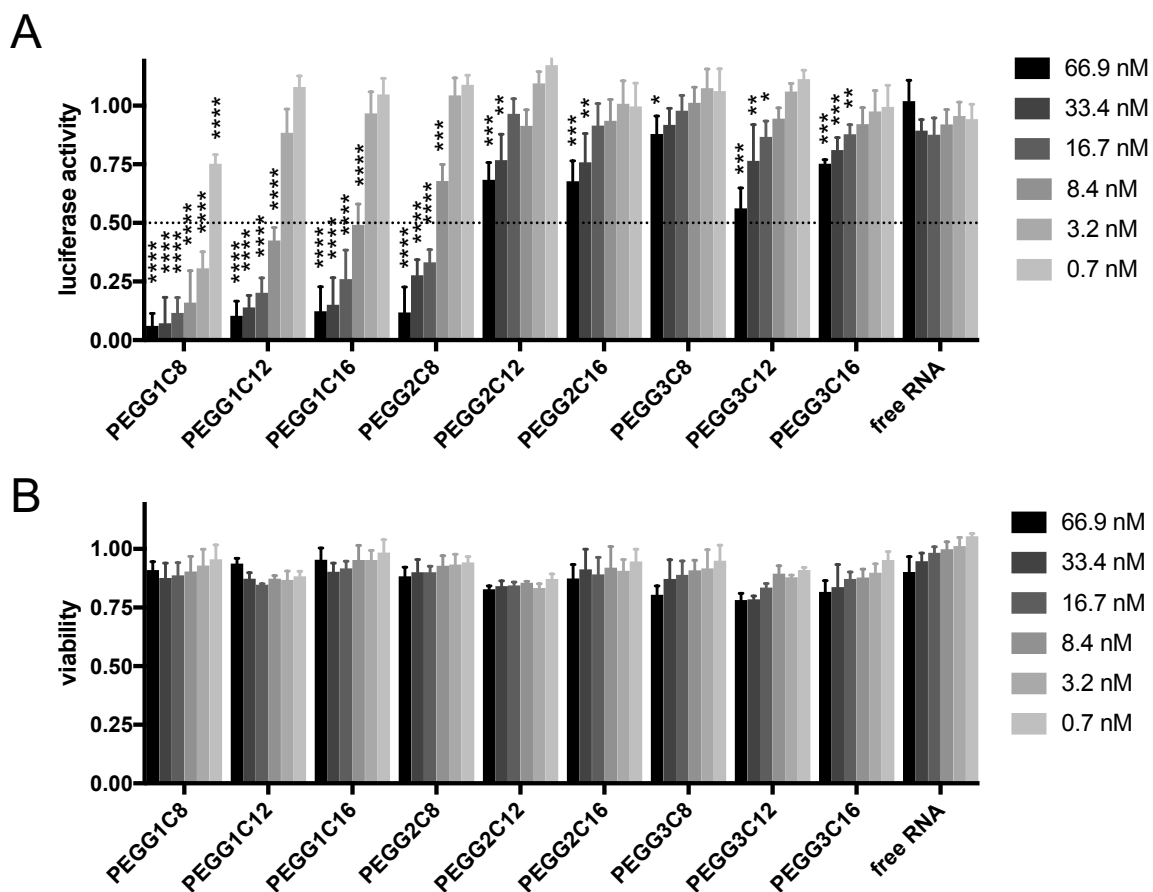


Figure 2.2.4. The dendritic structure of PEG-GnCm has an impact on the siRNA delivery efficacy *in vitro*. (A) Dose-dependent gene silencing and (B) Dose-dependent cell viability of cells treated with 5A2-SC8 DLNPs formulated with all nine linear dendritic PEG lipids. Stars indicate significant difference based on a comparison of the gene silencing and viability between each of RNA concentrations of 5A2-SC8 DLNPs and the concentration of 0.7 nM free RNA. (* $p < 0.05$, ** $p < 0.01$, * $p < 0.001$, and **** $p < 0.0001$, Student's two-tailed t-test).**

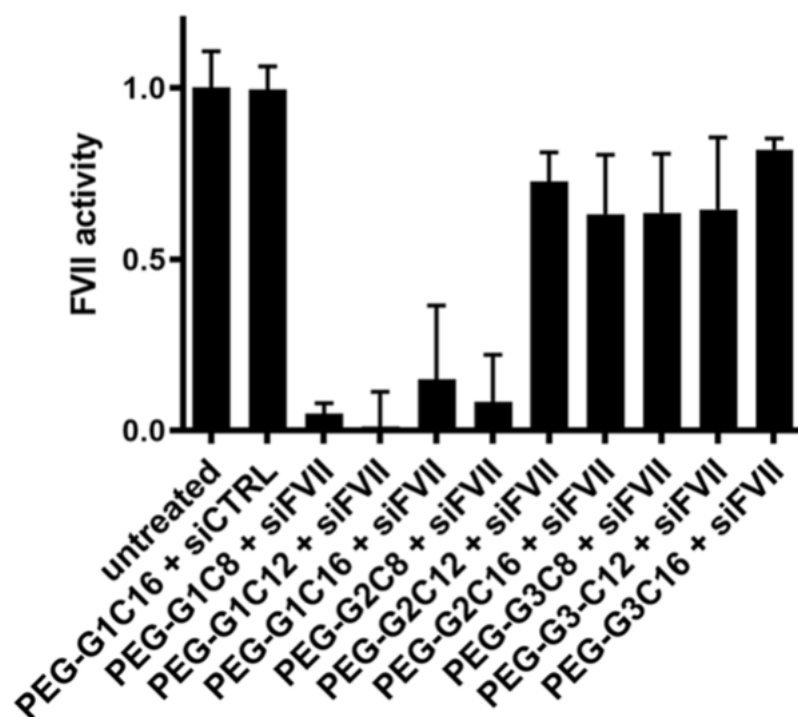


Figure 2.2.5. The dendritic structure of PEG-GnCm has an impact on siRNA delivery efficacy *in vivo*. *In vivo* FVII protein knockdown efficacy of 5A2-SC8 DLNPs formulated with nine linear dendritic PEG lipids (n=3). siCtrl-loaded PEG-GC16 5A2-SC8 DLNPs were evaluated for the control (n=3).

To assess the *in vivo* siRNA delivery of DLNPs with different PEGGn-Cm, we used the Factor VII (FVII) gene silencing assay that monitors the FVII protein, a blood-clotting factor produced in hepatocytes and secreted into the blood circulation, because this can be readily quantified from a small serum sample. 5A2-SC8 DLNPs were formulated with an siRNA against FVII (siFVII) and injected intravenously into mice at a dose of 0.5 mg/kg siRNA. FVII activity was quantified 3 days post injection. We found that the PEG lipids have the similar trend *in vitro* and *in vivo* impacting siRNA delivery of DLNPs (**Figure 2.2.4 and**

Figure 2.2.5). First generation PEG lipids (PEG-G1C8, PEG-G1C12, and PEG-G1C16) enabled 5A2-SC8 DLNPs to deliver siFVII efficaciously into the hepatocytes in the liver, while DLNPs formulated with second and third generation PEG lipids could not silence the FVII expression (except PEG-G2C8). We also formulated PEG-G1C16 5A2-SC8 DLNPs with control siRNA (siCTRL) and performed the FVII assay. No FVII gene silencing was observed, further supporting on target efficacy of siFVII DLNPs. The above data for siRNA delivery collectively indicated that the chemical structure of the dendritic block resulted in an almost binary effect on the siRNA delivery of 5A2-SC8 DLNPs.

2.2.4 Examination of endosomal escape for dendrimer-based lipid nanoparticles (DLNPs) containing different PEGGnCm.

Efficacious RNA delivery requires overcoming a series of extracellular and intracellular barriers. According to the above data, the PEG lipids have the similar trend in impacting both *in vitro* and *in vivo* delivery of 5A2-SC8 DLNPs. It led us to conclude that PEG lipids affect the RNA delivery of the 5A2-SC8 DLNPs through affecting the ability of the 5A2-SC8 DLNPs to overcome intracellular barriers. To test this, we investigated cellular uptake, hemolysis, and lysosome colocalization of 5A2-SC8 DLNPs formulated with different PEGGnCm. HeLa cells were incubated with 5A2-SC8 DLNPs that were formulated with Cy5.5-labeled siLuc. Cellular uptake was evaluated 24 hours after incubation using confocal microscopy imaging. We found that all 5A2-SC8 DLNPs across the nine different PEG lipids were internalized into the HeLa cells with similar average fluorescence intensity (**Figure 2.2.6**). This indicates that the PEG lipid chemical structure did not impact the cellular uptake

of the 5A2-SC8 DLNPs. We next focused on endosomal escape, which is one of the key intracellular RNA delivery barriers. We analyzed the lysosome colocalization of 5A2-SC8 DLNPs inside of HeLa cells. No significant difference of lysosome colocalization of 5A2-SC8 DLNPs was observed across the nine different PEG lipids after 24 hours.

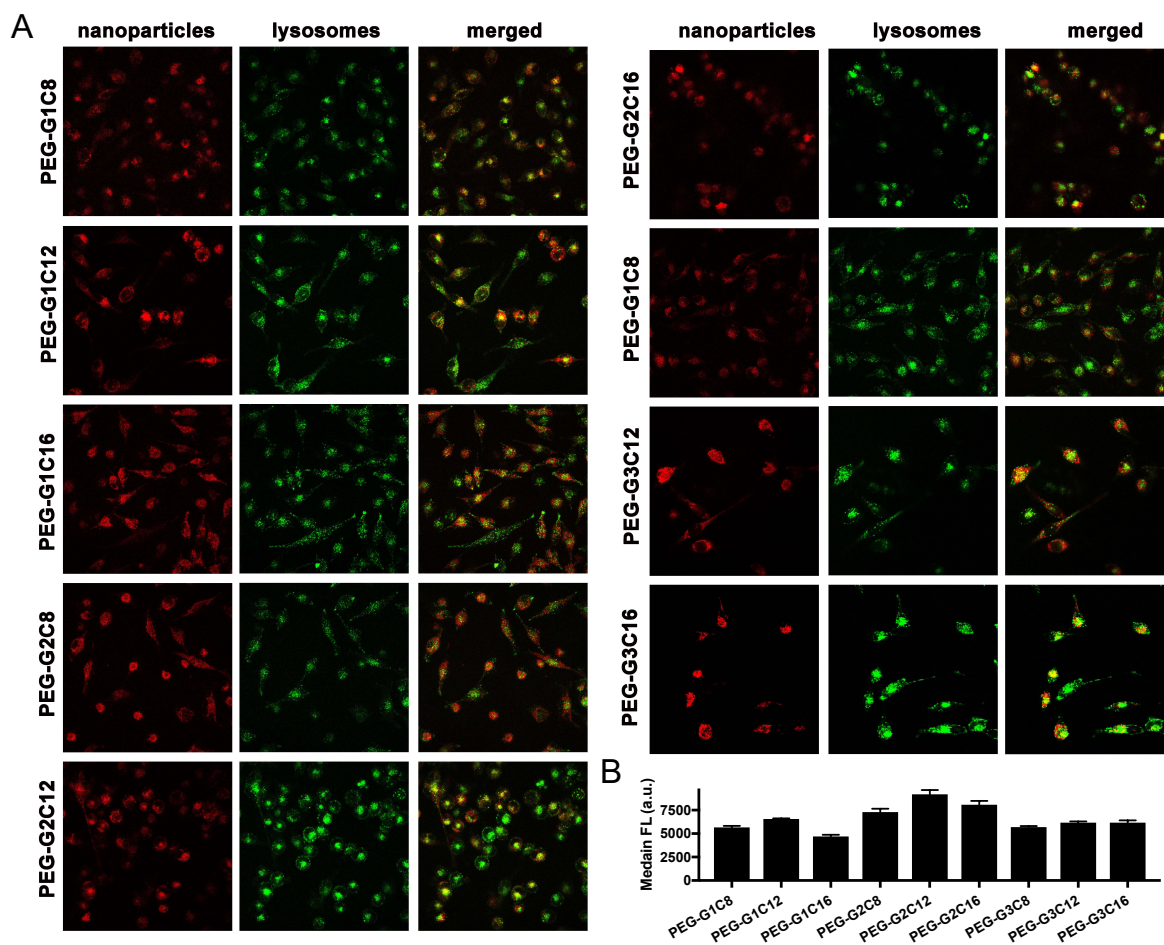


Figure 2.2.6. 5A2-SC8 DLNPs formulated with varying PEG lipid structures effectively internalize into HeLa cells. (A) Confocal images of cellular uptake into HeLa cells. (B) The mean fluorescence signal of 5A2-SC8 DLNPs formulated with nine PEG-lipids after 24-hour incubation in HeLa cells.

To further examine whether the PEG lipids could affect the ability of 5A2-SC8 DLNPs to escape from endosomes, three PEG lipids: PEG-G1C16, PEG-G2C12, and PEG-G3C12 were chosen for further study. These DLNPs were chosen because the three PEG lipids form similar 5A2-SC8 DLNPs that had distinct *in vitro* and *in vivo* RNA delivery potency. We first assessed the stability of PEG-G1C16, PEG-G2C12, and PEG-G3C12 5A2-SC8 DLNPs at the conditions of 20% FBS at 37 °C temperature with pH at 6.5, 6.0, and 5.0, respectively, by mimicking the pH conditions of early endosomes, late endosomes, and lysosomes.^{143,144} It was found that PEG-G1C16, PEG-G2C12, and PEG-G3C12 5A2-SC8 DLNPs were stable up to 48 hours and there was no significant difference of 5A2-SC8 DLNP stability across these conditions (**Figure 2.2.7**).

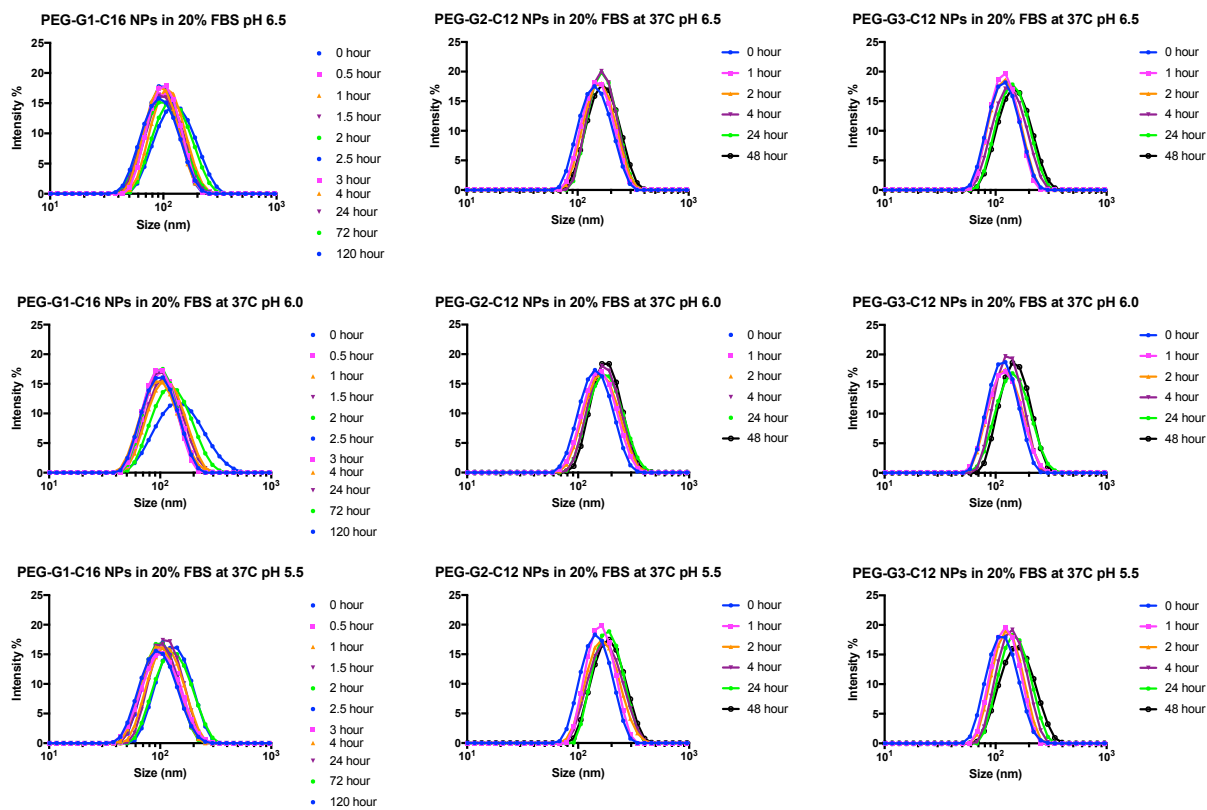


Figure 2.2.7. PEG-G1C16, PEG-G2C12 and PEG-G3C12 5A2-SC8 DLNPs remain stable under endosome mimicking conditions. The size of PEG-G1C16, PEG-G2C12 and PEG-G3C12 5A2-SC8 DLNPs was measured over time after incubation in 20% FBS with pH at 6.5, 6.0, and 5.0, respectively.

Next, the hemolysis of PEG-G1C16, PEG-G2C12, and PEG-G3C12 5A2-SC8 DLNPs was assessed at different pH values and concentrations. It was observed that these nanoparticles led to high hemolysis at pH 5.5 as the concentrations increased (**Figure A1**). There was no significant difference of hemolysis between PEG-G1C16, PEG-G2C12, and PEG-G3C12 5A2-SC8 DLNPs. Afterwards, the lysosome colocalization with of the PEG-

G1C16, PEG-G2C12, and PEG-G3C12 5A2-SC8 DLNPs with different incubation times: 4 and 24 hours was examined. The nanoparticles were still formulated with Cy5.5-labeled siLuc. Results indicated that with the 4-hour incubation, PEG-G1C16 5A2-SC8 DLNPs had significantly less lysosome colocalization than both PEG-G2C12 and PEG-G3C12 5A2-SC8 DLNPs (**Figure 2.2.8**). Interestingly, there was no difference of the lysosome colocalization between PEG-G1C16, PEG-G2C12 and PEG-G3C12 5A2-SC8 DLNPs when the incubation was extended to 24 hours. Comparison of the 4- and 24-hour time points indicated that PEG lipids did not impact the cellular uptake of 5A2-SC8 DLNPs. However, the anchoring part of these PEG lipids has a significant impact on siRNA escape from the endosomes at the early cell incubation time points, which explains the difference in efficacy. Since the low generation PEG lipid, PEG-G1C16, had significantly lower lysosomal colocalization at early time points compared to PEG-G2C12 and PEG-G3C12, we speculate that higher generation PEG lipids (PEG-G2C12 and PEG-G3C12) are less likely able to escape the endosomes and release siRNA due to chemical structures and greater hydrophobicity. The combined observations of gene silencing and early time point endosomal escape with varying PEG lipid DLNPs allowed us to identify a structure activity relationship (SAR) between PEG lipid length/ chemical composition and siRNA delivery efficacy. Due to the weak anchoring of PEG-G1C16 with 5A2-SC8 DLNPs, we can consider that there is a faster detaching of PEG-G1C16 from 5A2-SC8 DLNPs and this destabilization would enhance the endosomal escape.^{87, 120, 145}

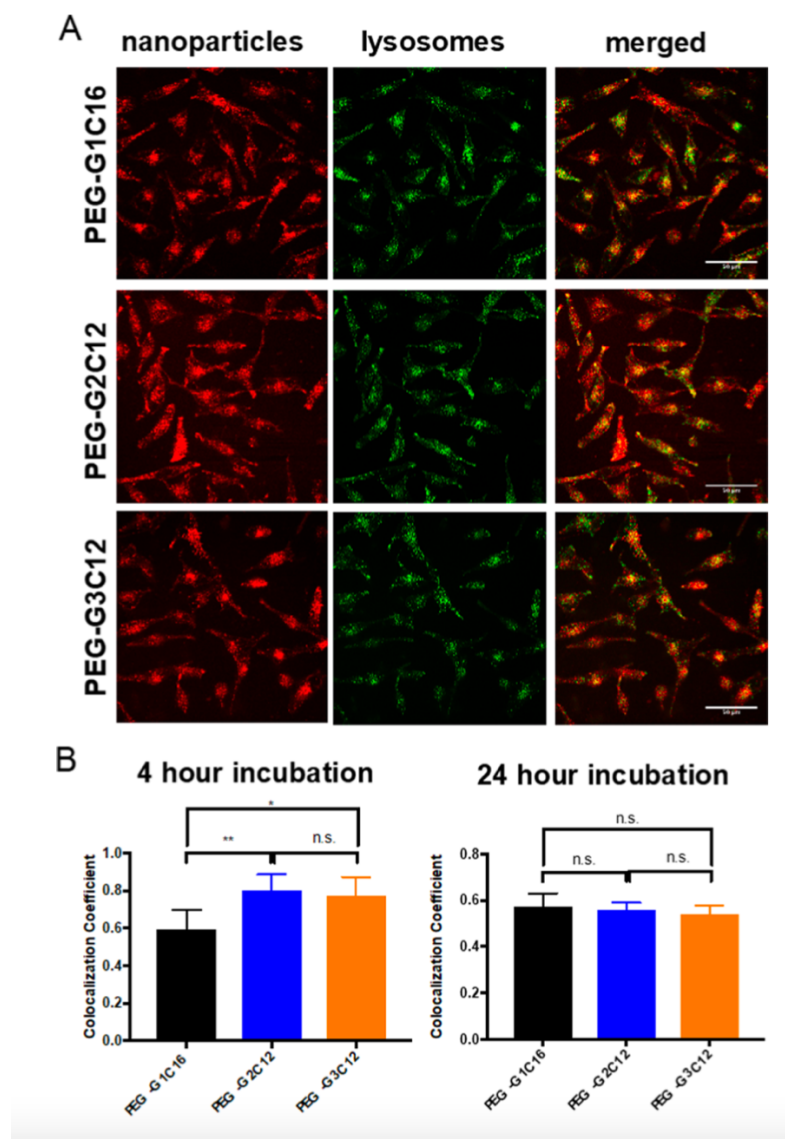


Figure 2.2.8. The hydrophobic domain of the PEG Lipid impacts endosomal escape at early time points. (A) Representative confocal images of cellular uptake of 5A2-SC8 DLNPs following 4-hour incubation. Scale bar = 50 μ m. (B) Analysis of colocalization between 5A2-SC8 DLNPs and lysosome organelles with 4- and 24-hour incubation. Statistical significance was calculated between the different groups with Student's two-tailed t-test. n.s. non-significant, * $p < 0.05$, ** $p < 0.01$, and *** $p < 0.001$.

2.2.5 In vivo small RNA delivery of the dendrimer-based lipid nanoparticles (DLNPs) in tumors.

Encouraged by the finding that the PEG lipids affect the RNA delivery of the 5A2-SC8 DLNPs to the liver through altering the ability of the 5A2-SC8 DLNPs to escape from endosomes, we wanted to examine the siRNA delivery capability of the PEG-G1C12 and PEG-G2C12 5A2-SC8 DLNPs in a cancer model as a potential therapeutic application. Subcutaneous tumor xenografts were formed in immunocompromised mice using HeLa-Luc cells, an aggressive type of cervical tumor. The mice were injected intravenously with the PEG-G1C12 and PEG-G2C12 5A2-SC8 DLNPs formulated with siLuc at the dosage of 1 mg/kg. We normalized the luciferase signal to that of day 0 when the mice were treated with 5A2-SC8 DLNPs because the tumors grew every day (**Figure 2.2.9A**). With no treatment, the luciferase signal of the tumor increased from day 0 to 2 due to the tumor growth. With the treatment of PEG-G2C12 5A2-SC8 DLNPs that cannot deliver siRNA effectively, the luciferase signal of the tumor also increased (similar to control animals). With the treatment of PEG-G1C12 5A2-SC8 DLNPs that can deliver siRNA effectively, the luciferase signal of the tumor was decreased at day 2. The luciferase signal was normalized to the luciferase signal of mice with no treatment to minimize the effect of the fast tumor growth that led to the increase of tumor luciferase signal (**Figure 2.2.9C**). The results indicated that the luciferase signal of the tumor decreased at day 1 after the treatment of PEG-G1C12 5A2-SC8 DLNPs while the luciferase signal of the tumor did not change after the treatment of PEG-G2C12 5A2-SC8 DLNPs. It is important to note here that the tumor xenograft tumors in the study grow rapidly and thus new cells being generated also express luciferase. Due to this fact, we adjusted the

analysis of luciferase in the tumors as explained above. In contrast to our other *in vivo* study, hepatocyte growth is slower and the FVII protein expression is relatively constant, thus it is easier to measure the decreased levels of FVII protein.

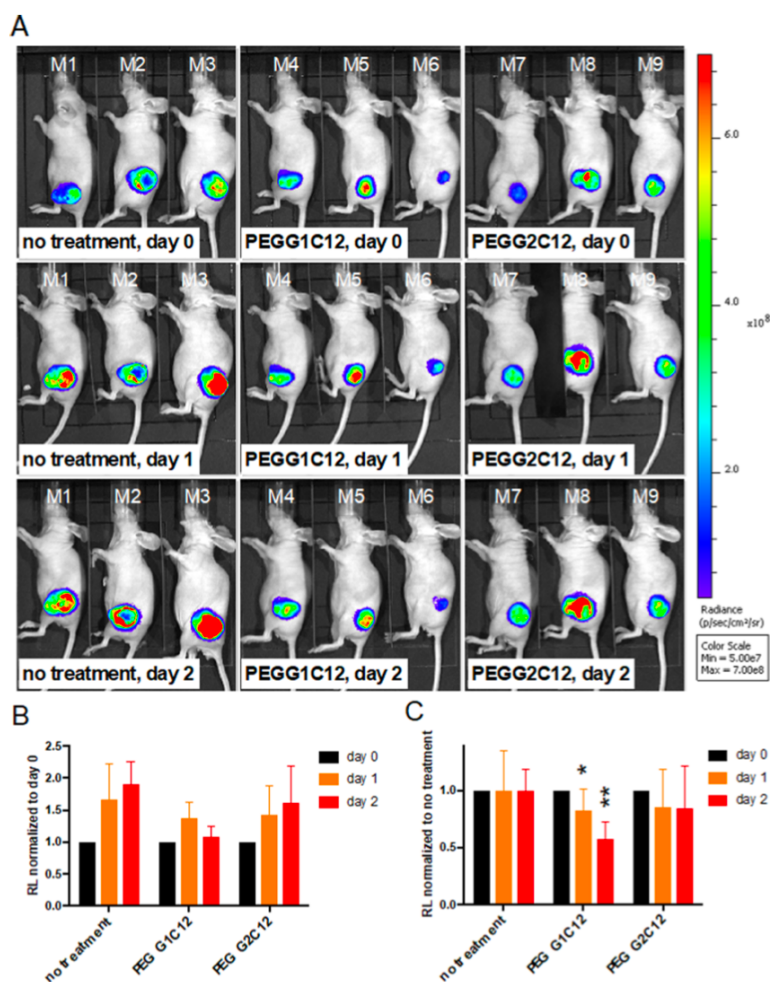


Figure 2.2.9 The siRNA delivery capability of the PEG-G1C12 and PEG-G2C12 5A2-SC8 DLNPs evaluated in a cancer model (A) Luciferase signal of HeLa-Luc xenograft tumors 0, 1, and 2 days after the intravenous injection of PEG-G1C12 or PEG-G2C12 5A2-SC8 DLNPs formulated with siLuc (1 mg/kg siLuc). (B) Normalization of the luciferase signal to that of day 0 when the mice were treated with 5A2-SC8 DLNPs (n =3). (C) Further

normalization of the luciferase signal to that of the untreated mice. Stars indicate significant difference based on a comparison of the luciferase knockdown between the treated groups and untreated groups. * $p < 0.05$ and ** $p < 0.01$ (Student's two-tailed t-test)

To address potential off target effects, the delivery of control siRNA in PEG-G2C12 5A2-SC8 DLNPs to HeLa-Luc cells was evaluated and it was observed that no off-target toxicity or off-targeting gene silencing occurred (**Figure A2**). This is in agreement with our prior application of 5A2-SC8 DLNPs to deliver siRNAs to mediate gene silencing in healthy mice,^{125, 127} multiple cancer models with therapeutic siRNA/miRNA sequences to extend survival,¹²⁵⁻¹²⁷ and mRNA encoding for functional proteins.⁶⁷ The data collectively indicates that PEG lipids affect the RNA delivery of the 5A2-SC8 DLNPs not only to the liver, but also to tumors.

2.3 EXPERIMENTAL SECTION

2.3.1 Materials. All amines, thiols, and otherwise unspecified chemicals were purchased from Sigma-Aldrich. 1,2-distearoyl-sn-glycero-3-phosphocholine (DSPC) was purchased from Avanti Lipids. 2-(acryloyloxy)ethyl methacrylate (AEMA) was synthesized according to our previous reports and purified by distillation under reduced pressure.¹²⁵ 5A2-SC8 dendrimer was synthesized following our established method.¹²⁵ mPEG-N₃ ($M_n = 2000$ g/mol) were purchased from Jenkem Technology. All organic solvents were purchased from Fisher Scientific and purified with a solvent purification system (Innovative Technology). The One

Glo + Tox assay kit was purchased from Promega. The lysotracker was purchased from Life technology. The FVII assay kit was purchased from Hyphen Biomed.

2.3.2 Characterization. ^1H and ^{13}C NMR were performed on a Varian 500 MHz spectrometer. MS was performed on a Voyager DE-Pro MALDI TOF. Flash chromatography was performed on a Teledyne Isco CombiFlash Rf-200i chromatography system equipped with UV-vis and evaporative light scattering detectors (ELSD). The molecular weight was measured by Gel Permeation Chromatography (GPC) (Viscotek) equipped with RI detection and ViscoGEL I-series columns (Viscotek I-MBLMW-3078) using DMF as the eluent at 0.75 mL/min and 45 °C. Particle sizes and zeta potentials were measured by Dynamic Light Scattering (DLS) using a Malvern Zetasizer Nano ZS (He-Ne laser, $\lambda = 632$ nm).

2.3.3 Methods

2.3.3.1 Synthesis of first, second, and third generation dendrimers TB-GnDB. The dendrimers TB-GnDB were prepared according to the previous method. Propargylamine TB-NH₂ (2.4 mL, 37.4 mmol) reacted with three equivalents (20.6 g, 112.2 mmol) of 2-(acryloyloxy)ethyl methacrylate (AEMA) in the presence of 5 mol% radical inhibitor BHT at 50 °C for 24 hours. The reaction was purified by column chromatography with the eluent of Hexane and Ethyl Acetate to give the clear product, the first generation dendrimer TB-G1DB (yield: 86%). As to the synthesis of second generation dendrimer TB-G2DB, TB-G1DB (13.5 g, 32 mmol), was dissolved in 20 mL DMSO and then 2-aminoethanethiol (6.0 g, 77 mmol) was

added. The reaction was stirred at room temperature for 30 min. Then 400 mL dichloromethane was added into the reaction solution and was washed with cold brine water (50 mL \times 3) to remove extra 2-aminoethanethiol. The organic phase was dried with magnesium sulfate and condensed via rotary evaporation to use directly for next step. AEMA (35 g, 192 mmol) and 5 mol% radical inhibitor BHT was added. After the reaction was complete, the reaction was purified by column chromatography with the eluent of Hexane and Ethyl Acetate to give the clear products TB-G2DB (yield: 74%). As to the synthesis of third generation dendrimer TB-G3DB, TB-G2DB (10.5 g, 8 mmol) was dissolved in 20 mL DMSO and then 2-aminoethanethiol (3.0 g, 38 mmol) was added. The reaction was stirred at room temperature for 30 min. Then 400 mL dichloromethane was added into the reaction solution and was washed with cold brine water (50 mL \times 3) to remove extra 2-aminoethanethiol. The organic phase was dried with magnesium sulfate and condensed via rotary evaporation to use directly for next step. AEMA (13 g, 72 mmol) and 5 mol% radical inhibitor BHT was added. After the reaction was complete, the reaction was purified by column chromatography with the eluent of Hexane and Ethyl Acetate to give the clear products TB-G3DB (yield: 63%).

2.3.3.2 Synthesis of linear-dendritic poly(ethylene glycol) (PEG) lipids PEG-GnCm.

PEG lipids PEG-GnCm were synthesized by two step reactions: TB-GnDB reacted with poly(ethylene glycol) azide (mPEG-N₃) through copper(I)-catalyzed azide-alkyne cycloaddition to give PEG-GnDB and then PEG-GnDB reacted with 1-octanethiol (C8-SH), 1-dodecanethiol (C12-SH), or 1-hexadecanethiol (C16-SH) through sulfa-Michael addition. Here is the description of syntheses of PEG-G1DB and PEG-G1C16. mPEG-N₃ (4.0 g, 2.0

mmol), TB-G1DB (0.27 g, 3.0 mmol), sodium ascorbate (30 mg, 0.15 mmol) and CuSO₄ (16 mg, 0.1 mmol) were added a flask with 10 mL oxygen-free DMF and 5 mL oxygen-free deionized water. The reaction was stirred at room temperature overnight. 300 mL DCM was added into the reaction solution and the organic phase was washed with brine (50 mL × 3) and dried with magnesium sulfate. After the solvent was removed, the residual was purified by running silica column with a gradient eluent of DCM and methanol to give a white solid PEG-G1DB (3.1 g, 64%). PEG-G1DB (1.0 g, 0.41 mmol) was dissolved in 5 mL DMSO. Then 1-hexadecanethiol (378 μL, 1.23 mmol) and DMPP (8.7 μL, 62 μmol) was added and the reaction was stirred at 60 °C for 48 hours. 300 mL DCM was added into the reaction solution and the organic phase was washed with brine water (50 mL × 3) and dried with magnesium sulfate. After the solvent was removed, the residual was purified running the silica column with a gradient eluent of DCM and methanol to give a white solid PEG-G1C16 (0.81 g, 67%)

2.3.3.3 Formulation of DLNPs. 5A2-SC8 DLNPs were prepared using a microfluidic mixing instrument with herringbone rapid mixing features (Precision Nanosystems NanoAssemblr). Ethanol solutions of dendrimer, DSPC, cholesterol, and PEG-GnCm (molar ratio of 50:10:38:2) were rapidly combined with acidic solutions of siRNA (citrate buffer, pH 3.8) at a ratio of the aqueous solution to the EtOH solution of 3/1 by volume and a flow rate of 12 mL/minute. The DLNPs were purified by dialysis in sterile 1X PBS with 3.5 kD cut-off and the size was measured by Dynamic Light Scattering (DLS) prior to *in vivo* studies. siRNA encapsulation was measured using the Ribogreen binding assay (Invitrogen) by taking the small amount of solution and following the manufacturer's protocol.

2.3.3.4 Evaluation of *in vitro* RNA delivery of 5A2-SC8 DLNPs. HeLa cells stably expressing firefly luciferase (HeLa-Luc) were seeded (10,000 cells/well) into each well of an opaque white 96-well plate (Corning) and allowed to attach overnight in phenol red-free DMEM supplemented with 5% FBS. 5A2-SC8 DLNPs formulated with anti-luciferase siRNA (siLuc) were added into the cells at the dosage of 0.7, 3.2, 8.4, 16.7 33.4 and 66.9 nM. After 24 h, firefly luciferase activity and viability were analyzed using One Glo + Tox assay kits (Promega). Results were normalized to untreated cells (n=4)

2.3.3.5 Evaluation of cellular uptake, stability, and hemolysis of 5A2-SC8 DLNPs. HeLa-Luc cells were seeded at a density of 30,000 cells per well in 4-chambered cover glass slides and allowed to attach for 24 hours. 5A2-SC8 DLNPs formulated with Cy5.5-labeled siRNA were added to the cells at the siRNA dose of 100 nM. After 4 or 24 h incubation, the medium was aspirated, the cells were washed with PBS, and the lysosomes were stained with the lysotracker according to the manufacturer's protocol. Confocal microscopy imaging was performed using a Zeiss LSM-710 confocal microscopy. The cellular uptake of 5A2-SC8 DLNPs was quantified by analyzing more than 50 cells with the ImageJ software. The colocalization of 5A2-SC8 DLNPs with the lysosomes was analyzed with the Zeiss LSM-710 software. The stability of 5A2-SC8 DLNPs was examined by measuring their size and RNA binding in multiple conditions and environments. The conditions included temperature, serum presence (20% FBS), varying pH values, DLNPs in PBS, and storage time. We chose the following pH values 6.5, 6.0, 5.0, respectively, in order to mimic the conditions of the early endosomes (pH ~ 6.5), later endosome (pH ~ 6.0), and lysosomes (pH ~ 5.0).^{143, 144} Mouse red

blood cells (RBCs) were washed 5X with a 150mM NaCl solution. After washing, the RBC solution was diluted 5-fold with 150 mM NaCl solution. In a v-bottom 96-well plate, 20 μ L of 5A2-SC8 DLNPs of set concentrations were added to 160 μ L of set pH buffer, 20 μ L of RBC were added to every well. Controls of 2% Triton X and DI water were added. The plate was incubated at 37 °C and 5% CO₂ for one hour. Afterwards, the plate was centrifuged at conditions of 4 °C and 500G for 5 minutes; 100 μ L of the supernatant was transferred into a clear bottom 96-well and absorbance was read at 540 nm.

2.3.3.6 Evaluation of *in vivo* RNA delivery of 5A2-SC8 DLNPs. All experiments were approved by the Institutional Animal Care and Use Committees of The University of Texas Southwestern Medical Center and were consistent with local, state and federal regulations as applicable. C57BL/6 mice and athymic nude Foxn1nu mice were purchased from Harlan Laboratories (Indianapolis, IN). For *in vivo* small RNA delivery to hepatocytes, C57BL/6 mice received tail vein i.v. injections of PBS (negative control, n=3) or 5A2-SC8 DLNPs containing anti-Factor VII siRNA (siFVII, n=3) diluted in PBS (200 μ L, 0.5 mg/kg of siRNA). After 48 h mice were anaesthetized by isoflurane inhalation for blood sample collection by retro-orbital eye bleed. Serum was isolated with serum separation tubes (Becton Dickinson) and Factor VII protein levels were analyzed by a chromogenic assay (Biophen FVII, Aniara Corporation). A standard curve was constructed using samples from PBS-injected mice and relative Factor VII expression was determined by comparing treated groups to an untreated PBS control. For *in vivo* siRNA delivery to xenograft tumors, HeLa-Luc cells were trypsinized, washed with PBS, and re-suspended in Hanks' balanced salt solution (HBSS) with 50% Matrigel (vol/vol). 5

million cells (100 μ L of HeLa-Luc suspension) were implanted in the right hind leg of athymic mice to generate tumor xenografts. Tumors subsequently formed with volume of ca. 110 mm³ (~ 6 mm in diameter) in 20 days. The PEG-G1C12 and PEG-G2C12 5A2-SC8 DLNPs formulated with siLuc were injected intravenously with the dosage of 1 mg/kg siLuc. The luciferase signal of the tumors was examined at day 0, 1, and 2 with the IVIS Lumina imaging system (n=3).

CHAPTER THREE

LIPID NANOPARTICLE (LNP) CHEMISTRY CAN ENDOW UNIQUE IN VIVO RNA DELIVERY DATES WITHIN THE LIVER THAT ALTER THERAPEUTIC OUTCOMES IN A CANCER MODEL

This chapter is based on a research article written by the author that was recently submitted (Johnson et al. 2022)

3.1 INTRODUCTION

Lipid nanoparticles (LNPs) are the most clinically advanced drug delivery system for RNA medicines.⁴⁸⁻⁵² In 2018, the first short interfering RNA (siRNA) LNP drug, Onpattro, was approved by the United States Food and Drug Administration (FDA) for treating the hereditary amyloidogenic transthyretin (hATTR) amyloidosis following intravenous (i.v.) infusion. More recently, similar LNPs were used to deliver messenger RNA (mRNA) encoding for the spike protein of the SARS-Cov-2 virus to vaccinate against COVID-19 following intramuscular injection.^{26, 53}

Nucleic acid therapeutics, including RNA interference (RNAi), are promising drugs for liver cancer and other diseases, due to their high efficacy, selectivity and numerous target choices. Liver cancer has limited treatment options because many current drugs have intrinsic hepatotoxicity which can exacerbate underlying liver disease and drastically limit a patient's treatment options.⁹⁹ As evidenced by the recent FDA approval of four siRNA drugs, it has been demonstrated that RNAi is a safe and effective therapeutic modality.¹⁴⁶ However, RNA

delivery still faces challenges with respect to understanding and controlling cell specific delivery. Significant progress has been made in hepatic and extrahepatic delivery. For example, selective organ targeting (SORT) LNPs were developed that can control RNA delivery to the lungs, spleen, or liver.^{69, 70, 147} We showed that the chemical identity of the SORT molecule can affect biodistribution, pKa, and protein corona formation to alter organ specific functional mRNA delivery.⁷⁰ While SORT and other methods of active and endogenous targeting are beginning to open the door to organ level delivery, the specific cellular fate of LNPs *within the organ* remains poorly defined (including in the liver).

Understanding the cellular fate of LNPs within the organ is especially important in the context of therapeutic LNPs, as delivery to an unexpected cell type could relate to adverse events. For instance, the clinical progress of nucleic acid therapy has been stymied by unexpected nanoparticle-induced stimulation of immune cells. For example, the Phase I HCC trial of a miR-34a nanoparticle MRX34 was halted after severe immune-related adverse events driven by off target nanoparticle uptake.^{104, 148} This clinical trial failure highlights that nanoparticle cellular tropism can have negative consequences and thus is essential to understand when developing therapeutic LNP candidates.

All traditional LNPs, including those used in ONPATRO and the COVID-19 vaccines, are comprised of four lipid components: an ionizable amino lipid, a phospholipid (typically DSPC), cholesterol, and a poly(ethylene glycol) (PEG) lipid.^{13, 26, 27, 48, 149} The ionizable amino lipid is one of the most critical components in LNPs because they bind negatively charged nucleic acids and release the encapsulated cargo of the LNP into the cytoplasm via lipid charge acquisition in acidic endosomes. Although many ionizable amino

lipids have been studied with diverse chemical structures, applications of i.v. administered LNPs have largely been limited to one organ (the liver) and a single cell type (hepatocytes). Analogous to very-low-density lipoprotein (V-LDL), this fate of LNPs has been shown to involve apolipoprotein E (ApoE) adsorption in the blood that subsequently mediates uptake into hepatocytes via the low-density lipoprotein receptor (LDL-R).^{13, 70} For this study, we hypothesized that the chemical structure of the ionizable amino lipid may modulate the biofate of LNPs within the liver, which could then affect therapeutic outcomes in the treatment of liver cancer.

In our previous work, we developed a chemically diverse library of ionizable cationic lipids and identified a successful amino lipid named 5A2-SC8 that when formulated into 5A2-SC8/DSPC/Chol/PEG-DMG LNPs was able to effectively deliver siRNA, miRNA, and mRNA to the liver for therapeutic benefit.^{67, 150} This LNP was shown to have high potency in liver hepatocytes and cancer cells, while avoiding off target toxicity to the remaining liver tissue. It is often assumed that the majority of LNPs are primarily taken up by hepatocytes and that liver delivery is a relatively easy and solved problem in terms of targeting. However, upon reexamination of our chemical library of ionizable cationic lipids for siRNA LNP delivery, we made an unexpected observation. A structurally similar lipid, 3A5-SC14, with higher siRNA delivery potency *in vitro* compared to 5A2-SC8 LNPs and comparable liver accumulation *in vivo* to that of 5A2-SC8 LNPs, was ineffective for functional siRNA delivery to liver hepatocytes. This observation of two related and similar LNPs, 5A2-SC8 and 3A5-SC14, that accumulated equally within the liver but had distinct *in vivo* functional RNA delivery capabilities prompted further examination.

The phenomenon inspired us to characterize the biochemical and physical properties of 5A2-SC8 and 3A5-SC14 LNPs and to determine what factors impact the cellular location of RNA LNPs in the liver and whether cellular tropism within an organ could alter the outcomes of cancer therapy. Herein, we formulated 4-component LNPs that only differed in 1 component - the ionizable cationic lipid. 5A2-SC8 and 3A5-SC14 LNPs each had similar physical properties such as size, charge, RNA encapsulation, and pKa. In addition, 5A2-SC8 and 3A5-SC14 LNPs were able to deliver siRNA to silence reporter luciferase expression *in vitro*, as well as accumulate in the liver on a gross analysis level *in vivo*. Despite being more potent for siRNA delivery *in vitro*, 3A5-SC14 LNPs were ineffective for siRNA-mediated gene silencing in hepatocytes *in vivo*. This phenomenon was intriguing and challenges the dogma that the majority of LNPs targeting the liver are consumed by hepatocytes. This unique observation in differential hepatocyte delivery inspired further exploration of the two structurally similar yet functionally distinct LNPs. Through a series of *in vitro* studies, we found that different protein coronas help guide the biofate of LNPs in the liver. We hypothesized that the chemistry of the amino lipid plays a prominent role in which proteins bind to the surface of LNPs when administered in the bloodstream and ultimately dictates the biofate of LNPs in the liver. We further explored if this unique biofate could impact the therapeutic outcomes in a genetically engineered model of MYC-driven liver cancer and found that only 5A2-SC8 let-7g miRNA LNPS were able to extend survival in the aggressive liver cancer model.

Overall, this body of work focused on understanding the biochemical and biophysical factors of two similar yet unique LNPs. We learned that although two LNPs are structurally

similar and share the suggested characteristics for successful liver hepatocyte targeting, these similarities do not always correlate to successful hepatocyte delivery and therapeutic efficacy. Our results illustrate the importance of understanding the sub-organ cellular destination of RNA delivery and incorporating further checkpoints when choosing nanoparticles beyond biochemical and physical characterization, especially in the context of therapeutic LNPs. We anticipate that these findings can help guide others in the selection of nanoparticles for disease treatment as cellular tropism impacts cancer therapy.

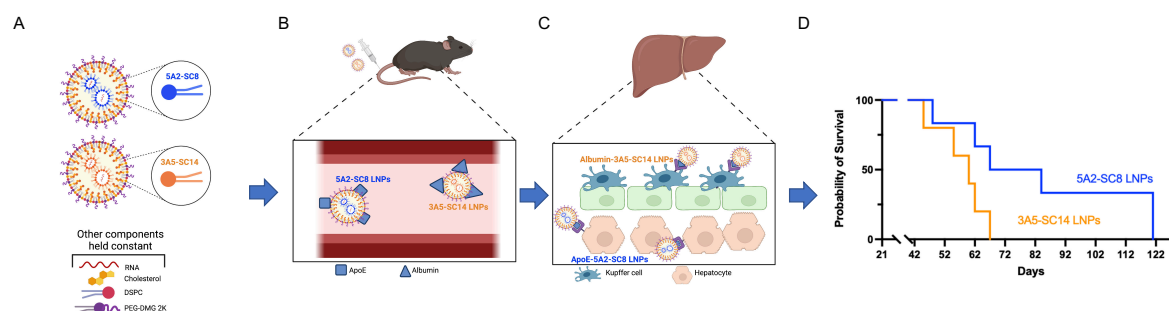


Figure 3.1 Small changes in LNP chemistry can have an impact on cellular tropism within liver and cancer therapeutic efficacy. (A) 5A2-SC8 and 3A5-SC14 form LNPs with similar physiochemical properties. **(B)** Unique serum proteins recognize the surface of 5A2-SC8 and 3A5-SC14 LNPs after they are administered into the blood stream forming different protein coronas. **(C)** Serum protein recognition helps direct the biofate of LNPs within the liver. **(D)** The cell tropism within the liver of 5A2-SC8 and 3A5-SC14 LNPs had a significant impact on liver cancer efficacy.

3.2 RESULTS AND DISCUSSION

3.2.1 5A2-SC8 and 3A5-SC14 LNPs possess similar physical properties.

During the development of LNPs, physical characterization of particle size, surface charge, and pKa are important parameters that can correlate with efficacy.⁵⁸ 4-component LNPs are comprised of an ionizable cationic lipid, phospholipid, cholesterol, and PEG lipid. To examine these properties, we formulated 5A2-SC8 LNPs and 3A5-SC14 LNPs (**Figure 3.2.1A**), differing only in the chemistry of the ionizable amino lipid (5A-SC8 or 3A5-SC14) while keeping the other 3 components (PEG-lipid, cholesterol, and DSPC) constant. While 5A2-SC8 and 3A5-SC14 are structurally similar dendritic amino lipids, they do have a few unique chemical differences. Both 5A2-SC8 and 3A5-SC14 have polyamine cores, they differ in the number of hydrophobic branches (5 versus 3, respectively). Further, 3A5-SC14's alkyl tail length is comprised of 14 carbons compared to the 8 carbons on 5A2-SC8 alkyl tail. These amine and alkyl differences could lead to different biological interactions with serum proteins and endosomal membranes. Each LNP was formulated using the same molar ratios of ionizable dendrimer (either 5A2-SC8 or 3A5-SC14), DSPC, cholesterol, and PEG2000-DMG (**Figure 3.2.1 B-C**) (50/38/10/2, mol/mol). We then measured physical properties including size, surface charge, and RNA encapsulation (**Figure 3.2.1 D-G**). Both 5A2-SC8 and 3A5-SC14 LNPs shared similar physical properties. 5A2-SC8 and 3A5-SC14 LNPs diameters were each around 80 nm with similar surface charge and similar encapsulation of siRNA. It has been shown in the literature that efficacious liver targeting LNPs possess a pKa value ranging from 6.2-6.5.⁵⁸ We measured apparent pKa for 5A2-SC8 and 3A5-SC14 LNPs using the 6-(p-

toluidino)-2-naphthalenesulfonic acid (TNS) assay. Both 5A2-SC8 and 3A5-SC14 LNPs have an identical pKa value of 6.5, which falls within the preferable range for hepatocyte delivery (**Figure 3.2.1 F**). Further, neither 5A2-SC8 or 3A5-SC14 LNPs elevated liver (AST and ALT) and kidney function enzymes (CREA and BUN) when delivering siRNA. (**Figure 3.2.2 A-C**), indicating observed differences would also not be due to toxicity. Taken together, we found that both 5A2-SC8 and 3A5-SC14 LNPs exhibit similar physical properties. These physical attributes, therefore, could not sufficiently explain differences in their activities within the liver. We wanted to explore if this potential factor attributing to the different activities within the liver was a mechanistic difference between the two LNPs or a difference in overcoming the delivery barrier to reach specific liver cells.

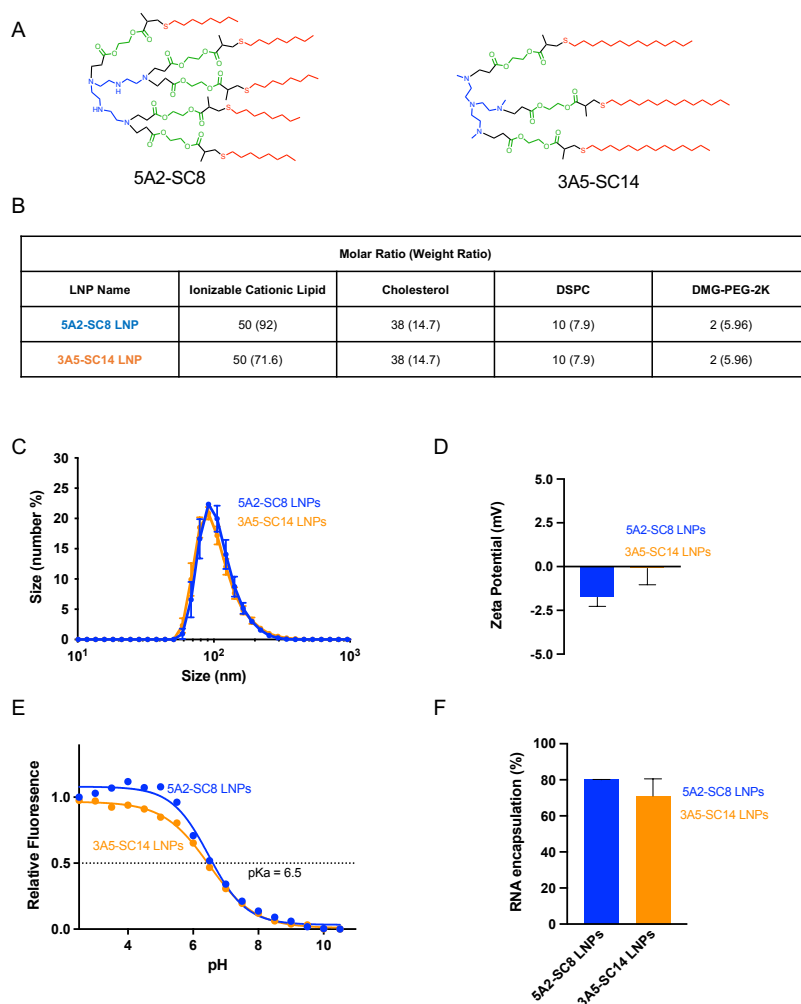


Figure 3.2.1. 5A2-SC8 and 3A5-SC14 LNPs containing siRNA form LNPs with similar physical properties. (A) Chemical structures of selected ionizable cationic amino lipids, 5A2-SC8 and 3A5-SC14. (B) Formulation composition of 5A2-SC8 and 3A5-SC14 LNPs. (C) Size of 5A2-SC8 siFVII LNPs and 3A5-SC14 siFVII LNPs. (D) Zeta potential surface charge of 5A2-SC8 siFVII LNPs and 3A5-SC14 siFVII LNPs (E) pKa of 5A2-SC8 LNPs and 3A5-SC14 LNPs containing a negative control siRNA. (F) RNA encapsulation of 5A2-SC8 siFVII LNPs and 3A5-SC14 siFVII LNPs.

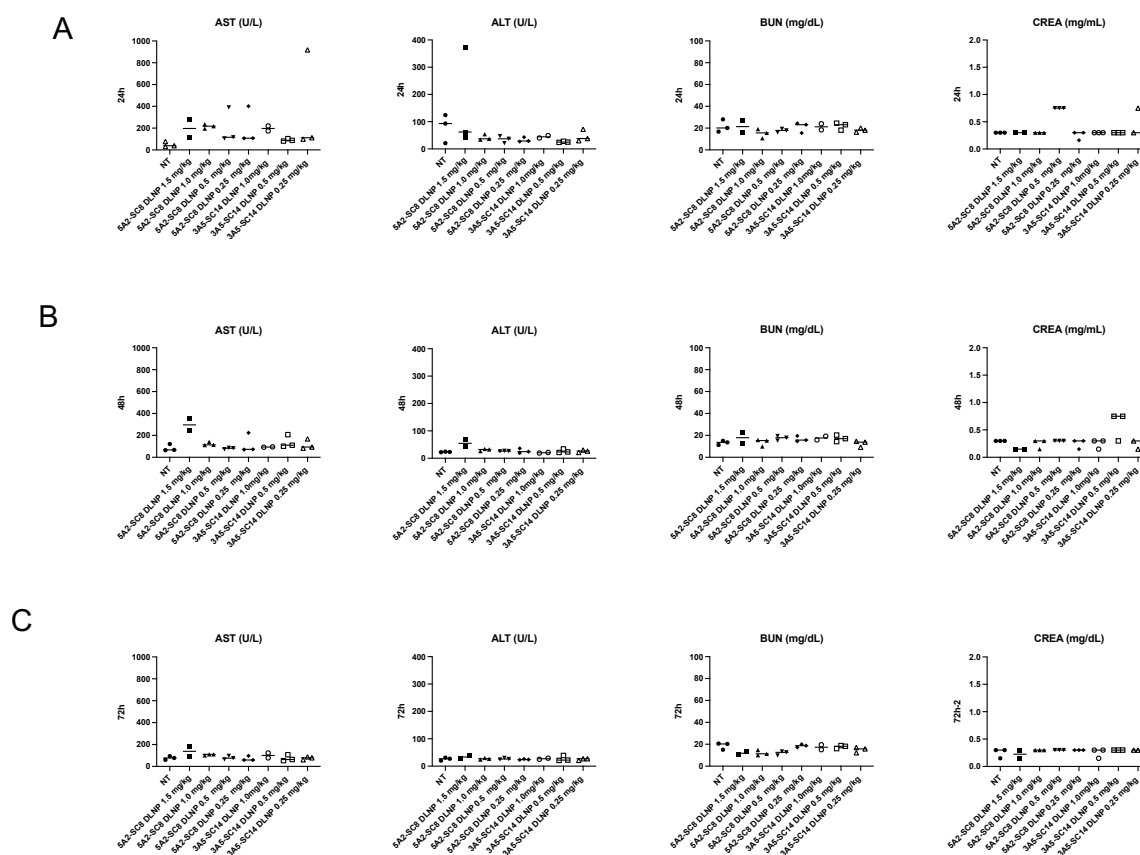


Figure 3.2.2. siFVII 5A2-SC8 and 3A5-SC14 LNPs were well tolerated in vivo at varying doses (0.25 mg/kg, 0.5 mg/kg, 1.0 mg/kg, and 1.5 mg/kg). LNPs were administered to mice via IV injection and PBS was used as a negative control. **(A)** At 24 hours after injection the serum was collected. Kidney function (BUN and CREA), and liver function (AST and ALT) were evaluated. **(B)** At 48 hours serum was collected and kidney function (BUN and CREA) and liver function (AST and ALT) were evaluated. **(C)** At 72 hours the serum was collected. Kidney function (BUN and CREA), and liver function (AST and ALT) were evaluated. There were no significant differences between siFVII LNPs compared to the PBS groups. Data are represented as the mean and standard error (n=3).

3.2.2 5A2-SC8 and 3A5-SC14 LNPs exhibit differential siRNA delivery capabilities to hepatocytes.

To examine first the barriers of cellular uptake and endosomal escape of siRNA, we compared the activity of 5A2-SC8 and 3A5-SC14 LNPs *in vitro*. 5A2-SC8 and 3A5-SC14 LNPs containing anti-luciferase siRNA (siLuc) were delivered into HeLa cells which were stably expressing the Luciferase gene (HeLa-Luc). After 24 hours, cytotoxicity and luciferase activity were quantified. Both 5A2-SC8 and 3A5-SC14 were not toxic to cells (**Figure 3.2.3A**). While both 5A2-SC8 siLuc LNPs and 3A5-SC14 siLuc LNPs were able to silence luciferase in HeLa-Luc cells, 3A5-SC14 LNPs were more potent (**Figure 3.2.3B**). These results indicated that both LNPs can overcome intracellular barriers such as cellular uptake and endosomal escape to deliver siRNA effectively *in vitro*. To examine the accumulation of 5A2-SC8 and 3A5-SC14 LNPs *in vivo*, we i.v. administered Cy5.5 dye labeled siRNA encapsulated inside 5A2-SC8 and 3A5-SC14 LNPs and quantified the explanted tissue fluorescence using *in vivo* imaging. 5A2-SC8 and 3A5-SC14 LNPs were comparably sequestered in the liver as the major organ of accumulation (**Figure 3.2.3C** and **Figure 3.2.4**). In order to test functional RNA delivery to the liver *in vivo*, we prepared both LNPs encapsulating mFluc and administered i.v. at a time point of 6 hours and a dose of 0.1 mg/kg. The results indicated that both 5A2-SC8 and 3A5-SC14 LNPs delivered functional mRNA to the liver (**Figure A3**). We next examined, *in vivo* siRNA mediated gene silencing in the liver. We choose Factor VII (FVII) siRNA (siFVII) as the *in vivo* RNA delivery efficacy test because the assay is well established and commonly used to assess functional delivery to the hepatocytes in the liver.⁶³ FVII, a blood clotting protein, is specifically produced by the hepatocytes and secreted into the blood, where

it can be readily measured in serum. We administered 5A2-SC8 and 3A5-SC14 LNPs containing siFVII to mice through i.v. injection. After 72 hours, the FVII levels in the serum were quantified utilizing chromogenic FVII kit. Interestingly, only 5A2-SC8 LNPs could enable FVII silencing in hepatocytes. 3A5-SC14 LNPs were unable to silence FVII at doses of 0.25 and 0.5 mg/kg despite having such similar physical properties and similar *in vitro* efficacy as 5A2-SC8 LNPs. The FVII activity for 5A2-SC8 LNP treated groups was reduced by 87% compared with the nontreated groups. However, the FVII activity in the groups treated with 3A5-SC14 LNPs was not reduced and remained comparable to the nontreated groups (**Figure 3.2.3 D**). Hepatocytes make up 80% of the liver cell mass, and LNPs have to first pass through the endothelial and Kupffer cell barriers to reach hepatocytes.¹⁵¹ However, the distinct FVII activity reduced by 5A2-SC8 and 3A5-SC14 LNPs illustrates the unique cell tropism of these LNPs *in vivo*.

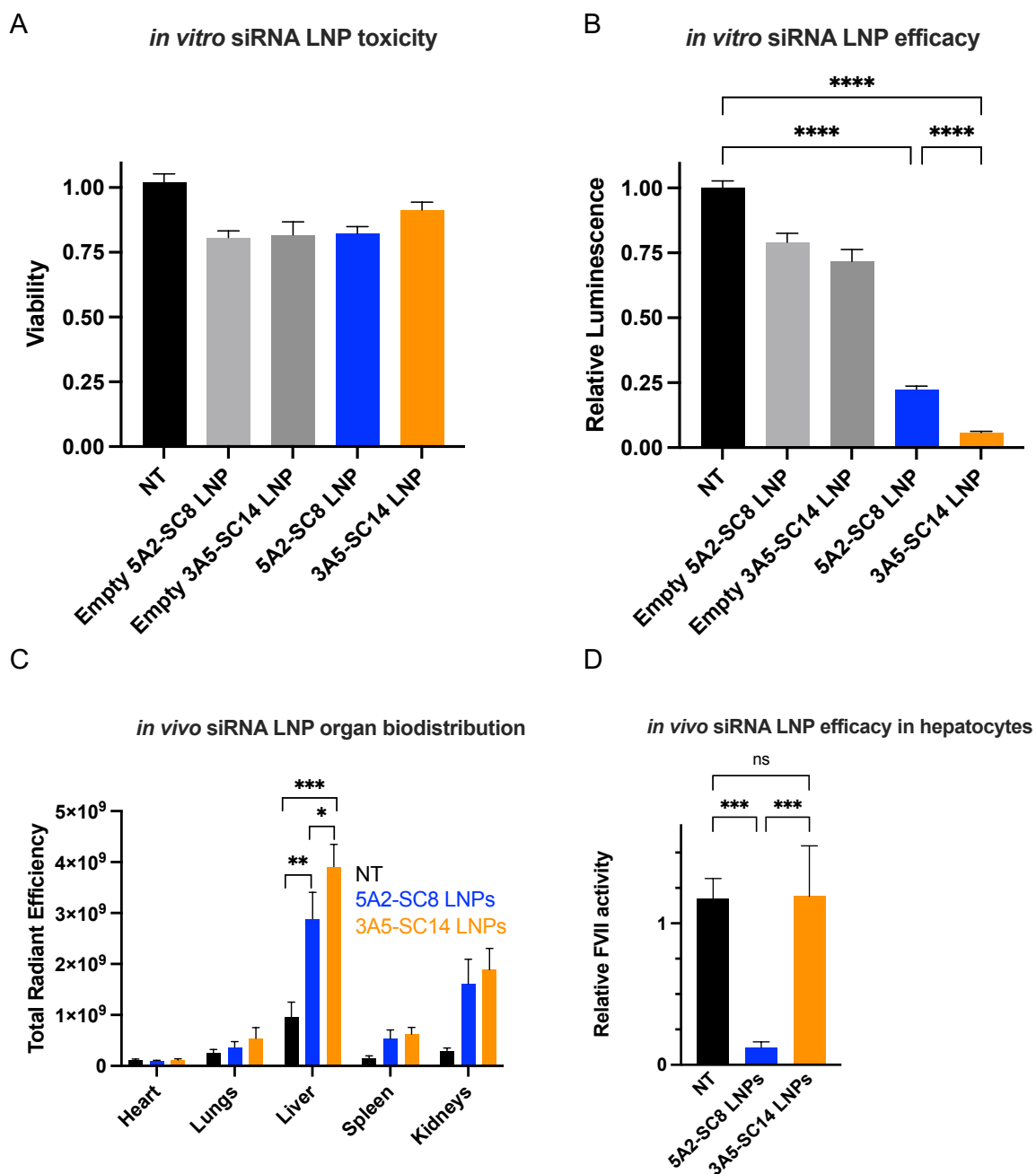


Figure 3.2.3. 5A2-SC8 and 3A5-SC14 LNPs containing siRNA have distinct *in vivo* activity in regards to hepatocyte delivery. (A) Cell viability after *in vitro* siLuc delivery to HeLa-Luc cells using 5A2-SC8 and 3A5-SC14 LNPs containing siLuc at dose of 25 nM for

24 hours. Control LNPs were LNPs containing no siRNA. (B) *In vitro* siLuc delivery to HeLa-Luc cells using 5A2-SC8 and 3A5-SC14 LNPs containing siLuc at a dose of 25 nM for 24 hours. Control LNPs were LNPs containing no siRNA. (C) Quantification of organ biodistribution of 5A2-SC8 and 3A5-SC14 LNPs containing siFVII Cy5.5 (0.5mg/kg) (6 hours). (D) Quantification of *in vivo* FVII gene silencing activity of 5A2-SC8 and 3A5-SC14 LNPs containing siFVII at 0.5 mg/kg (72 hours). Data are shown as mean +/- SEM. Statistical significance was determined using a One-Way ANOVA with multiple comparisons test (*p<0.05, **p<0.005, ****p<0.0001).

3.2.3 Kupffer cells impact 3A5-SC14 LNPs RNA delivery to hepatocytes and do not affect 5A2-SC8 LNPs.

Since 5A2-SC8 LNPs silenced FVII in liver hepatocytes but 3A5-SC14 LNPs did not, we hypothesized that the cellular distribution of these LNPs to cells within the liver are different. The liver structure is complex and is comprised of multiple cell types, where 60-80% of parenchymal cells are hepatocytes and the remaining 20% are non-parenchymal cells such as Kupffer cells, endothelial cells, and hepatic stellate cells.⁷⁵ Hepatocytes are involved in functions such as protein synthesis, protein storage, detoxification, and metabolism.⁷⁶ When LNPs are administered i.v. and enter the liver, one of the first cell types they are exposed to is the Kupffer cell.⁷⁵ Kupffer cells are an important first line of defense to foreign materials as these cells are tissue resident macrophages that will phagocytose and destroy pathogens and other foreign materials within the blood.⁷⁵ They are responsible for the majority of phagocytic

activity within the liver and make up of 80-90% of the total macrophage population within the body.^{75, 77} We aimed to investigate whether the Kupffer cells were playing a role in the difference in RNA delivery of 5A2-SC8 and 3A5-SC14 LNPs, theorizing that Kupffer cells could be acting as a barrier for delivery to hepatocytes.

We designed a series of experiments to determine the impact of liver Kupffer cells on siRNA delivery of LNPs to hepatocytes (**Figure 3.2.4A**). First, we depleted the Kupffer cells in the liver using dichloromethylenediphosphonic acid (clodronate) liposomes.¹⁵² Immunohistochemistry (IHC) was used to demonstrate that Kupffer cells in liver were successfully removed after 24 h treatment of clodronate liposomes (**Figure 3.2.4A**). When Kupffer cells were depleted, 5A2-SC8 and 3A5-SC14 LNPs still accumulated strongly within the liver following i.v. administration of 5A2-SC8 and 3A5-SC14 LNPs containing Cy5.5 dye labeled siFVII (**Figure 3.2.4B**). Next, 5A2-SC8 and 3A5-SC14 LNPs containing FVII siRNA were administrated into mice via i.v. injection at three different doses (0.25, 0.5, and 1 mg/kg siRNA) 24 hours after depletion of Kupffer cells. Mouse serum was collected 72 hours later for quantification for FVII levels. After administration of 5A2-SC8 siFVII LNPs, FVII levels were distinctly reduced in wild type (WT) mice and Kupffer cell depleted mice (**Figure 3.2.4C**). The presence or absence of Kupffer cells did not significantly affect siRNA delivery to hepatocytes using 5A2-SC8 siFVII LNPs at all doses tested (0.25, 0.5, and 1 mg/kg). In contrast, Kupffer cell depletion was required for 3A5-SC14 siFVII LNP mediated siRNA gene silencing in hepatocytes. 3A5-SC14 siFVII LNPs were only able to modestly affect FVII levels in WT mice at the highest doses tested (0.5 and 1 mg/kg). However, FVII levels were significantly reduced after Kupffer cells were depleted including at the lowest dose tested (0.25

mg/kg) (**Figure 3.2.4C**). These data suggest that 5A2-SC8 siFVII LNPs pass through the first barrier of Kupffer cells in the liver and internalize into hepatocytes whereas 3A5-SC14 siFVII LNPs may end up trapped within Kupffer cells, unable to pass through this barrier in order to reach hepatocytes. We next aimed to understand, mechanistically, whether the endogenous identify of LNPs formed when the LNPs come in contact with the plasma could explain their transport to Kupffer cells and hepatocytes.

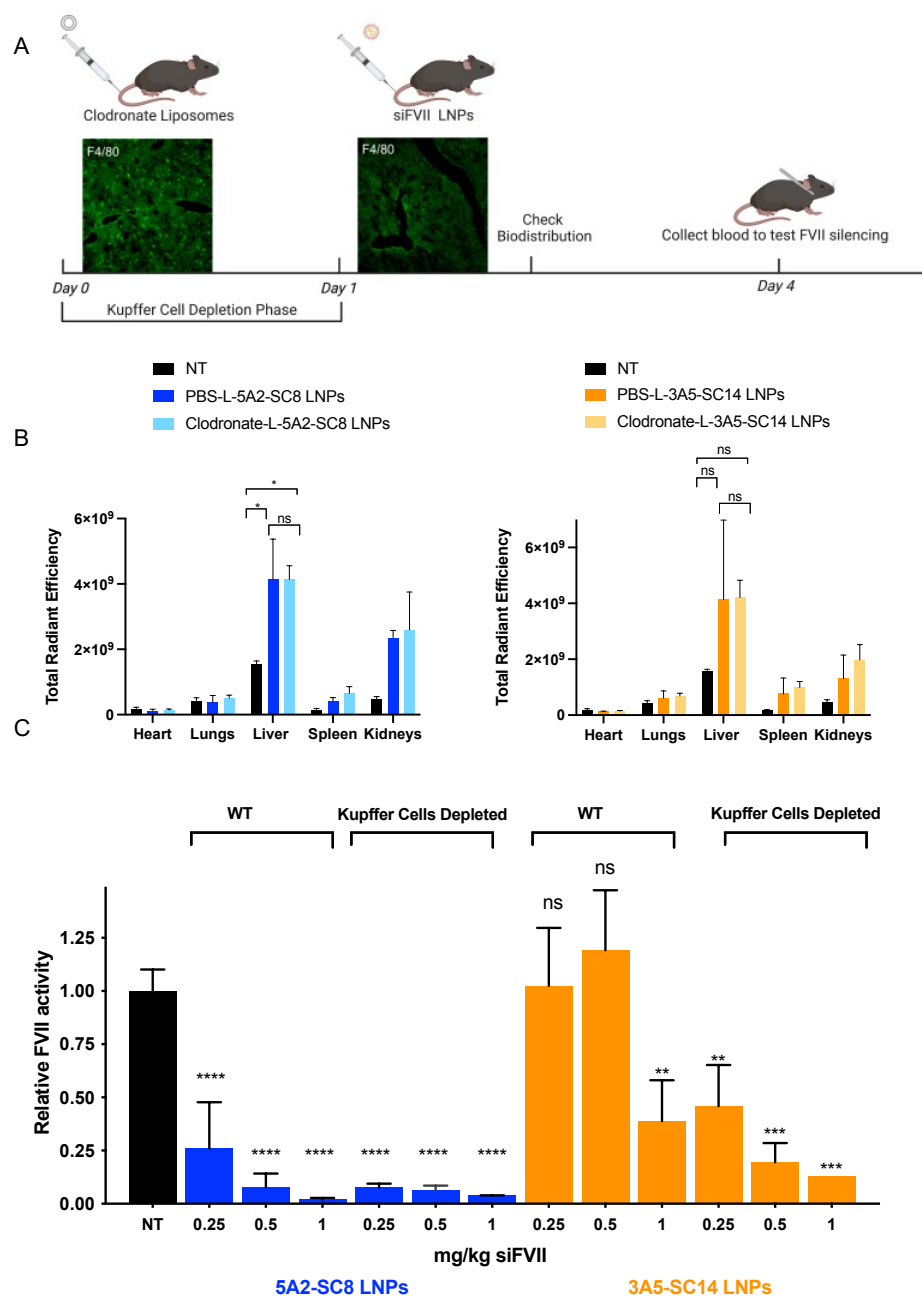


Figure 3.2.4 Depletion of Kupffer cells enables RNA delivery of 3A5-SC14 LNPs to hepatocytes but does not impact the RNA delivery of 5A2-SC8 LNPs. (A) Experimental

design scheme for evaluating siFVII LNPs after the depletion of Kupffer cells using clodronate liposomes (5 mg/kg). PBS liposomes (PBS-L) were used as a control and the treatment groups consist of clodronate liposomes (clodronate-L) i.v. administered 24 hours prior to i.v. administration of 5A2-SC8 siFVII LNPs or 3A5-SC14 siFVII LNPs. F4/80 Antibody staining was used to validate Kupffer cell depletion. **(B)** Quantification of organ biodistribution for 5A2-SC8 siFVII Cy5. LNPs and 3A5-SC14 siFVII Cy5.5 LNPs (0.5 mg/kg) (6 hours) and the non-treatment (NT) group was untreated C57/BL6 mice. Data are shown as mean +/- SEM. Statistical significance was determined using one-way ANOVA with multiple comparisons (* $p < 0.05$) **(C)** The evaluation of siFVII delivery *in vivo* using 5A2-SC8 and 3A5-SC14 LNPs at 0.25, 0.5, and 1 mg/kg siFVII (n=3). Data are shown as mean +/- SEM. Statistical significance was determined using one-way ANOVA with multiple comparisons. Each data set group was compared the non-treatment (NT) group (** $p < 0.001$, *** $p < 0.0001$).

3.2.4 The protein corona formed on 5A2-SC8 and 3A5-SC14 LNPs aids or restricts delivery to hepatocytes.

To further explore the mechanism of the *in vivo* biofate of 5A2-SC8 and 3A5-SC14 LNPs (**Figure 3.2.4D**), we examined the interaction of LNPs with serum proteins. Once LNPs are administered into the bloodstream, the nanoparticle's surface becomes modified by a layer of proteins from the biological fluid, known as the protein corona, which creates an endogenous identity with biological impact.^{153, 85} For example, individual proteins associated with the nanoparticle surface can serve as ligands guiding nanoparticles to specific cell surface

receptors.¹⁵⁴ For LNP delivery to the liver, adsorbed ApoE enables by hepatocyte uptake via binding to the LDL-R on the surface of hepatocytes and undergoing receptor-mediated endocytosis.^{88, 154} Furthermore, in our previous work, it was shown that LNPs undergo a three step endogenous targeting mechanism in order to reach specific organs (such as the lungs, liver, or spleen).⁷⁰ PEG lipid displacement first exposes underlying molecules on the LNP, in this case 5A2-SC8 or 3A5-SC14, to serum proteins in the blood. Next, distinct proteins bind to the surface of the LNP. Third, interactions between specific surface bound proteins and cognate receptors can drive endogenous targeting.⁷⁰

Thus, it is reasonable to expect that the chemistry of surface exposed amino lipids (5A2-SC8 or 3A5-SC14) could control protein adsorption that would affect cellular uptake within the liver. LNPs were incubated with mouse plasma and the plasma proteins which bind to the surface of 5A2-SC8 and 3A5-SC14 LNPs were isolated using differential centrifugation.¹⁵⁵ Once the LNPs protein coronas were isolated, we utilized an SDS-PAGE gel to separate the different proteins present on the protein coronas of 5A2-SC8 and 3A5-SC14 LNPs. While the set of plasma proteins on the surface of 5A2-SC8 and 3A5-SC14 LNPs share similarities, there was a striking difference at a molecular weight of around 35 kDa (**Figure 3.2.5A**), which is close to the molecular weight of ApoE. Western blotting (WB) using an ApoE antibody demonstrated that 5A2-SC8 LNPs were enriched in ApoE, while there was little to no ApoE present on 3A5-SC14 LNPs. In addition, we noticed a pronounced band around 69 kDa, particularly for 3A5-SC14 LNPs. The WB result validated that this protein was Albumin. Therefore, these results indicate that 5A2-SC8 LNPs are enriched in ApoE, whereas 3A5-SC14 LNPs are enriched in Albumin (**Figure 3.2.5B**). Next, we quantified this

result using mass spectrometry proteomics, which confirmed that 5A2-SC8 LNP corona had a higher abundance of ApoE and 3A5-SC14 LNPs corona had a slightly higher abundance of Albumin (**Figure 3.2.5C-D**).

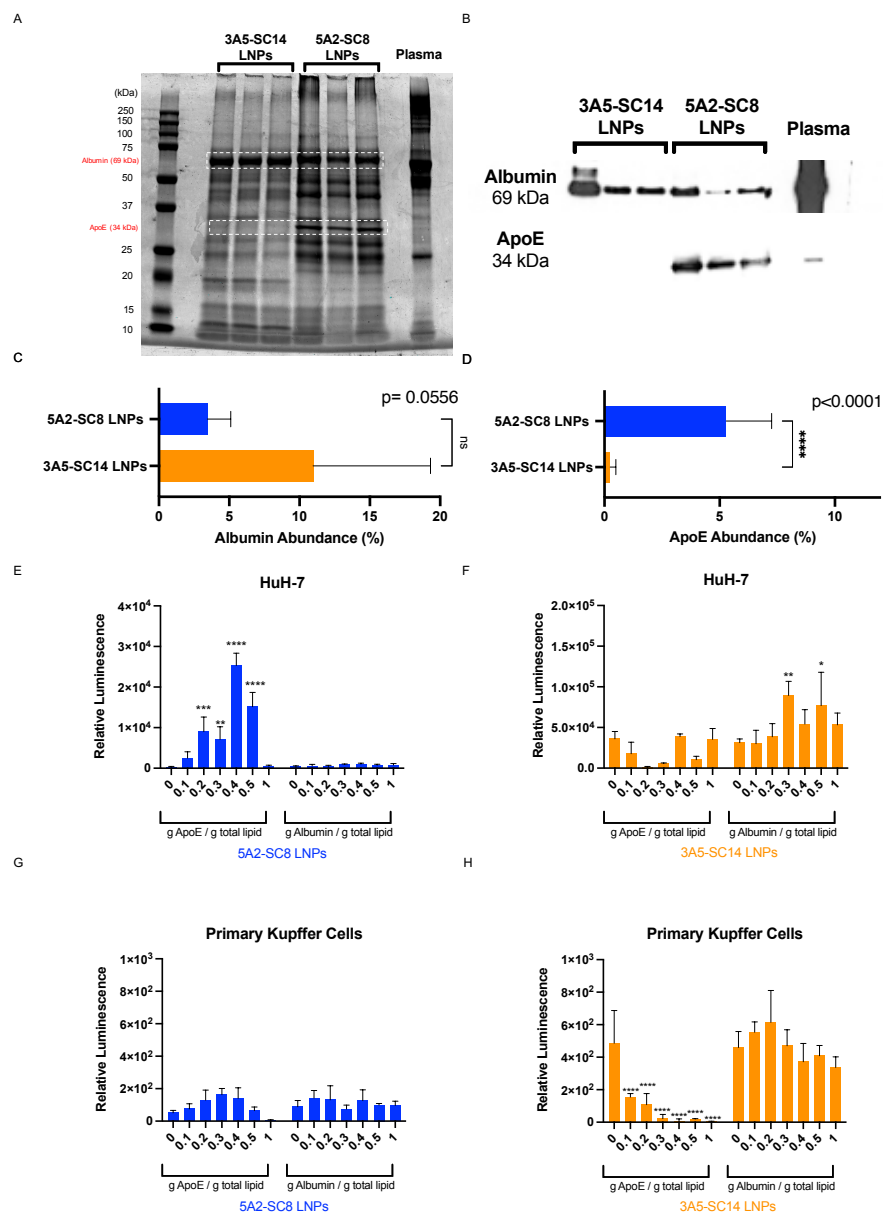


Figure 3.2.5. 3A5-SC14 and 5A2-SC8 LNPs have unique protein coronas. (A) SDS-PAGE of protein coronas isolated from 5A2-SC8 and 3A5-SC14 LNPs (B) ApoE and Albumin on

surface of 3A5-SC14 LNPs was validated by western blot. **(C)** Quantification of ApoE enrichment in the protein coronas of 5A2-SC8 LNPs using mass spectrometry proteomics (n=6). **(D)** Quantification of Albumin enrichment in the protein corona of 3A5-SC14 LNPs using mass spectrometry proteomics (n=6). Data are shown as mean +/- SEM. Statistical significance was determined using students t-test. **(E-F)** Activity of functional luciferase protein translated from uncoated or protein coated 5A2-SC8 and 3A5-SC14 LNPs in HuH-7 cells (25 ng mRNA, 24 h, n=4). **(G-H)** Activity of functional luciferase protein translated from uncoated or protein coated 5A2-SC8 and 3A5-SC14 LNPs in primary Kupffer cells (25 ng mRNA, 24 h, n=4). Data are shown as mean +/- SEM. Statistical significance was determined using one-way ANOVA with multiple comparisons. Each data set group was compared to the uncoated group (****p<0.0001, *** p< 0.0009, **p<0.005, *p<0.01).

To further investigate whether the proteins on the surface of 5A2-SC8 and 3A5-SC14 LNPs aid cell specific uptake, functional mRNA delivery experiments using 5A2-SC8 and 3A5-SC14 LNPs were performed *in vitro* using relevant cell lines. First, LDL-R expressing Hep-G2 and HuH-7 cells were used to examine ApoE mediated uptake. 5A2-SC8 and 3A5-SC14 LNPs encapsulating mFLuc were pre-incubated with recombinant ApoE or Albumin prior to the treatment of cultured cells. Next, luciferase activity was quantified after 24 hours of incubation as a readout for successful cellular uptake, endosomal escape, and mRNA translation to functional protein. The results indicated that when 5A2-SC8 LNPs were pre-incubated with ApoE, there was an improvement in mRNA delivery to HuH-7 (**Figure 3.2.5E**), Hep G2 (**Figure 3.2.6A** and **Figure 3.2.6E**), and primary hepatocytes (**Figure 3.2.7C**). Pre-

incubation of 5A2-SC8 with Albumin eliminated efficacy in both HuH-7 (**Figure 3.2.5E**) and HepG2 cells (**Figure 3.2.6A** and **Figure 3.2.6E**), suggesting that 5A2-SC8 LNPs may utilize ApoE LDL-R uptake pathways as previously identified.⁷⁰ In contrast, pre-incubation of 3A5-SC14 LNPs with ApoE did not improve mRNA delivery to HuH-7 (**Figure 3.2.5F**) or HepG2 cells (**Figure 3.2.6B**). It is speculated that the inability of 3A5-SC14 LNPs to bind ApoE led to free ApoE in the media that blocked LDL-R (**Figure 3.2.6B**). Pre-incubation of 3A5-SC14 LNPs with Albumin led to a slight increase in mRNA delivery to HuH-7 (**Figure 3.2.5F**) and HepG2 cells (**Figure 3.2.6B** and **3.2.6F**), suggesting possible ApoE-independent mechanisms although this will have to be further studied in the future.^{156, 157} To model delivery of LNPs to Kupffer cells, primary mouse Kupffer cells and RAW264.7 murine peritoneal macrophage cell lines were employed. 5A2-SC8 LNPs were unable to effectively deliver mRNA to primary Kupffer cells (**Figure 3.2.5G**) or RAW 264.7 (**Figure 3.2.6C** and **Figure 3.2.6G**) with or without ApoE or Albumin protein pre-incubation. In comparison, pre-incubation of 3A5-SC14 LNPs with Albumin did maintain efficacy in primary Kupffer cells (**Figure 3.2.5H**) and RAW 264.7 cells incubated with FBS media (**Figure 3.2.6D**). Together, these results confirm the mechanism of ApoE adsorption on 5A2-SC8 LNPs for delivery to LDL-R expressing cells, while also revealing possible ApoE-independent mechanisms. Multiple studies have reported that LNP delivery to liver hepatocytes is ApoE dependent,^{156, 157} evidenced by loss of efficacy in ApoE knockout mice.⁸⁸ Although Albumin is an abundant protein, reports have indicated that it can become structurally altered once bound to the surface of a nanocarrier. This altered form of Albumin can become a ligand for cell membrane receptors such as glycoprotein receptors and macrophage class A1 scavenger receptors (SR-A1).¹⁵⁸ It has also been suggested

that Albumin may aid in preferential uptake into macrophage populations and impact the mechanisms of endocytosis due to gp18 and gp30 receptor binding.¹⁵⁷⁻¹⁶⁰ Albumin has been identified on the protein corona of Syn-3 mRNA LNPs, wherein it aided liver delivery.¹⁵⁷ Together, these results show that protein corona adsorption can be linked to lipid chemistry and guide the biofate of LNPs within the liver.

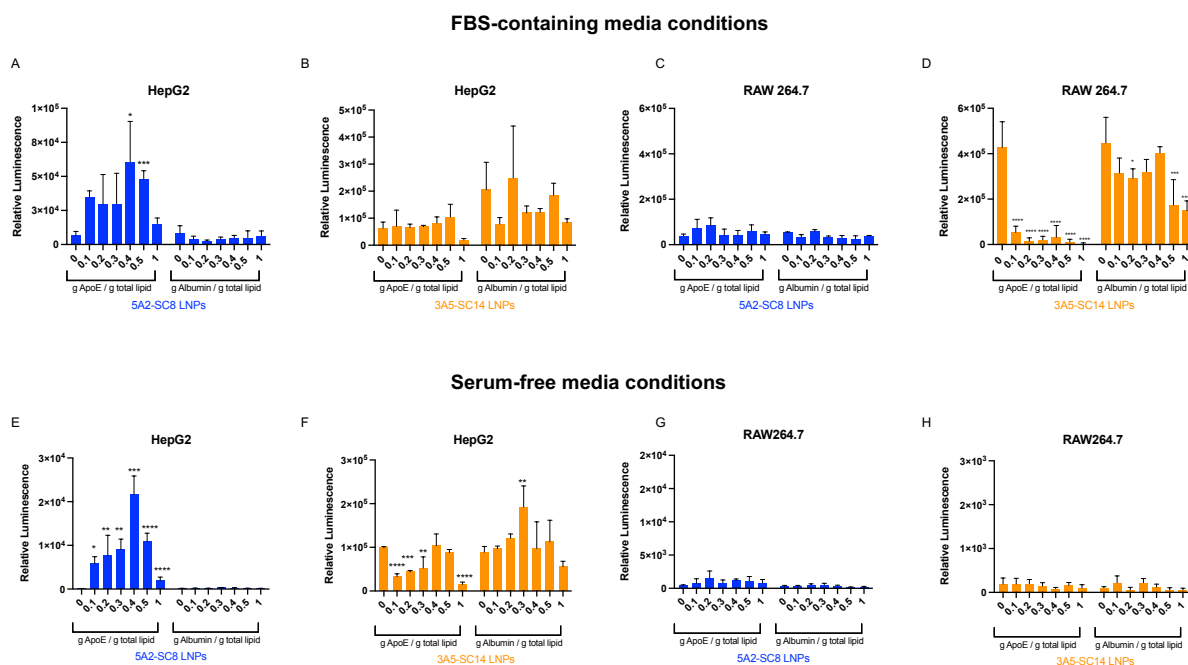


Figure 3.2.6. A comparison of the functional delivery of protein coated or uncoated 5A2-SC8 and 3A5-SC14 LNPs in vitro with and without serum containing media. (A-B) Activity of functional luciferase protein translated from uncoated or protein coated 5A2-SC8 and 3A5-SC14 LNPs in HepG2 cells (25 ng mRNA, 24 h, n=4). Uncoated or coated in ApoE and Albumin. Data are shown as mean +/- SEM. Statistical significance was determined using one-way AVOA with multiple comparisons. Each data set group was compared the NT group (***) $p < 0.0009$, (*) $p < 0.01$. (C-D) Activity of functional luciferase protein translated from

uncoated or protein coated 5A2-SC8 and 3A5-SC14 LNPs in RAW264.7 cells (25 ng mRNA, 24 h, n=4). Uncoated or coated in ApoE and Albumin. Data are shown as mean +/- SEM. Statistical significance was determined using one-way ANOVA with multiple comparisons. Each data set group was compared the NT group (***) $p < 0.0009$, * $p < 0.01$). **(E-F)** Activity of functional luciferase protein translated from uncoated or protein coated 5A2-SC8 and 3A5-SC14 LNPs in HepG2 cells (25 ng mRNA, 24 h, n=4). LNPs were either uncoated or coated in ApoE and Albumin and added to serum free media for 6 hours and then replaced with fresh media for the remainder of 24 hours. Data are shown as mean +/- SEM. Statistical significance was determined using one-way ANOVA with multiple comparisons. Each data set group was compared the NT group (***) $p < 0.0009$, * $p < 0.01$). **(G-H)** Activity of functional luciferase protein translated from uncoated or protein coated 5A2-SC8 and 3A5-SC14 LNPs in RAW264.7 (25 ng mRNA, 24 h, n=4). LNPs were either uncoated or coated in ApoE and Albumin and added to serum free media for 6 hours and then replaced with fresh media for the remainder of 24 hours. Data are shown as mean +/- SEM. Statistical significance was determined using one-way ANOVA with multiple comparisons. Each data set group was compared the NT group (***) $p < 0.0009$, * $p < 0.01$).

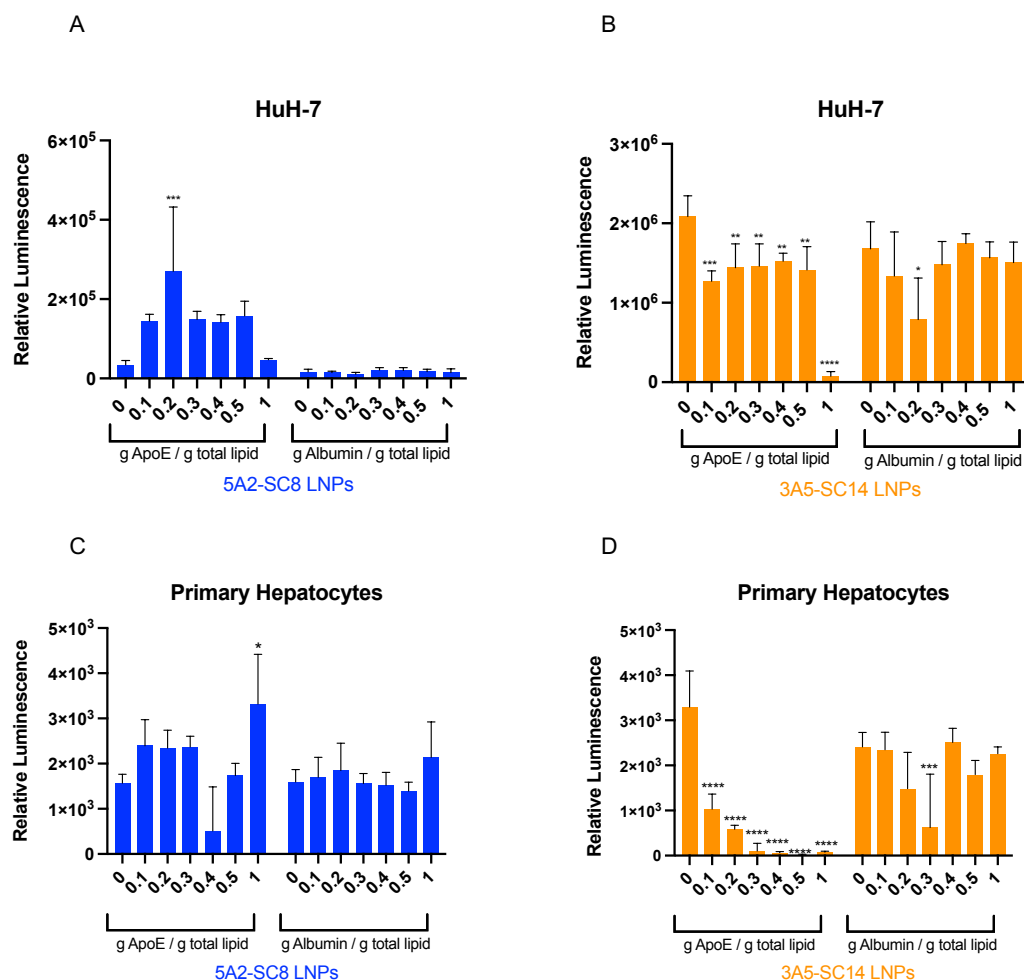


Figure 3.2.7. Functional luciferase mRNA delivery of uncoated or protein coated 5A2-SC8 and 3A5-SC14 LNP to HuH-7 cell line and primary hepatocytes. (A) Activity of functional luciferase protein translated from uncoated or protein coated 5A2-SC8 in HuH7 cells (25 ng mRNA, 24 h, n=4) where LNPs were incubated in FBS containing medium. Data are shown as mean +/- SEM. Statistical significance was determined using one-way ANOVA with multiple comparisons. Each data set group was compared the uncoated group (****p<0.0001, *** p< 0.0009, **p<0.005, *p<0.01). **(B)** Activity of functional luciferase protein translated from uncoated or protein coated 3A5-SC14 LNPs in HuH7 cells (25 ng

mRNA, 24 h, n=4) where LNPs were incubated in FBS containing medium. Data are shown as mean +/- SEM. Statistical significance was determined using one-way ANOVA with multiple comparisons. Each data set group was compared the uncoated group (****p<0.0001, *** p<0.0009, **p<0.005, *p<0.01). (C) Activity of functional luciferase protein translated from uncoated or protein coated 5A2-SC8 LNPs in primary Hepatocytes isolated from C57/BL6 mouse liver (25 ng mRNA, 24 h, n=4). Data are shown as mean +/- SEM. Statistical significance was determined using one-way ANOVA with multiple comparisons. Each data set group was compared the NT group (***p<0.0005, ** p<0.005). (D) Activity of functional luciferase protein translated from uncoated or protein coated 3A5-SC14 LNPs in primary Hepatocytes isolated from C57/BL6 mouse liver (25 ng mRNA, 24 h, n=4). Data are shown as mean +/- SEM. Statistical significance was determined using one-way ANOVA with multiple comparisons. Each data set group was compared the NT group (***p<0.0005, ** p<0.005).

3.2.5 Cellular tropism within the liver affects therapeutic outcomes in an aggressive liver cancer mouse model.

Understanding the biofate of LNPs can open up new avenues for therapeutic development as disease targets exist not only in specific organs but also in specific cell types. In order to move RNA LNPs into clinical development, an improved understanding of LNP cellular tropism within the liver and its impact on therapeutic efficacy will be valuable. We have seen in the context of failed clinical trials that it is crucial to understand cellular tropism.

We hypothesized that 5A2-SC8 LNPs would provide a therapeutic benefit when delivering a therapeutic RNA as this LNP was able to deliver RNA more effectively to hepatocytes. Liver cancer is one of the most common malignancies in the world with few promising effective treatments available and t current treatments only extend life by 3 months.^{93,98} One of the most frequently activated oncogenes associated with the pathogenesis of liver tumors in liver cancer is the MYC oncogene.¹⁶¹ Since MYC is an oncogene deregulated in hepatocellular carcinoma (HCC), an aggressive form of liver cancer, we chose to carry out our therapeutic study with a genetically engineered mouse model of *MYC*-driven cancer where cancer develops in the liver from hepatocytes and disease progresses quickly.¹⁵⁰

In this transgenic mouse model, overexpression of human c-MYC is controlled by a liver specific promoter wherein doxycycline (dox) is used to turn on or off MYC in hepatocytes.^{161, 162} Upon removal of dox, rapid tumor growth leads to death within 60 days without treatment. Importantly, hepatocytes differentiate into tumor cells in this model which further allowed us to test cellular tropism and consequences in regard to liver cancer treatment. Without any treatment, liver tumors become visible around day 20-26 and tumors take over the entire liver by day 45-55 (**Figure 3.2.8A**).

We followed a treatment regimen (**Figure 3.2.8B**) to test the therapeutic outcome of 5A2-SC8 and 3A5-SC14 LNPs. MYC is a challenging target and is an oncogene deregulated in many types of cancers.^{163, 164} Tumors with elevated MYC expression are a challenge to treat due to the highly proliferative and aggressive phenotypes.¹⁶⁵ When MYC is turned on, it drives cellular growth and proliferation.¹⁶⁵ microRNAs have emerged as key posttranscriptional regulators of gene expression, offering a promising approach for cancer therapy.¹⁶⁶ Let-7g is

part of the let-7 family and is known to be downregulated in many tumor types, especially in HCC.¹⁶⁷ We hypothesized that 5A2-SC8 LNPs would bind ApoE to aid delivery to LDL-R expressing hepatocytes and LDL-R expressing cancer cells, while 3A5-SC14 LNPs would not. Instead, albumin recognition on 3A5-SC14 LNPs are likely engulfed by the Kupffer cells are unable to deliver therapeutic miRNA to hepatocytes or cancer cells.

We administered 5A2-SC8 LNPs and 3A5-SC14 LNPs encapsulating let-7g miRNA to the cancer mouse model. Let7-g was chosen as the therapeutic small RNA because it is an important tumor suppressor that is down-regulated in liver cancer^{168, 169} and can lead to silencing of multiple oncogenes beneficial for cancer therapy.²³ The use of a validated therapeutic in the MYC model also allowed a direct comparison of 5A2-SC8 and 3A5-SC14 LNP efficacy. MYC was induced at birth by the removal of Dox water and male pups were randomly divided into 5 groups of non-treatment, empty 5A2-SC8 LNPs, empty 3A5-SC14 LNPs, 5A2-SC8 let-7g miRNA LNPs, and 3A5-SC14 let-7g miRNA LNPs. Let-7g miRNA was delivered twice a week with 5A2-SC8 and 3A5-SC14 let-7g miRNA LNPs at a dose of 0.5 mg/kg starting at day 21 and continuing until day 55 (**Figure 3.2.8A**). At specific time points, the liver tissue was collected for H&E staining to assess tumor burden (21 days, 26 days, 30 days, 45 days, and 55 days). By day 55, the liver was entirely full of tumors. (**Figure 3.2.8A**) The various treatment groups were monitored weekly for their abdomen size and body weight. The results showed that empty LNPs had comparable results to the non-treatment, both in terms of histology, abdomen size, and overall survival. The abdominal growth of groups treated with controls and 3A5-SC14 LNPs had a steady increase in the abdominal size, consistent with the livers becoming overcome by tumor growth (**Figure 3.2.9C-D**). In

comparison, 5A2-SC8 let-7g miRNA LNP treatment led to a slower increase in abdominal size that flattened out, consistent with our hypothesis of anti-cancer benefit and overall survival (**Figure 3.2.8C-D**).

Further, our results showed that 5A2-SC8 let-7g miRNA LNPs extended survival in the MYC mouse model to day 121 while 3A5-SC14 let-7g miRNA LNPs were not able to extend survival past day 67 (**Figure 3.2.8E**). Delivery of let-7g miRNA, or a therapeutic miRNA to hepatocytes and cancer cells is beneficial for treatment in this MYC driven liver cancer model. 3A5-SC14 LNPs are unable to release let-7g miRNA into hepatocytes and thus are not able to provide a therapeutic benefit, likely due to Kupffer cell engulfment and potential degradation. This result emphasizes an importance on understanding the cell type delivery of LNPs as two similar LNPs with promising liver targeting characteristics do not provide a similar therapeutic benefit. We anticipate that understanding the sub-organ cellular destination of RNA delivery can help guide others in the selection of nanoparticles for specific diseases and cancers.

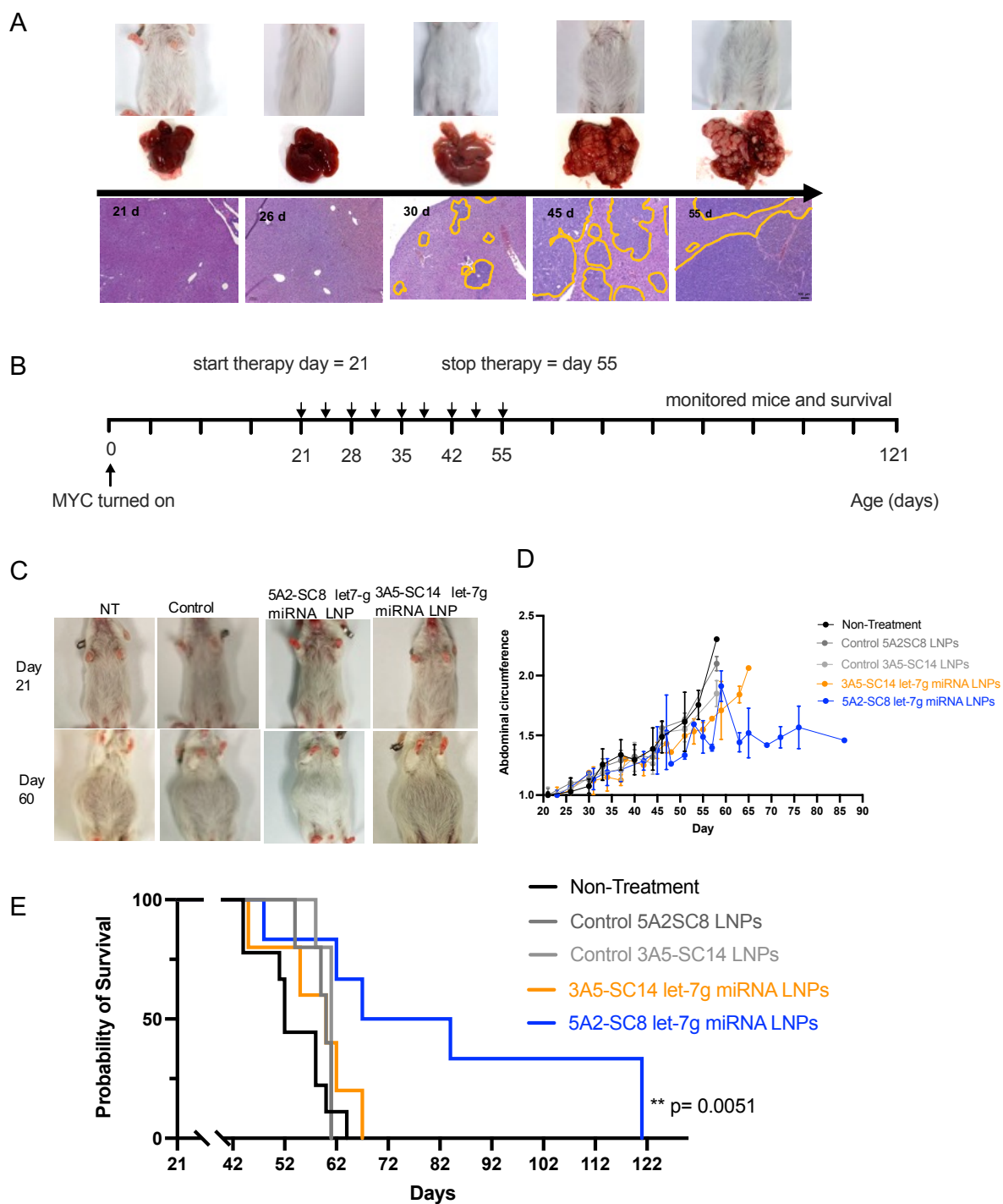


Figure 3.2.8. Therapeutic efficacy of 5A2-SC8 let-7g miRNA LNPs and 3A5-SC14 let-7g miRNA LNPs (0.5 mg/kg) were evaluated in *MYC*-driven liver cancer model. (A) Tumors

grow aggressively after initiation in the human c-MYC genetically engineered mouse model. Representative H&E liver sections are shown at 10X magnification. **(B)** 5A2-SC8 let-7g miRNA and 3A5-SC14 let-7g miRNA LNPs (0.5mg/kg) was administered i.v. to treatment groups twice a week starting at day 21 until day 55 (n=5). **(C)** Representative abdominal images of the various treatment groups at day 21 and day 60. **(D)** Abdominal circumference measurements spanning day 21 to day 87. **(E)** Kaplan-Meier survival curve of the various treatment groups. Treated mice were i.v. administered twice a week starting at day 21 until day 55 with 0.5 mg/kg of 5A2-SC8 let-7g miRNA LNPs (n=5) and 3A5-SC14 let-7g miRNA LNPs (n=5). A non-treatment group (n=9) and empty 5A2-SC8 and 3A5-SC14 LNPs group (n=5) were used as control groups. 5A2-SC8 let-7g miRNA LNPs treated groups had an improved survival.

3.3 EXPERIMENTAL SECTION

3.3.1 Materials and Reagents. 5A2-SC8 and 3A5-SC14 dendrimer amino lipids were synthesized according to our previously reported methods.¹⁵⁰ 1,2-distearoyl-sn-glycero-3-phosphocholine (DSPC) was purchased from Avanti Polar Lipids. DMG-PEG2000 (DMG-PEG2K) was purchased from NOF America Corporation (Sunbright GM-020). Cholesterol, Sucrose, SDS, and Pur-A-Lyzer Midi Dialysis Kits with a molecular weight cut off of 3.5 kDa were purchased from Sigma-Aldrich. Dynamic light scattering (DLS) ultramicro cuvettes, Quant-iT Ribogreen assay, Bovine Serum Albumin, and Simply Blue Safe Stain was purchased from Thermofisher Scientific. Clodronate Liposomes and PBS Liposomes were purchased from Liposoma. The One Glo+ Tox assay kit was purchased from Promega. The Biophen FVII

chromogenic assay kit was purchased from Hyphen Biomed Aniara Corporation. The nucleic acids utilized were purchased from Sigma Aldrich, Thermofisher Scientific and TriLink BioTechnologies. D-Luciferin (sodium salt) was purchased from Gold Biotechnology. The ReadyPrep 2-D Cleanup Kit, 12% Mini-PROTEAN TGX Precast Protein Gels, 2x Laemmli Buffer, 10x Tris/Glycine/SDS, nitrocellulose membrane, 10X Tris buffered saline, precision protein dual standards were purchased from Bio-Rad. Innovative Grade US Origin Mouse Plasma KD EDTA, Novus Biologicals Recombinant Human ApoE4 Protein, and O.C.T. compound for embedding frozen tissue samples was purchased from Fisher Scientific. The antibodies utilized can be found in the supporting information and were purchased from Biologend, Genetex, SantaCruz, and Bio-Rad.

3.3.2 Nucleic Acids Used

1. siFVII (siRNA against FVII) (Sigma Aldrich). 2'-Fluoro modified nucleotides are lower case.
 sense: 5'-GGAucAucucAAGucuuAc[dT][dT]-3'
 antisense: 3'-GuAAGAcuuGAGAuGAucc[dT][dT]-5'
2. siFVII-Cy5.5 (Sigma-Aldrich):
 sense: 5'- Cy5.5 GGAUCAUCUCAAGUCUUAC[dT][dT]-3'
 antisense: 3'-GUAAGACUUGAGAUGAUCC[dT][dT]-5'
3. siNegative Control: (Sigma-Aldrich)MISSION siRNA Universal Negative Control #1 (catalog number: SIC001) was used as a non-targeted siRNA in control experiments.

4. siNegative control Cy5: (Sigma-Aldrich) MISSION siRNA Universal Negative Control #1 Cy 5 (catalog number: [SIC005](#)) was used as a non-targeted siRNA in control experiments.
5. siLuc (siRNA against Luciferase). (Sigma Aldrich)
sense: 5'-GAUUAUGUCCGGUUAUGUA[dT][dT]-3'
antisense: 3'-UACAUAACCGGACAUAUAUC[dT][dT]-5'
6. Let-7g miRNA: (Thermofisher, Ambion) mirVana miRNA mimic (catalog number: 4464070, Assay ID: MC11758, name: hsa-let-7g). Exact sequence and modifications not disclosed by Ambion. Mimics mature human Let-7g.
7. Luciferase mRNA was purchased from TriLink BioTechnologies

3.3.3 Reagents Used for Biological Assays

- A) The QUANT-iT Ribogreen reagent was purchased from ThermoFisher Scientific.
- B) The One-Glo + Tox assay kit was purchased from Promega.
- C) The FVII assay was purchased from Hypen Biomed.

3.3.4 Antibodies Used

- A) Purified anti-ApoE Antibody (Biolegend)
- B) Albumin Antibody (Genetex)
- C) Secondary Goat anti-rat Ig (H+L) HRP (SantaCruz)
- D) Secondary Goat-anti-rabbit IgG (H+L) (Biorad)
- E) F4/80 (BM8.1) primary rat monoclonal antibody (Cell Signaling)

- F) Goat anti-Rat IgG (H+L) Cross-Adsorbed Secondary Antibody, Alexa 488 (Thermofisher)

3.3.5 Instrumentation

- a) **Nanoparticle size and surface charge:** Dynamic light scattering (DLS) was utilized to measure the nanoparticle size and Zeta Potential (surface charge) using a Malvern Zetasizer Nano ZS (He-Ne laser, $\lambda = 632$ nm). For both size and zeta potential, three measurements were taken at settings of 11 runs for a duration of 10 seconds per run.
- b) **Confocal laser scanning microscopy:** A Zeiss LSM-700 confocal laser scanning microscope was used to image liver tissue sections. Images were processed using ImageJ (NIH) and Zen 2.6 Blue Edition (Zeiss) Software.
- c) **Tissue sectioning:** Liver tissues were sectioned using a Leica CM1950 Cryostat.
- d) **Ex vivo animal imaging:** All *ex vivo* imaging of organs was taken using a Perkin Elmer IVIS Lumina system and images were processed using Living Image analysis software (Perkin Elmer).
- e) **In vitro luminescence and fluorescence assays:** Luminescence assays and fluorescence assays were performed using a Tecan Infinite M200 Pro plate reader.

3.3.6 Cell Culture Materials. Dulbecco's Modified Eagle Medium (DMEM) was purchased from Thermo Fisher Scientific containing high glucose, sodium pyruvate, L-glutamine, and phenol red. Penicillin Streptomycin (PS) (10,000 U/mL) was purchased from Fisher Scientific. Dulbecco's modified phosphate buffered saline (PBS), Trypsin-EDTA (0.25%) and fetal

bovine serum (FBS) were purchased from Sigma-Aldrich. RPMI-1640 was purchased from Sigma Aldrich. HeLa-Luc, Hep G2, HuH 7, and RAW264.7 cells were cultured in DMEM containing 10% FBS and 1% penicillin-streptomycin. Primary Kupffer cells were cultured in RPMI-1640 containing 10% FBS and 1% PS.

3.3.7 Experimental Procedures

3.3.7.1 Formulation and Characterization of 5A2-SC8 and 3A5-SC14 LNPs. 5A2-SC8 or 3A5-SC14, 1,2-distearoyl-sn-glycero-3-phosphocholine (DSPC), cholesterol, and PEG-DMG-2000 were dissolved in ethanol (molar ratio of 50:10:38:2) and all RNAs were dissolved in citrate buffer (10 mM citrate buffer at a pH 3.9). A 3:1 ratio of the aqueous solution to the EtOH solution (by volume) was used. Under vortex mixing, the ethanol solutions (40 μ L) were added into the RNA solution (120 μ L). The weight ratio of 5A2-SC8 or 3A5-SC14 amino lipid to RNA was set to 25:1 for all LNP formulations. The formulated 5A2-SC8 and 3A5-SC14 LNPs were incubated for 15 minutes at room temperature and then diluted with 1X PBS for *in vitro* studies. For *in vivo* studies, the LNPs were purified by dialysis in sterile 1X PBS with 3.5kD cut-off dialysis tubes for 2 hours. 5A2-SC8 and 3A5-SC14 LNPs containing luciferase mRNA were prepared using the same conditions as above. 5A2-SC8 and 3A5-SC14 LNPs were diluted to a concentration of 0.1mg/mL using 1X PBS prior to measuring size, and LNPs were diluted further to a volume of 800 μ L using 1X PBS for Zeta potential measurements. The LNP size and zeta potentials were measured by Dynamic Light Scattering (DLS) using a Malvern Zetasizer Nano ZS (He-Ne laser, $\lambda = 632$ nm) prior to *in vivo* studies. Nucleic acid

binding was determined using the Quant-iT Ribogreen assay (Fisher Scientific) following the recommended protocol and additional details can be found in the supporting information. Following a reported procedure, the TNS assay was used to determine the pKa of 5A2-SC8 and 3A5-SC14 siRNA LNPs comprised of dendrimer/DMG PEG-Lipid/ DSPC/Cholesterol (50/2/10/38 mol%) in PBS at a concentration of 100 μ M total lipid.¹⁵⁰ Briefly, the formulated LNPs were diluted to 60 μ M total lipid in 100 μ L volume per well in 96-well plates with a series of 10 mM HEPS/10 mM MES/10 mM ammonium acetate/130 mM NaCl buffer solution, where the pH values ranged from 2.5 to 11. The TNS buffer was diluted to 50 mM. The same volume (4 μ L) of TNS stock solution was added into each well to give a final concentration of 2 μ M. The plate was read with InfiniTe F/M200 Pro microplate reader (Tecan) using excitation and emission wavelength of 321 and 445nm shaking for 200 seconds. Four replicates were used for each data point. The data was normalized to the values at pH 2.5, and the data was analyzed using GraphPad Prism. A non-linear fit analysis of log (inhibitor) vs response was applied to the fluorescence data, and the pKa was measured as the pH value where the fluorescence intensity is half-maximum fluorescence (inflection point).

3.3.7.2 Nanoparticle size and surface charge measurement. The size and zeta potential of 5A2-SC8 and 3A5-SC14 LNPs were measured using the Malvern Zetasizer Nano ZS (He-Ne laser, $\lambda = 632$ nm). 5A2-SC8 and 3A5-SC14 LNPs were diluted to a concentration of 0.1mg/mL using 1x PBS prior to measuring the size by Dynamic Light Scattering. Next, the LNPs were diluted further to a volume of 800 μ L using 1x PBS for Zeta potential measurements.

3.3.7.3 RNA binding Ribogreen Assay. A 96-well black opaque polystyrene microplate was utilized for this assay (Corning-Fisher Scientific). Briefly, LNPs and a standard of appropriate nucleic acid solutions ranging with RNA concentrations of 0-10 ng/ μ L were prepared. 5 μ L of standard solution of LNPs were added per well (n=4). To measure free/unbound RNA, 50 μ L of diluted Ribogreen solution (1:200) were added to each well using a multi-channel micropipette. Using an orbital shaker, the plate was shaken for 5 minutes at room temperature while covered to protect from the light. Each well was then measured in the InfiniTe F/M200 Pro microplate reader (Tecan) for fluorescence using an excitation of 485nm and an emission 535nm. The amount of free siRNA was assessed once fitted to the standard curve. Free siRNA was used to determined encapsulated siRNA percentage using the following formula: $\frac{\text{total nucleic acid added} - \text{free nucleic acid}}{\text{total nucleic acid added}}$. To measure total RNA, 50 μ L of 0.5% Triton X-100 was added to each well. The plate was incubated under constant shaking for 5 min and fluorescence was measured. The percentage of encapsulated RNA was calculated as $100 * (\text{ng of total RNA} - \text{ng of free RNA}) / \text{ng of total RNA}$.

3.3.7.4 Evaluation of in vitro Luciferase delivery of 5A2-SC8 and 3A5-SC14 LNPs.

RAW 264.7, HuH-7, or Hep G2 cells were seeded into white-bottom 96-well plates at a density of 10,000 cells per well in 100 μ L final volume and incubated at 37 °C overnight with DMEM medium (10% FBS, 1% PenStep). After 24 hours, the old media was replaced with 100 μ L of fresh media. 5A2-SC8 and 3A5-SC14 LNP formulations containing firefly luciferase (FLuc) mRNA were added with fixed 25 ng mRNA per well (n=4). After 24 hours on LNP incubation, ONE-Glo + Tox (Promega) were used to detect Luciferase expression and cell viability using

Promega's recommended protocol. For the evaluation of in vitro luciferase delivery of LNPS in serum free HuH-7 cells, the cells were instead washed with PBS and then replaced with 100 uL serum free media for LNP incubation. After 6 hours, the serum free media was removed and replaced with regular media for the remainder of 24 hours.

3.3.7.5 Luciferase mRNA delivery assay with and without protein incubation to primary Kupffer cells and Hepatocytes: 25 ng of firefly luciferase mRNA (mFLuc) inside 5A2-SC8 and 3A5-SC14 LNPs was added into a white-bottom 96 well plate. Afterwards, 10,000 cells in 100 uL volume per well was added and mixed with LNPs. 5A2-SC8 and 3A5-SC14 LNPs incubated with either no serum protein, ApoE, or Albumin at a ratio of 0.1 g protein / 0.1 g total lipid, 0.2 g protein / 0.2 g total lipid, 0.3 g protein / 0.3 g total lipid, 0.4 g protein / 0.4 g total lipid, 0.5 g protein / 0.5 g total lipid, or 1 g protein / 1 g total lipid. The next day (24 hours later), a One-Glo+ Tox assay was performed according to the manufacturer's directions (Promega). All the data was normalized to cell viability. Cell culture conditions can be found in the supporting information.

3.3.7.6 Evaluation of in vivo toxicity of siFVII 5A2-SC8 and 3A5-SC14 LNPs at varying doses. C57BL/6 mice, with weights of 20g, were divided into four groups: n=3 per group. We selected four doses of siFVII, 1.5 mg/kg, 1.0mg/kg, 0.5 mg/kg, and 0.25 mg/kg. Two different LNP formulations were used 5A2-SC8 LNP and 3A5-SC14 LNP. Non-treated mice served as the negative control. At each time point (24 hours, 48hours, 72 hours), whole blood was collected into BD microtainer tubes. Serum was separated by centrifuging the tubes at 13,000

rpm for 10 minutes. Then, blood urea nitrogen (BUN), Creatinine (CREA) Alanine aminotransferase (ALT) and aspartate aminotransferase (AST) levels were measured using the UTSW metabolic phenotyping core.

3.3.7.7 Evaluation of Luciferase mRNA delivery in vivo. C57BL/6 mice weighing approximately 20 g (6-8 weeks of age) were i.v. injected with LNPs containing firefly luciferase mRNA at dose of 0.1 mg/kg. After 6 hours, mice were euthanized and major organs were removed (heart, lung, spleen, kidney, and liver) from each set. Luciferin was injected 10 minutes prior to *Ex vivo* Bioluminescence measurements. Organs were analyzed using IVIS Lumina Imaging technique (Caliper Life Sciences). Data analysis was done on IVIS Lumina software. Total luminescence of the heart, lungs, liver, spleen, and kidneys were measured using Living Image Software (PerkinElmer) by drawing regions of interest around each organ.

3.3.7.8 Evaluation of in vitro siRNA delivery of 5A2-SC8 and 3A5-SC14 LNPs. HeLa-Luc cells were seeded into white 96-well plates at a density of 10,000 cells per well 24 hours before transfection and cells were incubated with DMEM medium (10% FBS, 1% PenStep). The next day, 5A2-SC8 and 3A5-SC14 LNP formulations containing anti-luciferase siRNAs (siLuc) were added with fixed 24 nM siLuc per well. After incubation of 24 hours, ONE-Glo + Tox kits were used to detect luciferase expression and cytotoxicity based on Promega's recommended protocol. Cell viability was measured using the CellTiter-Glo Luminescent Cell Viability Assay following Promega's recommended protocol.

3.3.7.9 Animal Related Studies

All experiments were approved by the Institutional Animal Care and Use Committees (IACUC) of The University of Texas Southwestern Medical Center and were consistent with local, state, and federal regulations as application. Female C57BL/6 mice were used around 6-8 weeks of age. Transgenic mice bearing MYC-driven liver tumors were generated by crossing the TRE-MYC strain with LAP-tTA strain.^{161, 162} Mice bearing the LAP-tTa and TRE-MYC genotype were maintained on 1 mg/mL of dox, and MYC was induced by withdrawing dox at birth.

3.3.7.10 Evaluation of *in vivo* RNA delivery of 5A2-SC8 and 3A5-SC14 LNPs to hepatocytes.

For *in vivo* small RNA delivery to hepatocytes, C57BL/6 mice received i.v. injections of PBS (negative control, n=3), 5A2-SC8 LNPs containing anti-Factor VII siRNA (siFVII) diluted in PBS (200 μ L, 0.5 mg/kg of siFVII) or 3A5-SC14 LNPs containing siFVII diluted in PBS (200 μ L, 0.5 mg/kg of siFVII). After 72 h mice were anaesthetized by isoflurane inhalation for blood sample collection by cheek puncture. Serum was isolated with serum separation tubes (Becton Dickinson) and Factor VII protein levels were analyzed by a Biophen FVII chromogenic assay (Hyphen Biomed, Anisara Corporation) following the recommended protocol. A standard curve was constructed using samples from a PBS-injected mice and relative Factor VII expression was determined by comparing treated groups to an untreated PBS control.

3.3.7.11 Analysis of siFVII-Cy5.5 Biodistribution of 5A2-SC8 and 3A5-SC14 LNPs.

C57BL/6 mice weighing approximately 20 g (6-8 weeks of age) were administered i.v. 5A2-SC8 and 3A5-SC14 LNPs containing siFVII-Cy5.5 at dose of 0.5 mg/kg. After 6 hours, mice were euthanized and major organs were removed (heart, lung, spleen, kidney, and liver) from each set of mice. Ex vivo imaging (Cy5.5 filter setting) was done 6 hours post injection. Organs were analyzed using IVIS Lumina Imaging technique (Caliper Life Sciences). Data analysis was done on IVIS Lumina software and normalized to a PBS control. Total fluorescence of the heart, lungs, liver, spleen and kidneys were measured using Living Image Software (PerkinElmer) by drawing regions of interest around each organ.

3.3.7.12 Kupffer cell depletion and in vivo RNA delivery of 5A2-SC8 and 3A5-SC14 LNPs

to hepatocytes. C57BL/6 mice (6-8 weeks of age) were i.v. injected with Clodronate liposomes or PBS liposome controls purchased from Liposoma at dosage of 0.05 mg/mL (n=3). At 24 hours post injection, 5A2-SC8 or 3A5-SC14 LNPs containing siFVII were i.v. administered to the groups of mice. The dosages used were 0.25, 0.5 and 1 mg/kg of RNA. After 72 hours post LNP injection, blood was collected via cheek for FVII silencing following the Biophen FVII assay (Hyphen Biomed) above. In order to confirm Kupffer cell depletion was successful, after 24 hour of PBS liposome and clodronate liposome treatment, livers were removed and embedded in O.C.T to prepare frozen tissue sections. For confocal imaging, the tissue was cryo-sectioned (10 μ m) and fixed using 4% paraformaldehyde (PFA) at room temperature for 20 min. The slides were washed three times with PBS and blocked for 30 min in PBS with 2% BSA. Sections were then incubated overnight with F4/80 primary antibody (Cell Signaling,

1:300), Alexa 488 secondary (ThermoFisher, 1:200) in 2% BSA in PBS. The next day, slides were washed three times with PBS and stained with their secondary antibody for 1 hour. Afterwards, slides were washed and mounted using ProLong Gold Antifade (Life Technologies). Sections were imaged using an LSM 700 point scanning confocal microscope (Zeiss) equipped with a 20X objective.

3.3.7.13 Isolation of plasma proteins absorbed to 5A2-SC8 and 3A5-SC14 LNPs. 5A2-SC8 and 3A5-SC14 LNPs were prepared according to the previously described protocol and were diluted to a final lipid concentration of 1 g/L with 1X PBS.¹⁷⁰ The plasma proteins absorbed onto the LNPs were isolated following our reported methods.⁷⁰ Briefly, equal volume of 5A2-SC8 and 3A5-SC14 LNPs (at concentration of 1 mg/mL total lipid) were incubated in equal volumes mouse plasma (Innovative Grade US Origin Mouse Plasma KD EDTA purchased from Fisher Scientific) at a 1:1 ratio at 37°C for 15 minutes. Each sample was prepared in triplicates. A 0.7M sucrose gradient was prepared by dissolving solid sucrose in MilliQ water. The LNP and plasma solution were added to tubes containing a 0.7M sucrose gradient. The sucrose gradient tubes were prepared in advance by diluting 2M sucrose in MilliQ water. Samples were centrifuged at a speed of 25,000 G for 1 hour at 4°C. The supernatant was removed carefully and discarded. The samples were washed with 1X PBS 3 times at speed of 25,000 for 5 minutes. After 3 washes, samples were resuspended in 50 µL of a buffer comprised of Laemli sample buffer with 50% BME. Next, excess lipids were removed using the ReadyPrep 2D Clean up kit (Bio-Rad) following steps provided by the manufacturer. Samples were then stored at -20°C prior to processing.

3.3.7.14 Sodium dodecyl sulfate-polyacrylamide gel electrophoresis (SDS-PAGE) characterization of plasma proteins adsorbed onto 5A2-SC8 and 3A5-SC14 LNPs. The plasma proteins isolated from the surface of 5A2-SC8 and 3A5-SC14 LNPs were heated to 95°C for 5 minutes. 10 µL of sample in triplicates were loaded into the wells of 12 % mini-PROTEAN TGX precast gels (Bio-Rad). Mouse plasma was loaded as a control (1:100 dilution). The gel was run starting at 90V and then changed to 200 V and monitored regularly. Afterwards, the gel was washed 3 times in MilliQ water for 5 minutes per wash. The gel was stained with SimplyBlue Safe Stain (Bio-Rad) for 1 hour at room temperature gently shaking to visualize the protein bands. The gel was destained overnight using deionized water (DI) and imaged with a Licor Scanner the following day.

3.3.7.15 Validation of ApoE and Albumin adsorption on LNPs using Western Blot. The SDS PAGE gel used for the characterization of plasma proteins adsorbed onto the surface of 5A2-SC8 and 3A5-SC14 LNPs mentioned above was rinsed in 1X transfer buffer. After rinsing, the SDS gel was transferred using a nitrocellulose membrane via the Bio-Rad Trans-Blot transfer system according to Bio-Rad's recommended protocol. Next, the membrane was cut into two sections based on the molecular weight of ApoE and Albumin. The sample was blocked using a 5% dry milk solution (5% dry milk in 1X Tris-Buffered Saline and 0.1% Tween 20, TBST) for 1 hour. The samples were incubated overnight at 4°C with primary antibody ApoE (Biolegend, 1:500) and Albumin Antibody (Genetex, 1:1000) in 3% BSA in TBST overnight. After an overnight incubation, samples were washed 3X for 5 minutes each with TBST at room temperature while shaking. The samples were then cultured with secondary antibody goat-

anti-rabbit IgG (H+L) (Biorad, 1:3000) and secondary antibody goat anti-rat Ig (H+L) HRP (SantaCruz, 1:8000). The secondary antibodies were incubated for 1 hour at room temperature while gently shaking. Next, the substrate of HRP (Bio-rad) (1:1) was prepared. The protein was detected using the chemiluminescent method.

3.3.7.16 Preparation of plasma protein samples for mass spectrometry proteomics. Plasma proteins isolated from the surface of 5A2-SC8 or 3A5-SC14 LNPs were loaded onto a 12% mini PROTEAM TGX Precast Protein Gel at a volume of 10 μ L and run into the gel at 1 cm at 90V. Once the samples created an even line, the gel was removed and stained with SimplyBlue Safe Stain for 1 hour to fix and visualize the protein bands. After destaining for 1 hour, the protein bands were excised using a sterile razor blade and sliced into 1mm cubes. Next, the gel cubes were added to a 1.5 mL tube that had been rinsed with a 1:1 MilliQ water: Ethanol solution and stored at 4°C until being submitted to the UTSW Proteomics Core for mass spectrometry analysis. Data was analyzed via Microsoft excel and plotted using GraphPad Prism.

3.3.7.17 Luciferase mRNA delivery assay with and without protein incubation to cell lines.

10,000 cells per well were plated into a white-bottom 96 well plate. After 24 hours, the media was replaced with 100 μ L of fresh media and cells were treated with 25 ng of firefly luciferase mRNA (mFLuc) inside 5A2-SC8 and 3A5-SC14 LNPs incubated with either no serum protein, ApoE, or Albumin at a ratio of 0.1 g protein / 0.1 g total lipid, 0.2 g protein / 0.2 g total lipid, 0.3 g protein / 0.3 g total lipid, 0.4 g protein / 0.4 g total lipid, 0.5 g protein / 0.5 g total lipid,

or 1 g protein / 1 g total lipid. The next day, a One-Glo+ Tox assay was performed according to the manufacturer's directions (Promega). All the data was normalized to cell viability. The cell lines that were utilized in this experiment were HuH-7 cells, Hep G2, and RAW264.6 cells. Cell culture conditions and primary cell isolation details can be found in the supporting information.

3.3.7.18 Luciferase mRNA delivery assay with and without protein incubation to primary cells. 25 ng of firefly luciferase mRNA (mFLuc) inside 5A2-SC8 and 3A5-SC14 LNPs were incubated with either no serum protein, ApoE, or Albumin at a ratio of 0.1 g protein / 0.1 g total lipid, 0.2 g protein / 0.2 g total lipid, 0.3 g protein / 0.3 g total lipid, 0.4 g protein / 0.4 g total lipid, 0.5 g protein / 0.5 g total lipid, or 1 g protein / 1 g total lipid. The following LNPs were directly added into 96-well plates. 10,000 cells per well were plated into a white-bottom 96 well plate and mixed with the according LNPs. The next day, a One-Glo+ Tox assay was performed according to the manufacturer's directions (Promega). All the data was normalized to cell viability. The cells that were utilized in this experiment were primary Kupffer cells and primary Hepatocytes. Cell culture conditions and primary cell isolation details can be found in the supporting information.

3.3.7.19 Generation of MYC-driven aggressive cancer mouse model. Transgenic mice bearing MYC-driven liver tumors were generated by crossing the TRE-MYC strain with the LAP-tTA strain as reported in our previous publication.¹⁵⁰ Briefly, MYC was induced by withdrawing doxycycline (dox) water. For the therapy study, pups were removed from dox

water after birth (Day 0). Starting at Day 21, mice were divided into treatment groups. The groups consisted of non-treatment, 5A2-SC8 LNPs containing no miRNA, 5A2-SC8 LNPs containing 0.5mg/kg Let-7g miRNA and 3A5-SC14 LNPs containing 0.5 mg/kg Let-7g miRNA. The LNPs were administered i.v. twice a week.

3.3.7.20 *In vivo let-7g miRNA therapeutic study in aggressive liver cancer mouse model using 5A2-SC8 and 3A5-SC14 LNPs.* 21-day old male transgenic c-MYC mice bearing liver tumors were randomly divided into different treatment groups of non-treatment (n=9), 5A2-SC8 and 3A5-SC14 LNPs containing no miRNA (n=5) or 5A2-SC8 and 3A5-SC14 LNPs containing 0.5 mg/kg of let-7g miRNA (n=5). The groups received i.v. injections twice a week starting at day 21 and continuing until day 55. Their body weight, abdomen circumference, and survival were carefully monitored.

3.3.7.21 *Immunohistochemistry and histological tissue analysis.* Liver tissues from c-MYC mice were collected at 21 days, 26 days, 30 days, 45 days, and 55 days and placed in 10% formalin (Sigma Aldrich) for 72 hours for fixation. After 72-hour fixation, the formalin was replaced with PBS and the samples were sent to the UTSW tissue management shared resource core facility to perform Hematoxylin and Eosin (H&E) staining.

CHAPTER FOUR

CONCLUSIONS AND FUTURE DIRECTIONS

Understanding the chemistry behind individual LNP components and the cellular fate of LNPs is important in the context of disease therapy because delivery to an unexpected cell type could result in lack of efficacy and in adverse events. It has been shown that drugs have failed in clinical trials for these reasons. This dissertation highlights contributions towards understanding how the chemistry of the PEG lipid and the chemistry of the ionizable cationic lipid impact not only LNP formulation but RNA delivery and therapeutic efficacy.

In chapter two, a series of linear-dendritic poly(ethylene glycol) (PEG) lipids (PEG-GnCm) were synthesized through sequential aza- and sulfa-Michael additions to investigate the effect of the lipid tail dendritic chemical structures on the *in vitro* and *in vivo* siRNA delivery of our previously established 5A2-SC8 dendrimer-based lipid nanoparticles (DLNPs). The tail chemical structure of PEG-GnCm was modulated with different lipid length and different generations. It was found that the tail chemical structure of PEG-GnCm did not affect the formulation of 5A2-SC8 DLNPs including the nanoparticle size, RNA encapsulation, and stability. However, the tail chemical structure did dramatically affect RNA delivery efficacy of 5A2-SC8 DLNPs. First generation PEG lipids (PEG-G1C8, PEG-G1C12, and PEG-G1C16) and second-generation PEG lipid (PEG-G2C8) were able to yield 5A2-SC8 DLNPs that could deliver siRNAs effectively *in vitro* and *in vivo*. 5A2-SC8 DLNPs formulated with second generation PEG lipids (PEG-G2C12 and PEG-G2C16) and all three third generation PEG lipids (PEG-G3C8, PEG-G3C12 and PEG-G3C16) lost the ability to deliver siRNA *in vitro*

and *in vivo*. Through the studies reported in chapter two, a structure activity relationship was identified with respect to PEG lipids utilized in DLNPs and siRNA delivery efficacy. It was found the tail chemical structure of PEG lipids impacted the escape of 5A2-SC8 DLNPs from the endosomes at the early cell incubation time. The reports published in chapter two will provide new insights on formulation of lipid nanoparticles for delivering RNA therapeutics *in vitro* and *in vivo*.

In the nanomedicine delivery field, emphasis has focused on organ level delivery. Cell specific delivery has been underappreciated and not understood. Chapter three provides insights into cell specificity of LNP delivery and resulting anti-cancer potential. Understanding the cellular fate of LNPs within the liver is important in the context of cancer therapy because delivery to an unexpected cell type could result in lack of efficacy and even in adverse events. Here two LNPs, 5A2-SC8 and 3A5-SC14, that accumulate in the liver and share similar physical properties were studied. It was found that altering the chemistry of the amino lipid can affect protein corona formation, which then likely drives uptake into hepatocytes or Kupffer cells. It was identified ApoE and Albumin as key mediators of this difference between 5A2-SC8 and 3A5-SC14 LNPs. 3A5-SC14 LNPs were only able to silence gene expression in hepatocytes after Kupffer cells were depleted. Consequently, in a liver cancer model dependent on hepatocyte and cancer cell delivery, only 5A2-SC8 LNPs carrying let-7g miRNA provided a therapeutic benefit. Overall, these results in chapter three illustrate the importance of understanding the sub-organ cellular destination of RNA delivery and incorporating further checkpoints when choosing nanoparticles beyond biochemical and

physical characterization. The results from this body of research can help guide others in the future selection of nanoparticles for specific disease.

APPENDIX A

Supplementary Figures

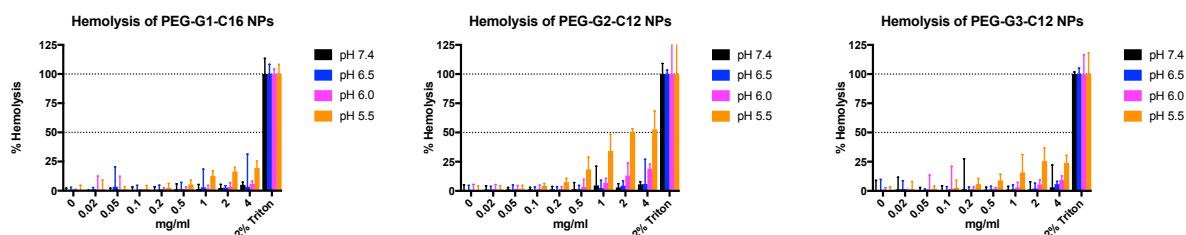


Figure A1. Hemolysis of PEG-G1C16, PEG-G2C12 and PEG-G3C12 5A2-SC8 DLNPs at different nanoparticle concentrations and pH values.

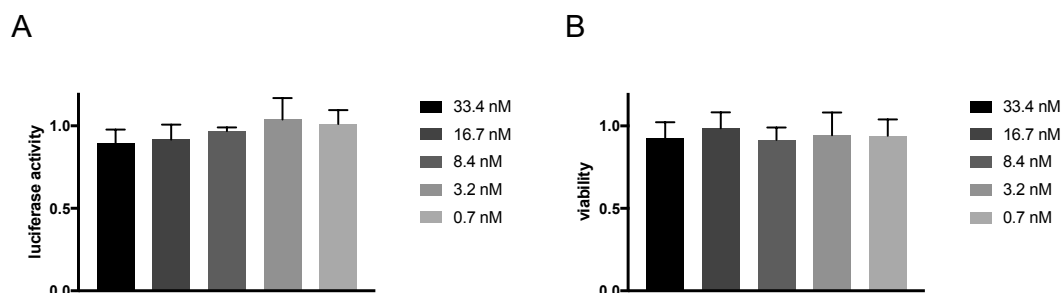


Figure A2. Dose-dependent (A) gene silencing and (B) cell viability of cells treated with 5A2-SC8 DLNPs formulated with PEG-G2-C12 linear dendritic PEG lipid. A control siRNA was encapsulated in the DLNPs (Sigma-Aldrich MISSION siRNA Universal Negative Control #1). Delivery of control siRNA in PEG-G2-C12 5A2-SC8 DLNPs did not lead to gene silencing and did not affect cell viability.

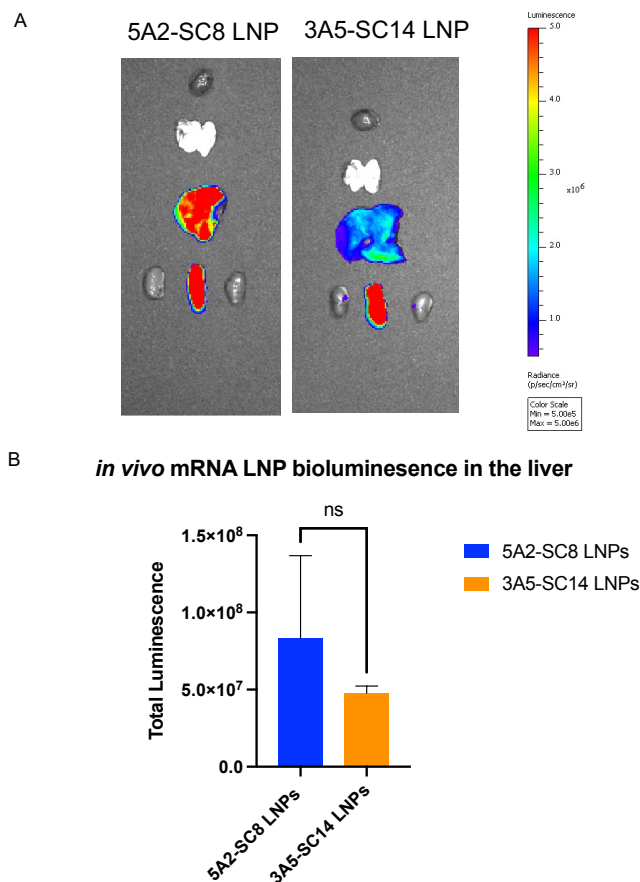


Figure A3. 5A2-SC8 and 3A5-SC14 LNPs deliver functional mRNA to the liver. (A) Organ biodistribution via IVIS Lumina Imaging for 6 hours biodistribution of 0.1 mg/kg Luciferase mRNA 5A2-SC8 and 3A5-SC14 LNP. (B) Quantification of total luminescence for 6 hours biodistribution of 0.1 mg/kg Luciferase mRNA 5A2-SC8 and 3A5-SC14 LNPs. Data are shown as mean +/- SEM. Statistical significance was determined using a student's t-test, where $p=0.3134$.

BIBLIOGRAPHY

1. Mendes, B. B.; Conniot, J.; Avital, A.; Yao, D.; Jiang, X.; Zhou, X.; Sharf-Pauker, N.; Xiao, Y.; Adir, O.; Liang, H.; Shi, J.; Schroeder, A.; Conde, J., Nanodelivery of nucleic acids. *Nat Rev Methods Primers* **2022**, *2*.
2. Crick, F., Central dogma of molecular biology. *Nature* **1970**, *227* (5258), 561-3.
3. Watson, J. D.; Crick, F. H., Molecular structure of nucleic acids; a structure for deoxyribose nucleic acid. *Nature* **1953**, *171* (4356), 737-8.
4. Tamura, R.; Toda, M., Historic Overview of Genetic Engineering Technologies for Human Gene Therapy. *Neurol Med Chir (Tokyo)* **2020**, *60* (10), 483-491.
5. Szybalska, E. H.; Szybalski, W., Genetics of human cell line. IV. DNA-mediated heritable transformation of a biochemical trait. *Proc Natl Acad Sci U S A* **1962**, *48*, 2026-34.
6. Gibbs, R. A., The Human Genome Project changed everything. *Nat Rev Genet* **2020**, *21* (10), 575-576.
7. Kulkarni, J. A.; Cullis, P. R.; van der Meel, R., Lipid Nanoparticles Enabling Gene Therapies: From Concepts to Clinical Utility. *Nucleic Acid Ther* **2018**, *28* (3), 146-157.
8. Damase, T. R.; Sukhovshin, R.; Boada, C.; Taraballi, F.; Pettigrew, R. I.; Cooke, J. P., The Limitless Future of RNA Therapeutics. *Front Bioeng Biotechnol* **2021**, *9*, 628137.
9. Rees, H. A.; Liu, D. R., Base editing: precision chemistry on the genome and transcriptome of living cells. *Nat Rev Genet* **2018**, *19* (12), 770-788.
10. Verve Therapeutics Doses First Human with an Investigational In Vivo Base Editing Medicine, VERVE-101, as a Potential Treatment for Heterozygous Familial Hypercholesterolemia. 2022.
11. Raguram, A.; Banskota, S.; Liu, D. R., Therapeutic in vivo delivery of gene editing agents. *Cell* **2022**.
12. de Fougerolles, A.; Vornlocher, H.-P.; Maraganore, J.; Lieberman, J., Interfering with disease: a progress report on siRNA-based therapeutics. *Nat. Rev. Drug Discov.* **2007**, *6* (6), 443-453.

13. Akinc, A.; Maier, M. A.; Manoharan, M.; Fitzgerald, K.; Jayaraman, M.; Barros, S.; Ansell, S.; Du, X. Y.; Hope, M. J.; Madden, T. D.; Mui, B. L.; Semple, S. C.; Tam, Y. K.; Ciufolini, M.; Witzigmann, D.; Kulkarni, J. A.; van der Meel, R.; Cullis, P. R., The Onpattro story and the clinical translation of nanomedicines containing nucleic acid-based drugs. *Nat. Nanotechnol.* **2019**, *14* (12), 1084-1087.
14. Hu, B.; Zhong, L.; Weng, Y.; Peng, L.; Huang, Y.; Zhao, Y.; Liang, X. J., Therapeutic siRNA: state of the art. *Signal Transduct Target Ther* **2020**, *5* (1), 101.
15. Xin, Y.; Huang, M.; Guo, W. W.; Huang, Q.; Zhang, L. Z.; Jiang, G., Nano-based delivery of RNAi in cancer therapy. *Mol Cancer* **2017**, *16* (1), 134-134.
16. Watts, J. K.; Corey, D. R., Silencing disease genes in the laboratory and the clinic. *J Pathol* **2012**, *226* (2), 365-79.
17. Dhuri, K.; Bechtold, C.; Quijano, E.; Pham, H.; Gupta, A.; Vikram, A.; Bahal, R., Antisense Oligonucleotides: An Emerging Area in Drug Discovery and Development. *J Clin Med* **2020**, *9* (6).
18. Marwick, C., First "antisense" drug will treat CMV retinitis. *JAMA* **1998**, *280* (10), 871.
19. Claudia, M.; Kristin, O.; Jennifer, O.; Eva, R.; Eleonore, F., Comparison of fluorescence-based methods to determine nanoparticle uptake by phagocytes and non-phagocytic cells in vitro. *Toxicology* **2017**, *378*, 25-36.
20. Dana, H.; Chalbatani, G. M.; Mahmoodzadeh, H.; Karimloo, R.; Rezaiean, O.; Moradzadeh, A.; Mehmandoost, N.; Moazzen, F.; Mazraeh, A.; Marmari, V.; Ebrahimi, M.; Rashno, M. M.; Abadi, S. J.; Gharagouzlo, E., Molecular Mechanisms and Biological Functions of siRNA. *Int J Biomed Sci* **2017**, *13* (2), 48-57.
21. Bartel, D. P., MicroRNAs: Genomics, biogenesis, mechanism, and function. *Cell* **2004**, *116* (2), 281-297.
22. Saliminejad, K.; Khorram Khorshid, H. R.; Soleymani Fard, S.; Ghaffari, S. H., An overview of microRNAs: Biology, functions, therapeutics, and analysis methods. *J Cell Physiol* **2019**, *234* (5), 5451-5465.
23. Lam, J. K.; Chow, M. Y.; Zhang, Y.; Leung, S. W., siRNA Versus miRNA as Therapeutics for Gene Silencing. *Mol Ther Nucleic Acids* **2015**, *4*, e252.
24. Chen, X.; Mangala, L. S.; Rodriguez-Aguayo, C.; Kong, X.; Lopez-Berestein, G.; Sood, A. K., RNA interference-based therapy and its delivery systems. *Cancer Metastasis Rev* **2018**, *37* (1), 107-124.

25. Wolff, J. A.; Malone, R. W.; Williams, P.; Chong, W.; Acsadi, G.; Jani, A.; Felgner, P. L., Direct gene transfer into mouse muscle in vivo. *Science* **1990**, *247* (4949 Pt 1), 1465-8.
26. Baden, L. R.; El Sahly, H. M.; Essink, B.; Kotloff, K.; Frey, S.; Novak, R.; Diemert, D.; Spector, S. A.; Rouphael, N.; Creech, C. B.; McGettigan, J.; Khetan, S.; Segall, N.; Solis, J.; Brosz, A.; Fierro, C.; Schwartz, H.; Neuzil, K.; Corey, L.; Gilbert, P.; Janes, H.; Follmann, D.; Marovich, M.; Mascola, J.; Polakowski, L.; Ledgerwood, J.; Graham, B. S.; Bennett, H.; Pajon, R.; Knightly, C.; Leav, B.; Deng, W. P.; Zhou, H. H.; Han, S.; Ivarsson, M.; Miller, J.; Zaks, T.; Grp, C. S., Efficacy and Safety of the mRNA-1273 SARS-CoV-2 Vaccine. *N. Engl. J. Med* **2021**, *384* (5), 403-416.
27. Polack, F. P.; Thomas, S. J.; Kitchin, N.; Absalon, J.; Gurtman, A.; Lockhart, S.; Perez, J. L.; Perez Marc, G.; Moreira, E. D.; Zerbini, C.; Bailey, R.; Swanson, K. A.; Roychoudhury, S.; Koury, K.; Li, P.; Kalina, W. V.; Cooper, D.; Frenck, R. W., Jr.; Hammitt, L. L.; Tureci, O.; Nell, H.; Schaefer, A.; Unal, S.; Tresnan, D. B.; Mather, S.; Dormitzer, P. R.; Sahin, U.; Jansen, K. U.; Gruber, W. C.; Group, C. C. T., Safety and Efficacy of the BNT162b2 mRNA Covid-19 Vaccine. *N Engl J Med* **2020**, *383* (27), 2603-2615.
28. Gillmore, J. D.; Maitland, M. L.; Lebowhl, D., CRISPR-Cas9 In Vivo Gene Editing for Transthyretin Amyloidosis. Reply. *N Engl J Med* **2021**, *385* (18), 1722-1723.
29. Mullard, A., Proof-of-principle Intellia trial shows in vivo CRISPR activity. *Nat Rev Drug Discov* **2022**, *21* (4), 249.
30. Jones, C. H.; Chen, C. K.; Ravikrishnan, A.; Rane, S.; Pfeifer, B. A., Overcoming nonviral gene delivery barriers: perspective and future. *Mol Pharm* **2013**, *10* (11), 4082-98.
31. Torres-Vanegas, J. D.; Cruz, J. C.; Reyes, L. H., Delivery Systems for Nucleic Acids and Proteins: Barriers, Cell Capture Pathways and Nanocarriers. *Pharmaceutics* **2021**, *13* (3).
32. Sartorius, K.; Antwi, S. O.; Chuturgoon, A.; Roberts, L. R.; Kramvis, A., RNA Therapeutic Options to Manage Aberrant Signaling Pathways in Hepatocellular Carcinoma: Dream or Reality? *Front Oncol* **2022**, *12*, 891812.
33. Conner, S. D.; Schmid, S. L., Regulated portals of entry into the cell. *Nature* **2003**, *422* (6927), 37-44.
34. Gilleron, J.; Querbes, W.; Zeigerer, A.; Borodovsky, A.; Marsico, G.; Schubert, U.; Manyoats, K.; Seifert, S.; Andree, C.; Stoter, M.; Epstein-Barash, H.; Zhang, L. G.; Koteliansky, V.; Fitzgerald, K.; Fava, E.; Bickle, M.; Kalaidzidis, Y.;

- Akinc, A.; Maier, M.; Zerial, M., Image-based analysis of lipid nanoparticle-mediated siRNA delivery, intracellular trafficking and endosomal escape. *Nat. Biotechnol.* **2013**, *31* (7), 638-U102.
35. Mendell, J. R.; Al-Zaidy, S. A.; Rodino-Klapac, L. R.; Goodspeed, K.; Gray, S. J.; Kay, C. N.; Boye, S. L.; Boye, S. E.; George, L. A.; Salabarria, S.; Corti, M.; Byrne, B. J.; Tremblay, J. P., Current Clinical Applications of In Vivo Gene Therapy with AAVs. *Mol Ther* **2021**, *29* (2), 464-488.
36. Dong, J. Y.; Fan, P. D.; Frizzell, R. A., Quantitative analysis of the packaging capacity of recombinant adeno-associated virus. *Hum Gene Ther* **1996**, *7* (17), 2101-2112.
37. Tornabene, P.; Trapani, I., Can Adeno-Associated Viral Vectors Deliver Effectively Large Genes? *Hum Gene Ther* **2020**, *31* (1-2), 47-56.
38. Lisowski, L.; Staber, J. M.; Wright, J. F.; Valentino, L. A., The intersection of vector biology, gene therapy, and hemophilia. *Res Pract Thromb Hae* **2021**, *5* (6).
39. Akinc, A.; Maier, M. A.; Manoharan, M.; Fitzgerald, K.; Jayaraman, M.; Barros, S.; Ansell, S.; Du, X.; Hope, M. J.; Madden, T. D.; Mui, B. L.; Semple, S. C.; Tam, Y. K.; Ciufolini, M.; Witzigmann, D.; Kulkarni, J. A.; van der Meel, R.; Cullis, P. R., The Onpatro Story and the Clinical Translation of Nanomedicines Containing Nucleic Acid-Based Drugs. *Nat. Nanotechnol.* **2019**, *14* (12), 1084-1087.
40. Gregoriadis, G., Liposomes in Drug Delivery: How It All Happened. *Pharmaceutics* **2016**, *8* (2).
41. Bangham, A. D.; Standish, M. M.; Watkins, J. C., Diffusion of univalent ions across the lamellae of swollen phospholipids. *J Mol Biol* **1965**, *13* (1), 238-52.
42. Working, P. K.; Dayan, A. D., Pharmacological-toxicological expert report. CAELYX. (Stealth liposomal doxorubicin HCl). *Hum Exp Toxicol* **1996**, *15* (9), 751-85.
43. Tenchov, R.; Bird, R.; Curtze, A. E.; Zhou, Q. Q., Lipid Nanoparticles-From Liposomes to mRNA Vaccine Delivery, a Landscape of Research Diversity and Advancement. *ACS Nano* **2021**, *15* (11), 16982-17015.
44. Khalil, I. A.; Younis, M. A.; Kimura, S.; Harashima, H., Lipid Nanoparticles for Cell-Specific in Vivo Targeted Delivery of Nucleic Acids. *Biol Pharm Bull* **2020**, *43* (4), 584-595.
45. Mukalel, A. J.; Riley, R. S.; Zhang, R.; Mitchell, M. J., Nanoparticles for nucleic acid delivery: Applications in cancer immunotherapy. *Cancer Lett* **2019**, *458*, 102-112.

46. Tai, W.; Gao, X., Functional peptides for siRNA delivery. *Adv Drug Deliv Rev* **2017**, *110-111*, 157-168.
47. Mitchell, M. J.; Billingsley, M. M.; Haley, R. M.; Wechsler, M. E.; Peppas, N. A.; Langer, R., Engineering precision nanoparticles for drug delivery. *Nat Rev Drug Discov* **2021**, *20* (2), 101-124.
48. Xiao, Y. L.; Shi, J. J., Lipids and the Emerging RNA Medicines. *Chem. Rev.* **2021**, *121* (20), 12109-12111.
49. Whitehead, K. A.; Langer, R.; Anderson, D. G., Knocking Down Barriers: Advances in siRNA Delivery. *Nat. Rev. Drug Discov.* **2009**, *8* (2), 129-138.
50. Hajj, K. A.; Whitehead, K. A., Tools for Translation: Non-Viral Materials for Therapeutic mRNA Delivery. *Nat. Rev. Mater.* **2017**, *2* (10).
51. Wei, T.; Cheng, Q.; Farbiak, L.; Anderson, D. G.; Langer, R.; Siegwart, D. J., Delivery of Tissue-Targeted Scalpels: Opportunities and Challenges for In Vivo CRISPR/Cas-Based Genome Editing. *ACS Nano* **2020**, *14* (8), 9243-9262.
52. Zhang, G.; Wang, Q.; Xu, R., Therapeutics Based on MicroRNA: A New Approach for Liver Cancer. *Curr. Genomics* **2010**, *11* (5), 311-325.
53. Chaudhary, N.; Weissman, D.; Whitehead, K. A., mRNA Vaccines for Infectious Diseases: Principles, Delivery and Clinical Translation. *Nat. Rev. Drug Discov.* **2021**, *20* (11), 817-838.
54. Pattni, B. S.; Chupin, V. V.; Torchilin, V. P., New Developments in Liposomal Drug Delivery. *Chem Rev* **2015**, *115* (19), 10938-66.
55. Witzigmann, D.; Kulkarni, J. A.; Leung, J.; Chen, S.; Cullis, P. R.; van der Meel, R., Lipid nanoparticle technology for therapeutic gene regulation in the liver. *Adv. Drug Deliv. Rev.* **2020**, *159*, 344-363.
56. Wu, Z.; Li, T., Nanoparticle-Mediated Cytoplasmic Delivery of Messenger RNA Vaccines: Challenges and Future Perspectives. *Pharm Res* **2021**, *38* (3), 473-478.
57. Bus, T.; Traeger, A.; Schubert, U. S., The great escape: how cationic polyplexes overcome the endosomal barrier. *J Mater Chem B* **2018**, *6* (43), 6904-6918.
58. Jayaraman, M.; Ansell, S. M.; Mui, B. L.; Tam, Y. K.; Chen, J.; Du, X.; Butler, D.; Eltepu, L.; Matsuda, S.; Narayanannair, J. K.; Rajeev, K. G.; Hafez, I. M.; Akinc, A.; Maier, M. A.; Tracy, M. A.; Cullis, P. R.; Madden, T. D.; Manoharan, M.; Hope, M. J., Maximizing the Potency of siRNA Lipid Nanoparticles for Hepatic Gene Silencing in vivo. *Angew. Chem. Int. Ed.* **2012**, *51* (34), 8529-33.

59. Yonezawa, S.; Koide, H.; Asai, T., Recent advances in siRNA delivery mediated by lipid-based nanoparticles. *Adv Drug Deliv Rev* **2020**, *154-155*, 64-78.
60. Han, X.; Zhang, H.; Butowska, K.; Swingle, K. L.; Alameh, M. G.; Weissman, D.; Mitchell, M. J., An ionizable lipid toolbox for RNA delivery. *Nat Commun* **2021**, *12* (1), 7233.
61. Bao, Y. J.; Jin, Y.; Chivukula, P.; Zhang, J.; Liu, Y.; Liu, J.; Clamme, J. P.; Mahato, R. I.; Ng, D.; Ying, W. B.; Wang, Y. T.; Yu, L., Effect of PEGylation on biodistribution and gene silencing of siRNA/lipid nanoparticle complexes. *Pharm. Res.* **2013**, *30* (2), 342-351.
62. Harris, J. M.; Chess, R. B., Effect of PEGylation on pharmaceuticals. *Nature Reviews Drug Discovery* **2003**, *2* (3), 214-221.
63. Chen, S.; Tam, Y. Y.; Lin, P. J.; Leung, A. K.; Tam, Y. K.; Cullis, P. R., Development of Lipid Nanoparticle Formulations of siRNA for Hepatocyte Gene Silencing Following Subcutaneous Administration. *J. Control. Release* **2014**, *196*, 106-12.
64. Chen, S.; Tam, Y. Y. C.; Lin, P. J. C.; Sung, M. M. H.; Tam, Y. K.; Cullis, P. R., Influence of particle size on the in vivo potency of lipid nanoparticle formulations of siRNA. *J Control Release* **2016**, *235*, 236-244.
65. Mui, B. L.; Tam, Y. K.; Jayaraman, M.; Ansell, S. M.; Du, X. Y.; Tam, Y. Y. C.; Lin, P. J. C.; Chen, S.; Narayanannair, J. K.; Rajeev, K. G.; Manoharan, M.; Akinc, A.; Maier, M. A.; Cullis, P.; Madden, T. D.; Hope, M. J., Influence of Polyethylene Glycol Lipid Desorption Rates on Pharmacokinetics and Pharmacodynamics of siRNA Lipid Nanoparticles. *Mol Ther-Nucl Acids* **2013**, *2*.
66. Cheng, X. W.; Lee, R. J., The role of helper lipids in lipid nanoparticles (LNPs) designed for oligonucleotide delivery. *Adv. Drug Deliv. Rev.* **2016**, *99*, 129-137.
67. Cheng, Q.; Wei, T.; Jia, Y.; Farbiak, L.; Zhou, K.; Zhang, S.; Wei, Y.; Zhu, H.; Siegwart, D. J., Dendrimer-Based Lipid Nanoparticles Deliver Therapeutic FAH mRNA to Normalize Liver Function and Extend Survival in a Mouse Model of Hepatorenal Tyrosinemia Type I. *Adv. Mater.* **2018**, *30* (52), e1805308.
68. Hou, X.; Zaks, T.; Langer, R.; Dong, Y., Lipid nanoparticles for mRNA delivery. *Nat Rev Mater* **2021**, *6* (12), 1078-1094.
69. Cheng, Q.; Wei, T.; Farbiak, L.; Johnson, L. T.; Dilliard, S. A.; Siegwart, D. J., Selective Organ Targeting (SORT) Nanoparticles for Tissue-Specific mRNA Delivery and CRISPR-Cas Gene Editing. *Nat. Nanotechnol.* **2020**, *15* (4), 313-320.

70. Dilliard, S. A.; Cheng, Q.; Siegwart, D. J., On the Mechanism of Tissue-Specific mRNA Delivery by Selective Organ Targeting Nanoparticles. *Proc. Natl. Acad. Sci. USA* **2021**, *118* (52).
71. Bertrand, N.; Leroux, J. C., The journey of a drug-carrier in the body: an anatomo-physiological perspective. *J. Controlled Release* **2012**, *161* (2), 152-163.
72. Zhang, Y.-N.; Poon, W.; Tavares, A. J.; McGilvray, I. D.; Chan, W. C. W., Nanoparticle–liver interactions: Cellular uptake and hepatobiliary elimination. *J. Controlled Release* **2016**, *240*, 332-348.
73. Yu, M. X.; Zheng, J., Clearance pathways and tumor targeting of imaging nanoparticles. *ACS Nano* **2015**, *9* (7), 6655-6674.
74. Almeida, J. P. M.; Chen, A. L.; Foster, A.; Drezek, R., In vivo biodistribution of nanoparticles. *Nanomedicine-Uk* **2011**, *6* (5), 815-835.
75. Zhang, Y. N.; Poon, W.; Tavares, A. J.; McGilvray, I. D.; Chan, W. C. W., Nanoparticle-Liver Interactions: Cellular Uptake and Hepatobiliary Elimination. *J. Control. Release* **2016**, *240*, 332-348.
76. Zhou, Z.; Xu, M. J.; Gao, B., Hepatocytes: A Key Cell Type for Innate Immunity. *Cell Mol. Immunol.* **2016**, *13* (3), 301-315.
77. Wang, H.; Thorling, C. A.; Liang, X.; Bridle, K. R.; Grice, J. E.; Zhu, Y.; Crawford, D. H. G.; Xu, Z. P.; Liu, X.; Roberts, M. S., Diagnostic Imaging and Therapeutic Application of Nanoparticles Targeting the Liver. *J. Mater. Chem. B.* **2015**, *3* (6), 939-958.
78. Bertrand, N.; Grenier, P.; Mahmoudi, M.; Lima, E. M.; Appel, E. A.; Dormont, F.; Lim, J. M.; Karnik, R.; Langer, R.; Farokhzad, O. C., Mechanistic understanding of in vivo protein corona formation on polymeric nanoparticles and impact on pharmacokinetics. *Nat. Commun.* **2017**, *8*.
79. Hadjidemetriou, M.; Kostarelos, K., Evolution of the nanoparticle corona. *Nat. Nanotechnol.* **2017**, *12*, 288.
80. Mahmoudi, M.; Bertrand, N.; Zope, H.; Farokhzad, O. C., Emerging understanding of the protein corona at the nano-bio interfaces. *Nano Today* **2016**, *11* (6), 817-832.
81. Kelly, P. M.; Aberg, C.; Polo, E.; O'Connell, A.; Cookman, J.; Fallon, J.; Krpetic, Z.; Dawson, K. A., Mapping protein binding sites on the biomolecular corona of nanoparticles. *Nat. Nanotechnol.* **2015**, *10* (5), 472-9.

82. Tenzer, S.; Docter, D.; Kuharev, J.; Musyanovych, A.; Fetz, V.; Hecht, R.; Schlenk, F.; Fischer, D.; Kiouptsi, K.; Reinhardt, C.; Landfester, K.; Schild, H.; Maskos, M.; Knauer, S. K.; Stauber, R. H., Rapid formation of plasma protein corona critically affects nanoparticle pathophysiology. *Nat. Nanotechnol.* **2013**, *8* (10), 772-781.
83. Monopoli, M. P.; Aberg, C.; Salvati, A.; Dawson, K. A., Biomolecular coronas provide the biological identity of nanosized materials. *Nat. Nanotechnol.* **2012**, *7* (12), 779-86.
84. Lundqvist, M.; Stigler, J.; Elia, G.; Lynch, I.; Cedervall, T.; Dawson, K. A., Nanoparticle size and surface properties determine the protein corona with possible implications for biological impacts. *Proc. Natl. Acad. Sci. USA* **2008**, *105* (38), 14265-14270.
85. Ritz, S.; Schottler, S.; Kotman, N.; Baier, G.; Musyanovych, A.; Kuharev, J.; Landfester, K.; Schild, H.; Jahn, O.; Tenzer, S.; Mailander, V., Protein Corona of Nanoparticles: Distinct Proteins Regulate the Cellular Uptake. *Biomacromolecules* **2015**, *16* (4), 1311-1321.
86. Yan, X. D.; Kuipers, F.; Havekes, L. M.; Havinga, R.; Dontje, B.; Poelstra, K.; Scherphof, G. L.; Kamps, J. A. A. M., The role of apolipoprotein E in the elimination of liposomes from blood by hepatocytes in the mouse (vol 328, pg 57, 2005). *Biochem Bioph Res Co* **2005**, *330* (4), 1320-1320.
87. Akinc, A.; Querbes, W.; De, S.; Qin, J.; Frank-Kamenetsky, M.; Jayaprakash, K. N.; Jayaraman, M.; Rajeev, K. G.; Cantley, W. L.; Dorkin, J. R.; Butler, J. S.; Qin, L.; Racie, T.; Sprague, A.; Fava, E.; Zeigerer, A.; Hope, M. J.; Zerial, M.; Sah, D. W.; Fitzgerald, K.; Tracy, M. A.; Manoharan, M.; Kotliansky, V.; Fougerolles, A.; Maier, M. A., Targeted delivery of RNAi therapeutics with endogenous and exogenous ligand-based mechanisms. *Mol. Ther.* **2010**, *18* (7), 1357-64.
88. Akinc, A.; Querbes, W.; De, S. M.; Qin, J.; Frank-Kamenetsky, M.; Jayaprakash, K. N.; Jayaraman, M.; Rajeev, K. G.; Cantley, W. L.; Dorkin, J. R.; Butler, J. S.; Qin, L. L.; Racie, T.; Sprague, A.; Fava, E.; Zeigerer, A.; Hope, M. J.; Zerial, M.; Sah, D. W. Y.; Fitzgerald, K.; Tracy, M. A.; Manoharan, M.; Kotliansky, V.; de Fougerolles, A.; Maier, M. A., Targeted Delivery of RNAi Therapeutics With Endogenous and Exogenous Ligand-Based Mechanisms. *Mol. Ther.* **2010**, *18* (7), 1357-1364.
89. Rinaldi, L.; Vetrano, E.; Rinaldi, B.; Galiero, R.; Caturano, A.; Salvatore, T.; Sasso, F. C., HCC and Molecular Targeting Therapies: Back to the Future. *Biomedicines* **2021**, *9* (10).
90. El-Serag, H. B., Hepatocellular carcinoma: recent trends in the United States. *Gastroenterology* **2004**, *127* (5 Suppl 1), S27-34.

91. El-Serag, H. B., Epidemiology of viral hepatitis and hepatocellular carcinoma. *Gastroenterology* **2012**, *142* (6), 1264-1273 e1.
92. El-Serag, H. B.; Kanwal, F., Epidemiology of hepatocellular carcinoma in the United States: where are we? Where do we go? *J. Hepatol.* **2014**, *60* (5), 1767-75.
93. Roberts, L. R., Sorafenib in Liver Cancer - Just the Beginning. *N. Engl. J. Med* **2008**, *359* (4), 420-422.
94. Scudellari, M., DRUG DEVELOPMENT: Try and try again. *Nature* **2014**, *516* (7529), S4-S6.
95. Boland, P.; Wu, J., Systemic therapy for hepatocellular carcinoma: beyond sorafenib. *Chin. Clin. Oncol.* **2018**, *7* (5).
96. Zhang, S.; Zhou, K.; Luo, X.; Li, L.; Tu, H. C.; Sehgal, A.; Nguyen, L. H.; Zhang, Y.; Gopal, P.; Tarlow, B. D.; Siegwart, D. J.; Zhu, H., The Polyploid State Plays a Tumor-Suppressive Role in the Liver. *Dev Cell* **2018**, *47* (3), 390.
97. Saffo, S.; Taddei, T. H., Systemic Management for Advanced Hepatocellular Carcinoma: A Review of the Molecular Pathways of Carcinogenesis, Current and Emerging Therapies, and Novel Treatment Strategies. *Digest Dis Sci* **2019**, *64* (4), 1016-1029.
98. Kobayashi, M.; Kudo, M.; Izumi, N.; Kaneko, S.; Azuma, M.; Copher, R.; Meier, G.; Pan, J.; Ishii, M.; Ikeda, S., Cost-effectiveness Analysis of Lenvatinib Treatment for Patients with Unresectable Hepatocellular Carcinoma (uHCC) Compared with Sorafenib in Japan. *J. Gastroenterol.* **2019**, *54* (6), 558-570.
99. Zhu, J.; Yin, T. L.; Xu, Y.; Lu, X. J., Therapeutics for advanced hepatocellular carcinoma: Recent advances, current dilemma, and future directions. *J. Cell. Physiol.* **2019**, *234* (8), 12122-12132.
100. Finn, R. S.; Qin, S.; Ikeda, M.; Galle, P. R.; Ducreux, M.; Kim, T. Y.; Kudo, M.; Breder, V.; Merle, P.; Kaseb, A. O.; Li, D.; Verret, W.; Xu, D. Z.; Hernandez, S.; Liu, J.; Huang, C.; Mulla, S.; Wang, Y.; Lim, H. Y.; Zhu, A. X.; Cheng, A. L.; Investigators, I. M., Atezolizumab plus Bevacizumab in Unresectable Hepatocellular Carcinoma. *N Engl J Med* **2020**, *382* (20), 1894-1905.
101. Foerster, F.; Gairing, S. J.; Ilyas, S. I.; Galle, P. R., Emerging immunotherapy for HCC: A guide for hepatologists. *J. Hepatol.* **2022**, *75* (6), 1604-1626.
102. Finn, R. S.; Bentley, G.; Britten, C. D.; Amado, R.; Busuttil, R. W., Targeting vascular endothelial growth factor with the monoclonal antibody bevacizumab inhibits

- human hepatocellular carcinoma cells growing in an orthotopic mouse model. *Liver Int* **2009**, *29* (2), 284-90.
103. Xu, C. F.; Wang, J., Delivery systems for siRNA drug development in cancer therapy. *Asian J. Pharm. Sci.* **2015**, *10* (1), 1-12.
104. Hanna, J.; Hossein, G. S.; Kocerha, J., The Potential for microRNA Therapeutics and Clinical Research. *Front. Genet.* **2019**, *10*.
105. Lin, C. P.; Liu, C. R.; Lee, C. N.; Chan, T. S.; Liu, H. E., Targeting c-Myc as a novel approach for hepatocellular carcinoma. *World J. Hepatol.* **2010**, *2* (1), 16-20.
106. Aravalli, R. N.; Steer, C. J., Immune-Mediated Therapies for Liver Cancer. *Genes* **2017**, *8* (2).
107. Lauth, W. W., In *Hepatic Circulation: Physiology and Pathophysiology*, San Rafael (CA), 2009.
108. Colagrande, S.; Inghilesi, A. L.; Aburas, S.; Taliani, G. G.; Nardi, C.; Marra, F., Challenges of advanced hepatocellular carcinoma. *World J. Gastroentero.* **2016**, *22* (34), 7645-7659.
109. Chakraborty, C.; Sharma, A. R.; Sharma, G.; Lee, S. S., Therapeutic advances of miRNAs: A preclinical and clinical update. *J. Adv. Res.* **2021**, *28*, 127-138.
110. Whitehead, K.; Langer, R.; Anderson, D., Knocking down barriers: Advances in siRNA delivery. *Nat. Rev. Drug Discovery* **2009**, *8* (2), 129-138.
111. Burnett, J. C.; Rossi, J. J., RNA-based therapeutics: Current progress and future prospects. *Chem. Biol.* **2012**, *19* (1), 60-71.
112. Ling, H.; Fabbri, M.; Calin, G. A., MicroRNAs and other non-coding RNAs as targets for anticancer drug development. *Nat. Rev. Drug Discovery* **2013**, *12* (11), 847-865.
113. Wu, S. Y.; Lopez-Berestein, G.; Calin, G. A.; Sood, A. K., RNAi therapies: Drugging the undruggable. *Sci. Transl. Med.* **2014**, *6* (240), 240-247.
114. Zuckerman, J. E.; Davis, M. E., Clinical experiences with systemically administered siRNA-based therapeutics in cancer. *Nat. Rev. Drug Discovery* **2015**, *14* (12), 843-856.
115. Kauffman, K. J.; Webber, M. J.; Anderson, D. G., Materials for non-viral intracellular delivery of messenger RNA therapeutics. *J. Controlled Release* **2016**, *240*, 227-234.

116. de Fougerolles, A.; Vornlocher, H. P.; Maraganore, J.; Lieberman, J., Interfering with disease: a progress report on siRNA-based therapeutics. *Nat. Rev. Drug Discovery* **2007**, *6* (6), 443-453.
117. Sahin, U.; Kariko, K.; Tureci, O., mRNA-based therapeutics: Developing a new class of drugs. *Nat. Rev. Drug Discovery* **2014**, *13* (10), 759-780.
118. Hajj, K. A.; Whitehead, K. A., Tools for translation: Non-viral materials for therapeutic mRNA delivery. *Nat. Rev. Mater.* **2017**, *2* (10), 17056.
119. Sullenger, B. A.; Nair, S., From the RNA world to the clinic. *Science* **2016**, *352* (6292), 1417-1420.
120. Akinc, A.; Maier, M. A.; Manoharan, M.; Fitzgerald, K.; Jayaraman, M.; Barros, S.; Ansell, S.; Du, X.; Hope, M. J.; Madden, T. D.; Mui, B. L.; Semple, S. C.; Tam, Y. K.; Ciufolini, M.; Witzigmann, D.; Kulkarni, J. A.; van der Meel, R.; Cullis, P. R., The Onpattro story and the clinical translation of nanomedicines containing nucleic acid-based drugs. *Nat. Nanotechnol.* **2019**, *14* (12), 1084-1087.
121. Mullard, A., FDA approves landmark RNAi drug. *Nat. Rev. Drug Discovery* **2018**, *17*, 613.
122. Zhang, Y.; Satterlee, A.; Huang, L., In vivo gene delivery by nonviral vectors: Overcoming hurdles? *Mol. Ther.* **2012**, *20* (7), 1298-1304.
123. Kanasty, R.; Dorkin, J. R.; Vegas, A.; Anderson, D., Delivery materials for siRNA therapeutics. *Nat. Mater.* **2013**, *12* (11), 967-977.
124. Dowdy, S. F., Overcoming cellular barriers for RNA therapeutics. *Nat. Biotechnol.* **2017**, *35*, 222.
125. Zhou, K.; Nguyen, L. H.; Miller, J. B.; Yan, Y.; Kos, P.; Xiong, H.; Li, L.; Hao, J.; Minnig, J. T.; Zhu, H.; Siegwart, D. J., Modular degradable dendrimers enable small RNAs to extend survival in an aggressive liver cancer model. *Proc. Natl. Acad. Sci. U.S.A.* **2016**, *113* (3), 520-525.
126. Zhang, S.; Nguyen, L. H.; Zhou, K.; Tu, H. C.; Sehgal, A.; Nassour, I.; Li, L.; Gopal, P.; Goodman, J.; Singal, A. G.; Yopp, A.; Zhang, Y.; Siegwart, D. J.; Zhu, H., Knockdown of anillin actin binding protein blocks cytokinesis in hepatocytes and reduces liver tumor development in mice without affecting regeneration. *Gastroenterology* **2018**, *154* (5), 1421-1434.
127. Zhang, S.; Zhou, K.; Luo, X.; Li, L.; Tu, H. C.; Sehgal, A.; Nguyen, L. H.; Zhang, Y.; Gopal, P.; Tarlow, B. D.; Siegwart, D. J.; Zhu, H., The polyploid state plays a tumor suppressive role in the liver *Dev. Cell* **2018**, *44* (4), 447-459.

128. Love, K.; Mahon, K.; Levins, C.; Whitehead, K.; Querbes, W.; Dorkin, J.; Qin, J.; Cantley, W.; Qin, L.; Racie, T.; Frank-Kamenetsky, M.; Yip, K.; Alvarez, R.; Sah, D.; de Fougerolles, A.; Fitzgerald, K.; Koteliensky, V.; Akinc, A.; Langer, R.; Anderson, D., Lipid-like materials for low-dose, in vivo gene silencing. *Proc. Natl. Acad. Sci. U.S.A.* **2010**, *107* (5), 1864-1869.
129. Semple, S. C.; Akinc, A.; Chen, J. X.; Sandhu, A. P.; Mui, B. L.; Cho, C. K.; Sah, D. W. Y.; Stebbing, D.; Crosley, E. J.; Yaworski, E.; Hafez, I. M.; Dorkin, J. R.; Qin, J.; Lam, K.; Rajeev, K. G.; Wong, K. F.; Jeffs, L. B.; Nechev, L.; Eisenhardt, M. L.; Jayaraman, M.; Kazem, M.; Maier, M. A.; Srinivasulu, M.; Weinstein, M. J.; Chen, Q. M.; Alvarez, R.; Barros, S. A.; De, S.; Klimuk, S. K.; Borland, T.; Kosovrasti, V.; Cantley, W. L.; Tam, Y. K.; Manoharan, M.; Ciufolini, M. A.; Tracy, M. A.; de Fougerolles, A.; MacLachlan, I.; Cullis, P. R.; Madden, T. D.; Hope, M. J., Rational design of cationic lipids for siRNA delivery. *Nat. Biotechnol.* **2010**, *28* (2), 172-176.
130. Whitehead, K. A.; Dorkin, J. R.; Vegas, A. J.; Chang, P. H.; Veisoh, O.; Matthews, J.; Fenton, O. S.; Zhang, Y. L.; Olejnik, K. T.; Yesilyurt, V.; Chen, D. L.; Barros, S.; Klebanov, B.; Novobrantseva, T.; Langer, R.; Anderson, D. G., Degradable lipid nanoparticles with predictable in vivo siRNA delivery activity. *Nat. Commun.* **2014**, *5*, 4277.
131. Kauffman, K. J.; Dorkin, J. R.; Yang, J. H.; Heartlein, M. W.; DeRosa, F.; Mir, F. F.; Fenton, O. S.; Anderson, D. G., Optimization of lipid nanoparticle formulations for mRNA delivery in vivo with fractional factorial and definitive screening designs. *Nano Lett.* **2015**, *15* (11), 7300-7306.
132. Wittrup, A.; Ai, A.; Liu, X.; Hamar, P.; Trifonova, R.; Charisse, K.; Manoharan, M.; Kirchhausen, T.; Lieberman, J., Visualizing lipid-formulated siRNA release from endosomes and target gene knockdown. *Nat. Biotechnol.* **2015**, *33* (8), 870-976.
133. Miller, J. B.; Zhang, S.; Kos, P.; Xiong, H.; Zhou, K.; Perelman, S. S.; Zhu, H.; Siegwart, D. J., Non-viral CRISPR/Cas gene editing in vitro and in vivo enabled by synthetic nanoparticle co-delivery of Cas9 mRNA and sgRNA. *Angew. Chem. Int. Ed.* **2017**, *56* (4), 1059-1063.
134. Hajj, K. A.; Ball, R. L.; Deluty, S. B.; Singh, S. R.; Strelkova, D.; Knapp, C. M.; Whitehead, K. A., Branched-tail lipid nanoparticles potently deliver mRNA in vivo due to enhanced ionization at endosomal pH. *Small* **2019**, *15* (6), 1805097.
135. Li, B.; Luo, X.; Deng, B.; Wang, J.; McComb, D. W.; Shi, Y.; Gaensler, K. M.; Tan, X.; Dunn, A. L.; Kerlin, B. A.; Dong, Y., An orthogonal array optimization of lipid-like nanoparticles for mRNA delivery in vivo. *Nano Lett.* **2015**, *15* (12), 8099-8107.

136. Zhang, X. W.; Wang, H.; Ma, Z. G.; Wu, B. J., Effects of pharmaceutical PEGylation on drug metabolism and its clinical concerns. *Expert Opin. Drug Met.* **2014**, *10* (12), 1691-1702.
137. Sato, Y.; Note, Y.; Maeki, M.; Kaji, N.; Baba, Y.; Tokeshi, M.; Harashima, H., Elucidation of the physicochemical properties and potency of siRNA-loaded small-sized lipid nanoparticles for siRNA delivery. *J. Controlled Release* **2016**, *229*, 48-57.
138. Ying, B.; Campbell, R. B., Delivery of kinesin spindle protein targeting siRNA in solid lipid nanoparticles to cellular models of tumor vasculature. *Biochem. Biophys. Res. Commun.* **2014**, *446* (2), 441-447.
139. Belliveau, N. M.; Huft, J.; Lin, P. J.; Chen, S.; Leung, A. K.; Leaver, T. J.; Wild, A. W.; Lee, J. B.; Taylor, R. J.; Tam, Y. K.; Hansen, C. L.; Cullis, P. R., Microfluidic synthesis of highly potent limit-size lipid nanoparticles for in vivo delivery of siRNA. *Mol. Ther. - Nucl. Acids* **2012**, *1*, e37.
140. Tao, W. K.; Davide, J. P.; Cai, M. M.; Zhang, G. J.; South, V. J.; Matter, A.; Ng, B.; Zhang, Y.; Sepp-Lorenzino, L., Noninvasive imaging of lipid nanoparticle-mediated systemic delivery of small-Interfering RNA to the liver. *Mol. Ther.* **2010**, *18* (9), 1657-1666.
141. Wurm, F.; Frey, H., Linear-dendritic block copolymers: The state of the art and exciting perspectives. *Prog. Polym. Sci.* **2011**, *36* (1), 1-52.
142. Kesharwani, P.; Jain, K.; Jain, N. K., Dendrimer as nanocarrier for drug delivery. *Prog. Polym. Sci.* **2014**, *39* (2), 268-307.
143. Casey, J. R.; Grinstein, S.; Orłowski, J., Sensors and regulators of intracellular pH. *Nat. Rev. Mol. Cell Bio.* **2010**, *11* (1), 50-61.
144. Kuhn, T.; Ihalainen, T. O.; Hyvaluoma, J.; Dross, N.; Willman, S. F.; Langowski, J.; Vihinen-Ranta, M.; Timonen, J., Protein diffusion in mammalian cell cytoplasm. *PLOS One* **2011**, *6* (8), 12.
145. Scheideler, M.; Vidakovic, I.; Prassl, R., Lipid nanocarriers for microRNA delivery. *Chem. Phys. Lipids* **2020**, 226.
146. Zhang, M. M.; Bahal, R.; Rasmussen, T. P.; Manautou, J. E.; Zhong, X. B., The Growth of siRNA-Based Therapeutics: Updated Clinical Studies. *Biochem. Pharmacol.* **2021**, *189*, 114432.
147. Liu, S.; Cheng, Q.; Wei, T.; Yu, X.; Johnson, L. T.; Farbiak, L.; Siegwart, D. J., Membrane-Destabilizing Ionizable Phospholipids for Organ-Selective mRNA Delivery and CRISPR-Cas Gene Editing. *Nat. Mater.* **2021**, *20* (5), 701-710.

148. Chakraborty, C.; Sharma, A. R.; Sharma, G.; Doss, C. G. P.; Lee, S. S., Therapeutic miRNA and siRNA: Moving from Bench to Clinic as Next Generation Medicine. *Mol. Ther. Nucleic Acids* **2017**, *8*, 132-143.
149. Cai, X.; Li, J. J.; Liu, T.; Brian, O.; Li, J., Infectious disease mRNA vaccines and a review on epitope prediction for vaccine design. *Brief. Funct. Genom.* **2021**, *20* (5), 289-303.
150. Zhou, K.; Nguyen, L. H.; Miller, J. B.; Yan, Y.; Kos, P.; Xiong, H.; Li, L.; Hao, J.; Minnig, J. T.; Zhu, H.; Siegwart, D. J., Modular Degradable Dendrimers Enable Small RNAs to Extend Survival in an Aggressive Liver Cancer Model. *Proc. Natl. Acad. Sci. USA* **2016**, *113* (3), 520-5.
151. Poon, W.; Zhang, Y. N.; Ouyang, B.; Kingston, B. R.; Wu, J. L. Y.; Wilhelm, S.; Chan, W. C. W., Elimination Pathways of Nanoparticles. *ACS Nano* **2019**, *13* (5), 5785-5798.
152. Tavares, A. J.; Poon, W.; Zhang, Y. N.; Dai, Q.; Besla, R.; Ding, D.; Ouyang, B.; Li, A.; Chen, J.; Zheng, G.; Robbins, C.; Chan, W. C. W., Effect of Removing Kupffer Cells on Nanoparticle Tumor Delivery. *Proc. Natl. Acad. Sci. USA* **2017**, *114* (51), E10871-E10880.
153. Monopoli, M. P.; Aberg, C.; Salvati, A.; Dawson, K. A., Biomolecular Coronas Provide the Biological Identity of Nanosized Materials. *Nat. Nanotechnol.* **2012**, *7* (12), 779-786.
154. Yan, X. D.; Kuipers, F.; Havekes, L. M.; Havinga, R.; Dontje, B.; Poelstra, K.; Scherphof, G. L.; Kamps, J. A. A. M., The Role of Apolipoprotein E in the Elimination of Liposomes from Blood by Hepatocytes in the Mouse. *Biochem. Biophys. Res. Commun.* **2005**, *330* (4), 1320-1320.
155. Docter, D.; Distler, U.; Storck, W.; Kuharev, J.; Wunsch, D.; Hahlbrock, A.; Knauer, S. K.; Tenzer, S.; Stauber, R. H., Quantitative Profiling of the Protein Coronas that Form Around Nanoparticles. *Nat. Protoc.* **2014**, *9* (9), 2030-2044.
156. Da Silva Sanchez, A. J.; Dobrowolski, C.; Cristian, A.; Echeverri, E. S.; Zhao, K.; Hatit, M. Z. C.; Loughrey, D.; Paunovska, K.; Dahlman, J. E., Universal Barcoding Predicts In Vivo ApoE-Independent Lipid Nanoparticle Delivery. *Nano Lett* **2022**, *22* (12), 4822-4830.
157. Miao, L.; Lin, J. Q.; Huang, Y. X.; Li, L. X.; Delcassian, D.; Ge, Y. F.; Shi, Y. H.; Anderson, D. G., Synergistic Lipid Compositions for Albumin Receptor Mediated Delivery of mRNA to the Liver. *Nat. Commun.* **2020**, *11* (1).

158. Vincent, M. P.; Bobbala, S.; Karabin, N. B.; Frey, M.; Liu, Y.; Navidzadeh, J. O.; Stack, T.; Scott, E. A., Surface Chemistry-Mediated Modulation of Adsorbed Albumin Folding State Specifies Nanocarrier Clearance by Distinct Macrophage Subsets. *Nat. Commun.* **2021**, *12* (1), 648.
159. Schnitzer, J. E.; Sung, A.; Horvat, R.; Bravo, J., Preferential Interaction of Albumin-Binding Proteins, Gp30 and Gp18, with Conformationally Modified Albumins - Presence in Many Cells and Tissues with a Possible Role in Catabolism. *J. Biol. Chem* **1992**, *267* (34), 24544-53.
160. Schnitzer, J. E.; Bravo, J., High Affinity Binding, Endocytosis, and Degradation of Conformationally Modified Albumins. Potential Role of gp30 and gp18 as Novel Scavenger Receptors. *J. Biol. Chem* **1993**, *268* (10), 7562-70.
161. Shachaf, C. M.; Kopelman, A. M.; Arvanitis, C.; Karlsson, A.; Beer, S.; Mandl, S.; Bachmann, M. H.; Borowsky, A. D.; Ruebner, B.; Cardiff, R. D.; Yang, Q. W.; Bishop, J. M.; Contag, C. H.; Felsher, D. W., MYC inactivation uncovers pluripotent differentiation and tumour dormancy in hepatocellular cancer. *Nature* **2004**, *431* (7012), 1112-1117.
162. Kistner, A.; Gossen, M.; Zimmermann, F.; Jerecic, J.; Ullmer, C.; Lubbert, H.; Bujard, H., Doxycycline-Mediated Quantitative and Tissue-Specific Control of Gene Expression in Transgenic Mice. *Proc. Natl. Acad. Sci. USA* **1996**, *93* (20), 10933-10938.
163. Whitfield, J. R.; Beaulieu, M. E.; Soucek, L., Strategies to Inhibit Myc and Their Clinical Applicability. *Front. Cell Dev. Biol.* **2017**, *5*.
164. Dang, C. V., c-Myc Target Genes Involved in Cell Growth, Apoptosis, and Metabolism. *Mol. Biol. Cell* **1999**, *19* (1), 1-11.
165. Dang, C. V., MYC, Metabolism, Cell Growth, and Tumorigenesis. *Cold Spring Harb. Perspect. Med.* **2013**, *3* (8).
166. Sun, J.; Lu, H.; Wang, X.; Jin, H., MicroRNAs in Hepatocellular Carcinoma: Regulation, Function, and Clinical Implications. *Sci. World J.* **2013**, *2013*, 924206.
167. Nguyen, L. H.; Robinton, D. A.; Seligson, M. T.; Wu, L. W.; Li, L.; Rakheja, D.; Comerford, S. A.; Ramezani, S.; Sun, X. K.; Parikh, M. S.; Yang, E. H.; Powers, J. T.; Shinoda, G.; Shah, S. P.; Hammer, R. E.; Daley, G. Q.; Zhu, H., Lin28b Is Sufficient to Drive Liver Cancer and Necessary for Its Maintenance in Murine Models. *Cancer Cell* **2014**, *26* (2), 248-261.
168. Roush, S.; Slack, F. J., The let-7 family of microRNAs. *Trends Cell Biol* **2008**, *18* (10), 505-16.

169. Wu, L.; Nguyen, L. H.; Zhou, K.; de Soysa, T. Y.; Li, L.; Miller, J. B.; Tian, J.; Locker, J.; Zhang, S.; Shinoda, G.; Seligson, M. T.; Zeitels, L. R.; Acharya, A.; Wang, S. C.; Mendell, J. T.; He, X.; Nishino, J.; Morrison, S. J.; Siegwart, D. J.; Daley, G. Q.; Shyh-Chang, N.; Zhu, H., Precise let-7 expression levels balance organ regeneration against tumor suppression. *Elife* **2015**, *4*, e09431.
170. Zhou, K. J.; Nguyen, L. H.; Miller, J. B.; Yan, Y. F.; Kos, P.; Xiong, H.; Li, L.; Hao, J.; Minnig, J. T.; Zhu, H.; Siegwart, D. J., Modular Degradable Dendrimers Enable Small RNAs to Extend Survival in an Aggressive Liver Cancer Model. *Proc. Natl. Acad. Sci. USA* **2016**, *113* (3), 520-525.